# Facile Approach to Synthesize Stimuli Responsive Polymer-Brush Constructed on a Silicon Substrate by Atom Transfer Radical Polymerization

*A thesis submitted to the department of Molecular Design & Engineering in the conformity with the requirments for the degree of Doctor of Engineering.*

Submitted by

**Muhammad Nurul Huda**

Student ID # 480866074

Molecular Assembly System Laboratory

Department of Molecular Design & Engineering

Graduate School of Engineering

Nagoya University

Nagoya, Japan

March 2011

To

My all Respected Teachers

&

Beloved Parents

# Acknowlwdgement

This dissertation would not have been possible without the guidance and the help of several individuals who in one way or another contributed and extended their valuable assistance in the preparation and completion of this study. Chapter two and chapter four of  of my dissertation, which was originally published in transaction of matyerial resource society Japan and Macromolecules respectively.

First and foremost, my utmost gratitude to **Professor  Dr. Y. Takeoka**, my academic supervisor, whose encouragement, guidance and support from the initial to the final level enabled me to develop an understanding of the subject. Above all and the most needed, he provided me unflinching encouragement and support in various ways. I gratefully acknowledge for his advice, supervision and crucial contribution which made him a backbone of this research and so the thesis. His friendship and technical guidance are valued.  I am heartily thankful to for his kind effort regarding my preparation for PhD defense also. I am quite lucky to find **Professor Takeoka** as my supervisor.

I would like to express the deepest appreciation to **Professor Dr. T. Seki**, who has the attitude and the substance of a genius: he continually and convincingly conveyed a spirit of adventure in regard to research and scholarship, and an excitement in regard to teaching. Without his guidance and persistent help this dissertation would not have been possible. His truly scientist intuition has made him as a constant oasis of ideas and passions in science, which exceptionally inspire and enrich my growth as a student, a researcher and a scientist want to be.

To the role model for hard workers in the lab, **Prof. Dr. S. Nagano**, I would like to thank him for being the person who helped in many ways by both his theoritical as well as experimental knowledge. I am proud to record that I had several opportunities to work with an exceptionally experienced scientist like him.

I am grateful to Professor **H. Iida** of  Polymer Materials Design department for his valuable advice regarding click chemistry.

I would like to thank specially **Mr. H. Suzuki**, former student of our laboratory and was acted my tutor as well. I have learnt a lot of experimental techniques from him.

I gratefully thank to most of the teachers of my Applied Chemistry & Chemical

Engineering, University of Dahak, Bangladesh, specially **Prof. Dr. Hamidul Kabir**. His perpetual energy and enthusiasm in research had motivated all his advisees, including me. In addition, he was always accessible and willing to help his students with their research. As a result, research life became smooth and rewarding for me.

Joining Nagoya University as a doctoral student was not only a turning point in my life, but also a wonderful experience. I cherished the prayers and support between me and them, and the friendships with my Japanese lab mates. I treasured all precious moments we shared and would really like to thank them. Many thanks go in particular to **Dr. A.B. Imran, Dr. H. Rashid, H. Ashraf, W. Li, M. Hara, Y. Goto D. Kondo** for their support and encouragement throughout my research.

Last but not the least, my family and the one above all of us, the omnipresent God. Thanks be to God for my life through all tests in the past three and half years. You have made my life more beautiful. May your name be exalted, honored, and glorified. for answering my prayers for giving me the strength to plod on despite my constitution wanting to give up and throw in the towel, thank you so much Dear Lord.

**Muhammad Nurul Huda**

March, 2011

Table of Contents

Chapter 1.

1-1. Introduction.....9

1-2. Polymer brush.....11

1-3. Grafting methods.....13

1-4. ATRP.....13

1-5. Components of ATRP.....15

1-6. Monomer.....15

1-7. Initiator.....15

1-8. Catalyst.....18

1-9. Solvent.....18

1-10. Poly(N-isopropylacrylamide).....18

1-11. Aim of the Experiment.....19

1-12. Reference.....21

Chapter 2

Abstract.....24

2.1. Introduction.....25

2.2. Experimental Section.....26

2.2.1. Self-Assembly of Initiator Monolayer on Silicon Wafers.....26

2.2.2. Synthesis procedure of the ATRP initiator.....30

2.2.3. ATRP of NIPA in bulk solution and on surface of ATRP initiator layer.....30

2.3. Result and discussion.....34

2.4. Conclusion.....41

References and Notes.....42

Chapter 3.

Abstract.....43

3.1. Introduction.....44

3.2. Experimental Section

3.2.1. Materials.....46

3.2.2. Synthesis of PNIPA-$N_3$.....47

3.2.3. Synthesis of PNIPA-COOH.....50

3.3. Results and discussion.....53

3.3.1. pH responsive contact angle.....56

3.4. Conclusion.....60

References and Notes.....61

Chapter 4

Abstract.....64

4.1. Introduction.....65

4.2. Experimental Section

4.2.1. Materials.....67

4.2.2. Sample Synthesis.

4.2.2.1.Preparation of [11-(2-chloro)propionyloxy]undecyl-dimethylchlorosilane

(CPU-dMCS) as Surface-Attachable ATRP Initiator.....68

4.2.2.2. Preparation of [11-(2-methyl)propionyloxy]undecyl-dimethylchlorosilane (MPU-dMCS) as an ATRP-Inactive Alkyldimethylsilane Derivative.....69

4.2.2.3. Preparation of ATRP Initiator-Deposited Silicon Wafer.....71

4.2.2.4.General Procedure for Synthesis of Grafted PNIPA from ATRP Initiator-Modified Silicon Wafers.....73
4.2.3. Characterization
4.2.3.1. XPS Analysis of monolayer.....73
4.2.3.3. Equilibrium Contact Angle Measurements.....74
4.2.3.4.Gel Permeation Chromatography (GPC).....76
4.2.3.5. $^{1}$H NMR spectroscopy.....76
4.2.3.6. Fourier Transform Infrared Spectroscopy (FT-IR).....76
4.3. Results and Discussion.....78
4.3.1. Preparation of Silicon Surface Modified with ATRP Initiator.....78
4.3.2. ATRP of NIPA for Preparation of Grafted Membrane.....85
4.3.3. Change in Thickness of High-Density Grafted Membrane of PNIPA in Water with Changing Temperature.....94
4.3.4. FT-IR to Observe Molecular Behavior of PNIPA in Grafted Membrane under Water.....96
4.3.5. Contact Angle of Air Bubble underneath PNIPA Grafted Membranes under Water.....102
4.4 Conclusions.....108
References and Notes.....110
Chapter 5
Abstract.....117
5.1. Introduction.....117

5.2. Experimental Section.....120

5.3. Self-Assembly of Initiator Monolayer on Silicon Wafers.....120

5.3.1. Synthesis procedure of the ATRP initiator.....121

5.3.2. Preparation of the Free Polymers and polymer Brushes simultaneously.....121

5.3.3. Treatment of the PNIPA Brushes by Different pH Aqueous Solution.....122

5.4. Characterization.....122

5.4.1. Fourier Transform Infrared Spectroscopy (FT-IR).....123

5.4.2. Atomic force microscopy (AFM).....123

5.5. Result and discussion.....125

5.6. Conclusion.....133

References and notes.....134

# Chapter 1

## General Introduction

## 1.1. Introduction.

Henri Braconnot's work in the 1830s is perhaps the first modern example of polymer science. Braconnot, along with Christian Schönbein and others, developed derivatives of the natural polymer cellulose producing new, semi-synthetic materials, such as celluloid and cellulose acetate. The term "polymer" was coined in 1833 by Jöns Jakob Berzelius, though Berzelius did little that would be considered polymer science in the modern sense. In the 1840s, Friedrich Ludersdorf and Nathaniel Hayward independently discovered that adding sulfur to raw natural rubber (polyisoprene) helped prevent the material from becoming sticky. In 1844 Charles Goodyear received a U.S. patent for vulcanizing rubber with sulfur and heat. Thomas Hancock had received a patent for the same process in the UK the year before. Vulcanized rubber represents the first commercially successful product of polymer research. In 1884 Hilaire de Chardonnet started the first artificial fiber plant based on regenerated cellulose, or viscose rayon, as a substitute for silk, but it was very flammable.[1] In 1907 Leo Baekeland invented the first synthetic polymer, a thermosetting phenol-formaldehyde resin called Bakelite.

Despite significant advances in polymer synthesis, the molecular nature of the polymer was not understood until the work of Hermann Staudinger in 1922. Prior to Staudinger's work, polymers were understood in terms of the association theory or aggregate theory which originated with Thomas Graham in 1861. Graham proposed that cellulose and other polymers were "colloids", aggregates of molecules small molecular mass connected by an unknown intermolecular force. Hermann Staudinger was the first to propose that polymers consisted of long chains of atoms held together by covalent bonds. It took over a decade for Staudinger's work to gain wide acceptance in the scientific community, work for which he was awarded the Nobel Prize in 1953.

The World War II era marked the emergence of a strong commercial polymer industry. The limited or restricted supply of natural materials such as silk and latex necessitated the increased production of synthetic substitutes, such as rayon and neoprene. In the intervening years, the development of advanced polymers such as Kevlar and Teflon have continued to fuel a strong and growing polymer industry.

The growth in industrial applications was mirrored by the establishment of strong academic programs and research institute. In 1946, Herman Mark established the Polymer Research Institute at Brooklyn Polytechnic, the first research facility in the United States dedicated to polymer research. Mark is also recognized as a pioneer in establishing curriculum and pedagogy for the field of polymer science.[2] In 1950, the POLY division of the American Chemical Society was formed, and has since grown to the second-largest division in this association with nearly 8,000 members. Fred W.Billmeyer, JR, a Professor of Analytical Chemistry had once said that "although the scarcity of education in polymer science is slowly diminishing but it is still evident in many areas. What is most unfortunate is that it appears to exist, not because of a lack of awareness but, rather, a lack of interest." (Source: Polymer Science, Wikipedia)

### 1.2. Polymer brush.

Polymer brush is a layer of polymers attached with one end to a surface. [3] The brushes may be either in a solvent state, when the dangling chains are submerged into a solvent, or in a melt state, when the dangling chains completely fill up the space available. Additionally, there is a separate class of polyelectrolyte brushes, when the polymer chains themselves carry an electrostatic charge.

The brushes are often characterized by the high density of grafted chains. The limited space then leads to a strong extension of the chains, and unusual properties of the system. Brushes can be used to stabilize colloids, reduce friction between surfaces, and to provide lubrication in artificial joints. [4] Polymer brushes have been modeled with Monte Carlo methods [5] or with Brownian dynamics simulations [6].

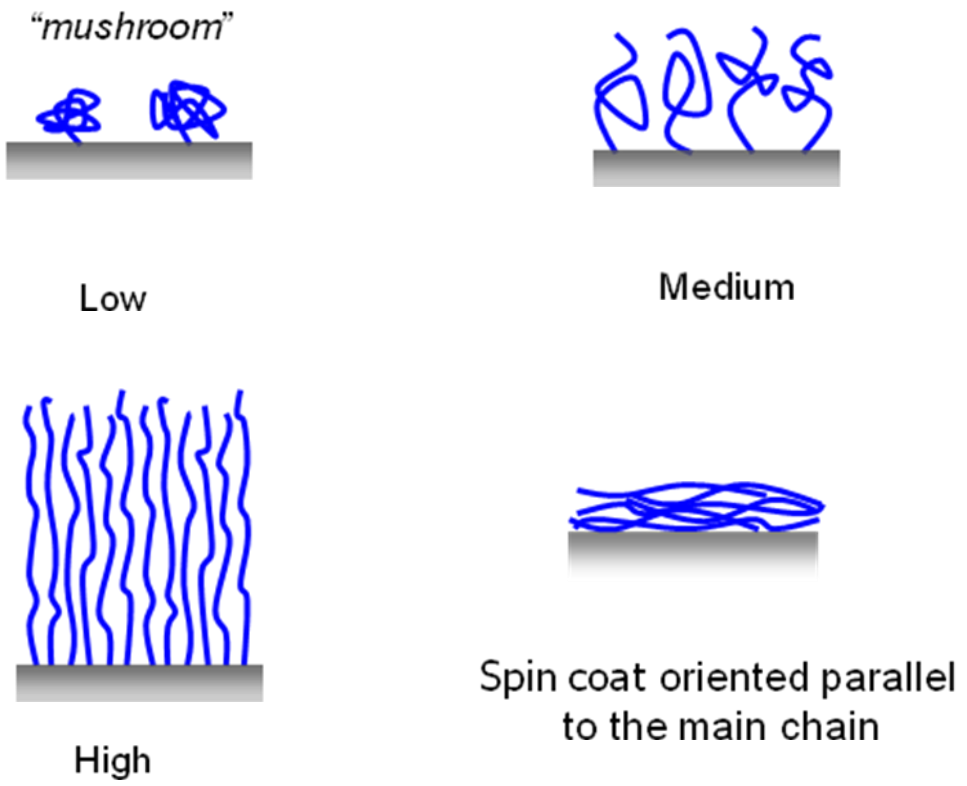


Figure 1-1: Schematic diagram of Polymer brushes with different graft densities

## 1.3. Grafting methods.

Most of these studies have focused on surface modification by means of either ‘‘grafting-to’’ or ‘‘grafting-from’’ techniques [7-14]. ‘‘Grafting-to’’ involves the bonding of a preformed end-functionalized polymer chains to the reactive surface groups on the substrate. The limitation in this technique is that the attachment of a small number of chains significantly hinders diffusion of additional polymer chains to the surface, thereby leading to very low grafting density. In the grafting-from technique, initiator species on the substrate surface are used to initiate polymerization upon exposure to a monomer solution under appropriate conditions, so that high grafting density can be achieved.

## 1.4. ATRP.

ATRP or atom transfer radical polymerization is an example of a living polymerization or a controlled/living radical polymerization (CRP). Like its counter part, ATRA or atom transfer radical addition, it is a means of forming carbon-carbon bond through transition metal catalyst. As the name implies, the atom transfer step is the key step in the reaction responsible for uniform polymer chain growth. ATRP (or transition metal-mediated living radical polymerization) was independently discovered by Mitsuo Sawamoto[15] and by Krzysztof Matyjaszewski and Jin-Shan Wang in 1995.[16] This is a typical ATRP reaction:

The uniformed polymer chain growth, which leads to low polydispersity, stems from the transition metal based catalyst. This catalyst provides an equilibrium between active, and therefore propagating, polymer and an inactive form of the polymer; known as the dormant form. Since the dormant state of the polymer is vastly preferred in this equilibrium, side reactions are suppressed. This equilibrium in turn lowers the concentration of propagating radicals, therefore suppressing unintentional termination and controlling molecular weights.

ATRP reactions are very robust in that they are tolerant of many functional groups like allyl, amino, epoxy, hydroxy and vinyl groups present in either the monomer or the initator. ATRP methods are also advantageous due to the ease of preparation, commercially available and inexpensive catalysts (copper complexes), pyridine based ligands and initiators (alkyl halides).[17]

**(a)**

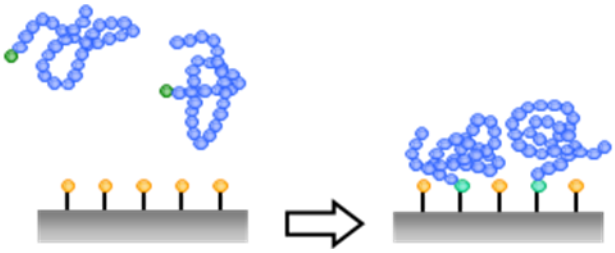

**(b)**

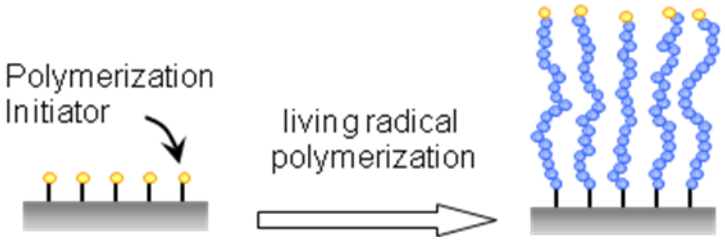


Figure 1-2: Schematic diagram of the technique of the surface modification by means of either (a) grafting-to (b) grafting-from

## 1.5. Components of ATRP.

There are five important variable components of Atom Transfer Radical Polymerizations. They are the monomer, initiator, catalyst, solvent and temperature. The following section breaks down the contributions of each component to the overall polymerization.

## 1.6. Monomer.

Monomers that are typically used in ATRP are molecules with substituents that can stabilize the propagating radicals; for example, styrenes, (meth)acrylates, (meth)acrylamides, and acrylonitrile.[18] ATRP are successful at leading to polymers of high number average molecular weight and a narrow polydispersity index when the concentration of the propagating radical balances the rate of radical termination. Yet, the propagating rate is unique to each individual monomer. Therefore, it is important that the other components of the polymerization (initiator, catalysts, ligands and solvents) are optimized in order for the concentration of the dormant species to be greater than the concentration of the propagating radical and yet not too great to slow down or halt the reaction.

## 1.7. Initiator.

The number of growing polymer chains is determined by the initiator. The faster the initiation, the fewer terminations and transfers, the more consistent the number of propagating chains leading to narrow molecular weight distributions.[19] Organic halides that are similar in the organic framework as the propagating radical are often chosen as initiators. Most initators for ATRP are alkyl halides. Alkyl halides such as alkyl bromides are more reactive than alkyl chlorides and both have good molecular weight control.[19] The shape or structure of your initiator can determine the architecture of your polymer. For example, initiators with multiple alkyl halide groups on a single core can lead to a star-like polymer shape.

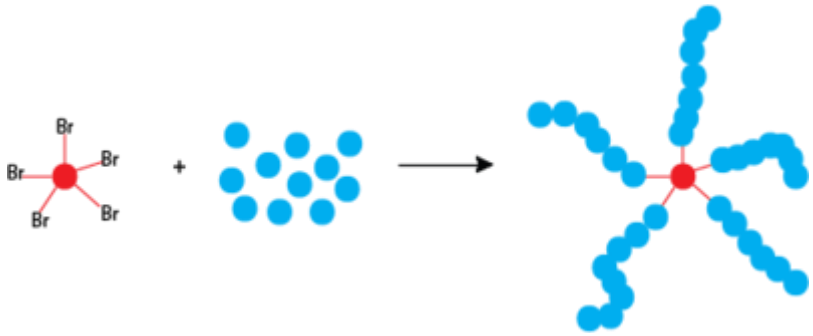


Figure 1-3: Illustration of a star initiator for ATRP

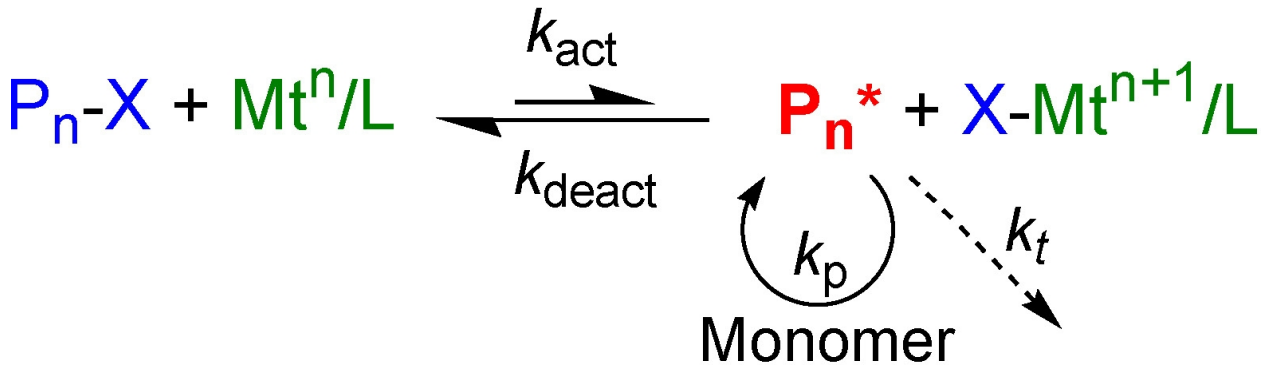


Figure 1-4:Mechanism of the Atomic Transfer Radical Polymerization method

## 1.8. Catalyst.

The catalyst is the most important component of ATRP because it determines the equilibrium constant between the active and dormant species. This equilibrium determines the polymerization rate and an equilibrium constant too small may inhibit or slow the polymerization while an equilibrium constant too large leads to a high distribution of chain lengths.[19]

There are several requirements for the metal catalyst:

1. there needs to be two accessible oxidation states that are separated by one electron
2. the metal center needs to have a reasonable affinity for halogens
3. the coordination sphere of the metal needs to be expandable when its oxidized so to be able to accommodate the halogen
4. a strong ligand complexation.

The most studied catalysts are those that polymerizations involving copper, which has shown the most versatility, showing successful polymerizations regardless of the monomer.

## 1.9. Solvent.

Toluene,1,4-dioxane, xylene, anisole, DMSO

## 1.10. **Poly(*N*-isopropylacrylamide)**.

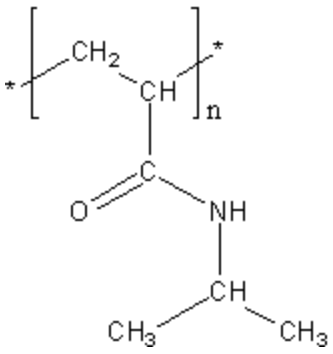


Poly(*N*-isopropylacrylamide) (variously abbreviated PNIPA, PNIPAAm, PNIPAA or PNIPAm) is a temperature-responsive polymer that was first synthesized in the 1950s.[20] It forms a three-dimensional hydrogel when crosslinked with *N,N'*-methylene-bis-acrylamide (MBAm) or *N,N'*-cystamine-bis-acrylamide (CBAm). When heated in water above 33°C, it undergoes a reversible lower critical solution temperature phase transition from a swollen hydrated state to a shrunken dehydrated state, losing about 90% of its mass. In dilute solution, it undergoes a corresponding coil-to-globule transition at similar conditions)[21]. Since PNIPAm expels its liquid contents at a temperature

near that of the human body, PNIPAm has been investigated by many researchers for possible applications in controlled drug delivery.[22-24]

### 1.11. **Aim of the Experiment.**

The surface initiated ATRP of NIPA onto a silicon wafer and Au-deposited mica has been reported, but in many cases, the authors do not give molecular weight and polydispersity data. [25-32] Judging by our additional examinations, many cases of surface-initiated ATRP of NIPA on a flattened surface such as silicon, the thickness of the grafted PNIPA membranes cannot be well-controlled according to the living polymerization system. Moreover, the densities of the grafted PNIPA membranes are in diluted or semi-diluted regions, and as a result, the intermolecular interaction between grafted polymers is not significant due to the poor choice of the polymerization systems. But Well defined polymer brushes are used for making materials with surfaces that have been designed on the nanoscale. Well controlled PNIPA is also used for cell sheet engineering (figure 1-5). For the preparation of cell sheets, the surface must be hydrophobic around the cultivation temperature, i.e., 37 $^{o}$C, and hydrophilic below the LCST. As a result, the cell sheets cultured at 37 $^{o}$C that are useful for tissue engineering are safely isolated from the membranes below the LCST. So aim of this study is to synthesis PNIPA grafted membrane on silicon surface by ATRP and precisely controlled their chain length and graft density, examination of the effect of chain-length and graft density on the surface characteristics, check the change of the wettability at hydration state in the polymer and finally check the stimuli responsive behavior of PNIPA grafted membrane on silicon surface. ATRP is attractive because it can provide good control over predictable polymer molecular weight, PDI and end groups as long as the conditions are suitable.

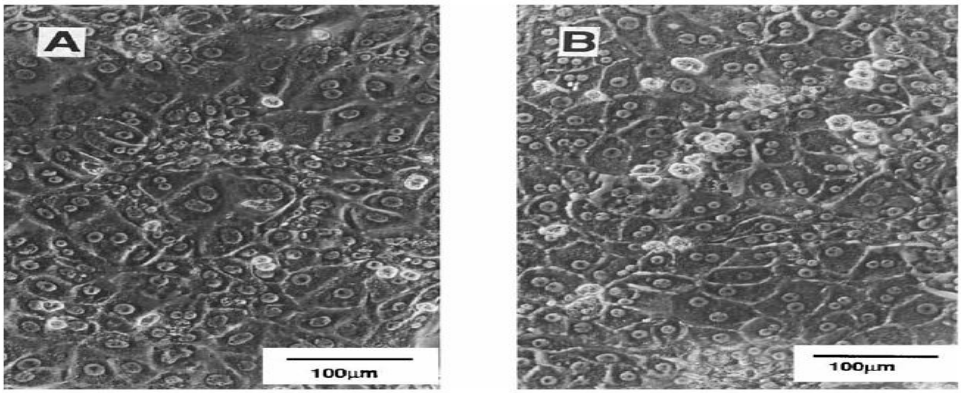


Phase-contrast photographs of rat primary hepatocytes cultured on PIPAAm-grafted (A) and control B) dishes. Rat primary hepatocytes were cultured for 4 days

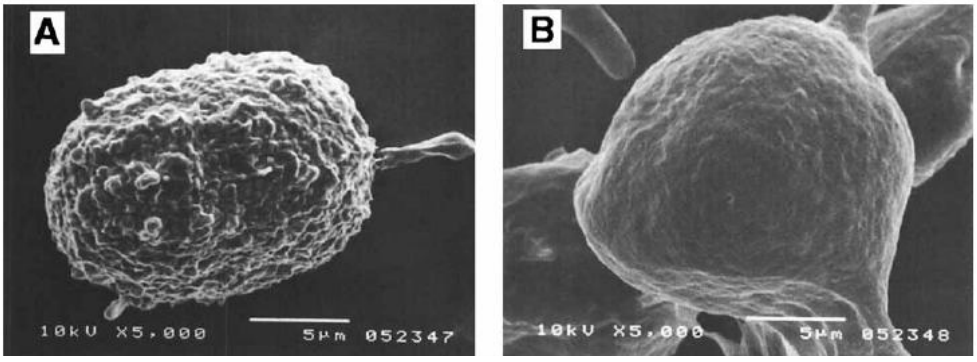


Scanning electron micrographs of hepatocytes recovered by low temperature treatment (A) and trypsin treatment (B).

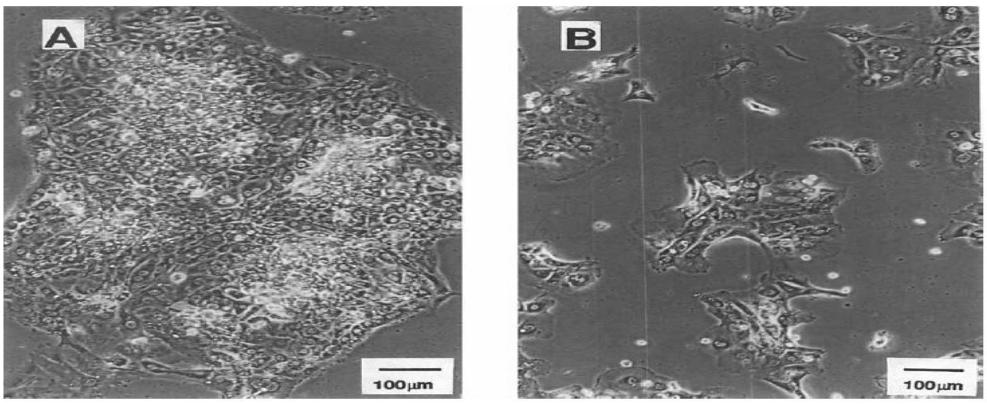


Phase-contrast micrographs of hepatocytes subcultured by low temperature treatment (A) and trypsin treatment *(8).* Primary hepatocytes were recovered by low temperature treatment from the PIPAAm-grafted dish and by trypsin treatment from the control dish. The recovered hepatocytes were subcultured for 3 days on control dishes.

**Figure 1-5:** Application of PNIPA gel. (Journal of Biomedical Materials Research, Vol. 27, 1243-1251 (1993))

**References and notes.**


1. Plastiquarian
2. "Polymer Research Institute". *National Historical Chemical Landmarks*. http://acswebcontent.acs.org/landmarks/landmarks/polymer/pol_1.html. Retrieved 2007-11-07.
3. Milner, S. T. Science 1991, 251, 905.
4. Halperin, A.; Tirrel, M.; Lodge, T. P. Adv. Polym. Sci. 1991, 100, 31.
5. Laradji, M; Guo, H.; Zuckermann, M. P.
6. Kaznessis, Y.N.; Hill, D.; Maginn, E.D. Macromolecules 1998, 31, 3116-3129
7. Mansky P, Liu Y, Huang E, Russell TP, Hawker CJ. Science 1997; 275:1458.
8. Geng Y, Discher DE, Justynska J, Schlaad H. Angew Chem Int Ed 2006; 45:7578.
9. Joester D, Klein E, Geiger B, Addadi L. J Am Chem Soc 2006;128:1119.
10. Choi WS, Park JH, Koo HY, Kim JY, Cho BK, Kim DY. Angew Chem Int Ed 2005;44:1096.
11. Ulbricht M, Yang H. Chem Mater 2005;17:2622.
12. Parrish B, Breitenkamp RB, Emrick T. J Am Chem Soc 2005;127: 7404.
13. Buga K, Majkowska A, Pokrop R, Zagorska M, Djurado D, Pron A, et al. Chem Mater 2005;17:5754.
14. Brack HP, Padeste C, Slaski M, Alkan S, Solak HH. J Am Chem Soc, 2004;126:1004.
15. Kato, M; Kamigaito, M; Sawamoto, M; Higashimura, T, *Macromolecules* 28: 1721–1723. doi:10.1021/ma00109a056.
16. Wang, J; Matyjaszewski, K , *J. Am. Chem. Soc*. 117: 5614–5615. doi:10.1021/ja00125a035.
17. Matyjaszewski, K. Fundamentals of ATRP Research (accessed 01/07, 2009).
18. Patten, T. E; Matyjaszewski, K (1998). *Adv. Mater*. 10: 901. doi:10.1002/(SICI)1521-4095(199808)10:12<901::AID-ADMA901>3.0.CO;2-B
19. Matyjaszewski, K; Xia, J (2001). "Atom Transfer Radical Polymerization". *Chem. Rev.* 101 (9): 2921–2990. doi:10.1021/cr940534g. ISSN 0009-2665. PMID 11749397.
20. Schild, H. G., 1992, 17 (2), 163–249.
21. Wu, C; Wang X (1998). *Physical Review Letters* **80** (18): 4092-4094.

22. Chung, J. E.; Yokoyama, M.; Yamato, M.; Aoyagi, T.; Sakurai, Y.; Okano, Journal of Controlled Release, 1999, 62, 115–127.
23. Hu Yan and Kaoru Tsujii. "Potential application of poly(N-isopropylacrylamide) gel containing polymeric micelles to drug delivery systems" Colloids and Surfaces B: Biointerfaces. 2005, 46, 142–146.
24. Antunes F. , Gentile L. , Tavano L. , Oliviero Rossi C. , " Rheological characterization of the thermal gelation of poly(N-isopropylacrylamide) and poly(N-isopropylacrylamide)co-Acrylic Acid". Applied Rheology, 2009, Vol. 19, n. 4, pp. 42064-42069.
25. Wang, S. Q.; Zhu, Y. X. Langmuir 2009, 25 (23), 13448–13455.
26. Teodorescu, M.; Matyjaszewski, K. Macromolecules 1999, 32 (15), 4826–4831.
27. Rademacher, J. T.; Baum, R.; Pallack, M. E.; Brittain, W. J.; Simonsick, W. J. Macromolecules 2000, 33 (2), 284–288.
28. Bontempo, D.; Li, R. C.; Ly, T.; Brubaker, C. E.; Maynard, H. D. Chem. Commun. 2005, No. 37, 4702–4704.
29. Xu, J.; Ye, J.; Liu, S. Y. Macromolecules 2007, 40 (25), 9103–9110.
30. Masci, G.; Giacomelli, L.; Crescenzi, V. Macromol. Rapid Commun. 2004, 25 (4), 559–564.
31. Millard, P.-E.;Mougin, N. C.;B€oker,A.;M€uller,A.H.E. Controlled/ Living Radical Polymerization: Progress in ATRP; Matyjaszewski, K., Ed.; ACS Symposum Series; American Chemical Society: Washington, DC, 2009; pp 127-137.
32. Jonas, A. M.; Glinel, K.; Oren, R.; Nysten, B.; Huck, W. T. S.

# Chapter 2

## Characteristics of High-Density Poly(N-isopropylacrylamide) (PNIPA) Brushes on Silicon Surface by Atom Transfer Radical Polymerization

## 2.1. Abstract.

High-density poly(*N*-isopropylacrylamide) (PNIPA) brushes were synthesized on silicon surfaces by surface initiated ATRP at various polymerization conditions. Polymerization was achieved using CuCl/tris(2-(dimethylamino)ethyl)amine ($Me_6$TREN) as a catalytic system in DMSO at 20$^{o}$C. The linear evolution of number average molecular weight ($M_n$) versus monomer conversion, the increase in layer thickness with polymerization time and relatively low molecular weight distribution (~ 1.2) indicate a well-controlled manner of polymerization. The average value of grafting density of PNIPA brushes was around 0.48 chain/nm$^2$: We obtained high-density PNIPA brushes. During the measurement of air bubble contact angle under the surface of the PNIPA brushes in water, the surface property of PNIPA brushes shows an interesting phenomenon, which is antithetic to that of typical PNIPA gel. With the increase of temperature from 10°C, the surfaces of the PNIPA brushes gradually change to more hydrophobic natures. But as temperature approaches the LCST, the brush surfaces turned back to hydrophilic state. This might be the effect of the change in the surface morphology of the polymer brushes and/or the change in physical state of the terminal end groups of the polymer, depending on temperature.

Keywords: atom-transfer radical polymerization (ATRP); monolayers; polymer brushes; surface-initiated polymerization.

## 2.1. INTRODUCTION.

Atom transfer radical polymerization (ATRP) is one of the attractive and versatile controlled or living radical polymerization techniques. A variety of monomer can be used, and the polymerization can be performed in bulk solutions and at surfaces to obtain a wide variety of functional materials. For designing "intelligent" materials that are sensitive to the change in environments, poly(*N*-isopropylacrylamide) (PNIPA) has a great interest as a thermo-sensitive polymer. It has a lower critical solution temperature (LCST) at ~32$^{o}$C in water, between room temperature and physiological temperature.[1-4] Below its LCST, the linear polymer in aqueous solution is in a random coil conformation. However, when the temperature is above the LCST, the linear polymer chains undergo a sharp phase transition, forming a collapsed globule state. A sharp change in the solubility of polymer chains in water is thus triggered by a moderate temperature stimulus. As a result of this property, thermoresponsive surfaces based on PNIPA covalently bounded on solid surfaces have been developed for various applications.[5-7] Thermoresponsive surfaces with temperature responsive properties are most important among smart surfaces since temperature can be easily controlled as a stimulant. By applying external stimuli (e.g. adhesion, wettability, friction, roughness, reactivity, biocompatibility, selectivity etc.) on "smart" materials, it switch and/or tune the properties of the coatings.[15] That's the reason for developing many thermoresponsive surfaces.[7] Naturally hydrophobic interactions are thermodynamic in nature. If water structure forms around hydrophobic groups, gained entropy is reduced by accomplishing hydrophobic species.[16] To study alteration of polymer brushes few research groups used AFM method and presumed if temperature raised over LCST brush thickness will decrease. Most of the controlled radical polymerization reactions at surfaces so far have been carried out at fairly elevated temperatures, mostly between 90 and 1208C. Polymerization at lower temperature would have several advantages: Firstly, such processes would be compatible with substrates that are sensitive to elevated temperatures. Additionally, spontaneous thermal polymerization and other side reactions, such as transesterification reactions, elimination reactions and thermal crosslinking, occurring in systems with sensitive monomers will be less likely. Accordingly, lower polymerization temperatures could lead to a better control of the polymerization reaction and improve the structural homogeneity of the grafted films.The

polymer-grafted surfaces can be prepared by "grafting to" or "grafting from" method. [8] Comparing to the "grafting to" method, high-density polymer grafted membrane, so-called "polymer brush", with well-controlled structure can be synthesized by the "grafting from" method. [9-12] In this work, we synthesized high-density polymer brushes of PNIPA on silicon surface by the "grafting from" method using [11-(2-chloro)propionyloxy]undecyl-dimethylchlorosilane modified silicon and propargyl 2-chloropropionate/CuCl/$Me_6$TREN (1:1:1) as the initiating system at 20°C and examined the kinetics of the ATRP system and the static structure of the resultant grafted membrane. Through variation of reaction time of polymerization, we showed that how the reaction time influenced the polymerization kinetics, evolution of number average molecular weight, $M_n$, molecular weight distribution, $M_w/M_n$, and the distinctive properties of the grafted membrane. Here we successfully showed that, ATRP of NIPA on silicon surface was precisely controlled to demonstrate a chain length of PNIPA as well as graft density. We also found a very interesting thermo-sensitivity of the PNIPA grafted membrane.

## 2.2. EXPERIMENTAL SECTION.

### 2.2.1. Self-Assembly of Initiator Monolayer on Silicon Wafers. [13]

The surface-attachable ATRP initiator ([11-(2-chloro)propionyloxy]undecyl-dimethylchlorosilane, CPU-dMCS), was synthesized by the hydrosilylation of 10-undecen-1-yl 2-chloropropionate with chlorodimethylsilane in the presence of Karsted catalyst at room temperature for 6 hours (Figure2-1). 10-undecen-1-yl 2-chloropropionate was synthesized by a substitution chloride in the presence of triethylamine in dry-THF. 100 μl CPU-dMCS as a silane coupling solution was added into 100ml dry toluene in a glove box. Treated silicon wafers were then immersed into the silane coupling solution and were kept into a thermostat chamber at 60 $^oC$ for 84 hours to form a self-assembled initiator monolayer. The surface modified silicon wafers were then removed from solution and ultrasonically cleaned by dry toluene, rinsed sequentially with toluene and methanol, and then dried through an argon stream. The successful synthesizes of the ATRP initiator layer was verified by X-ray photoelectron spectroscopy (XPS).

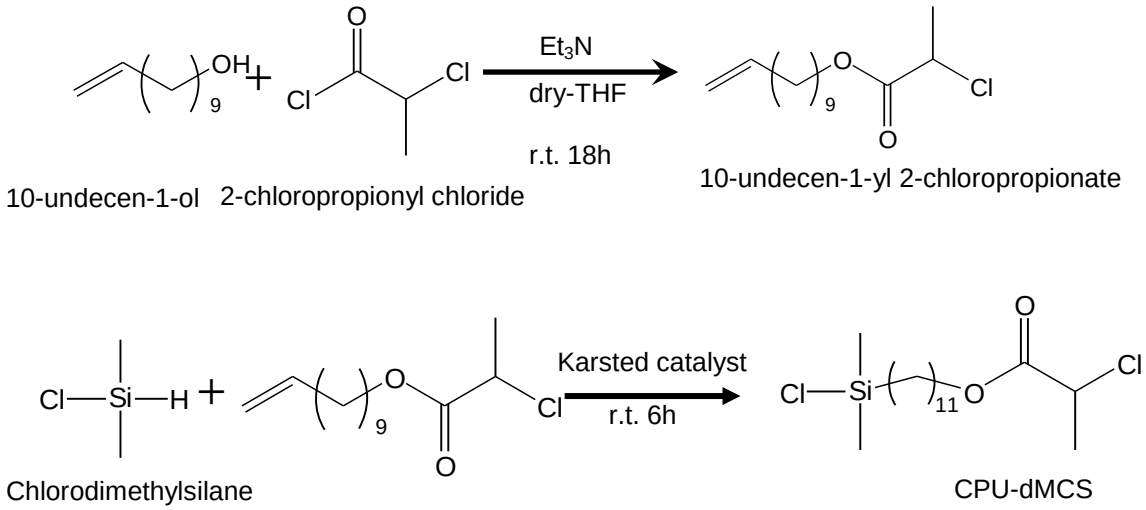


**Figure 2-1:** Synthetic route of [11-(2-Chloro)propionyloxy] undecyldimethylchlorosilane *CPU-dMCS*

.

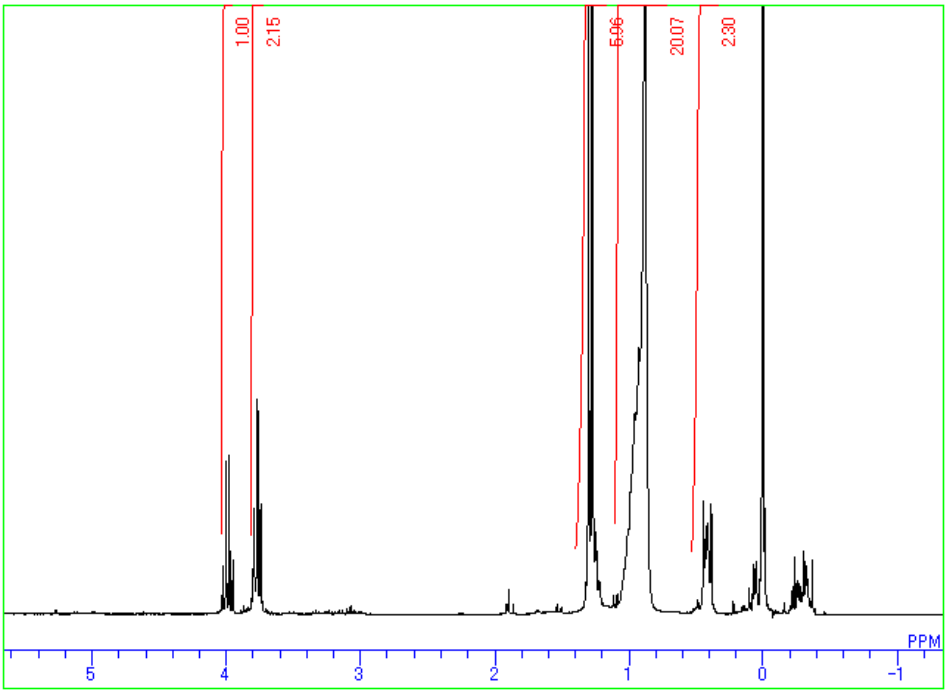


**Figure 2-2:** $^{1}H$ NMR spectrum of 11-(2-Chloro)propionyloxy] undecyldimethylchlorosilane *CPU-dMCS*

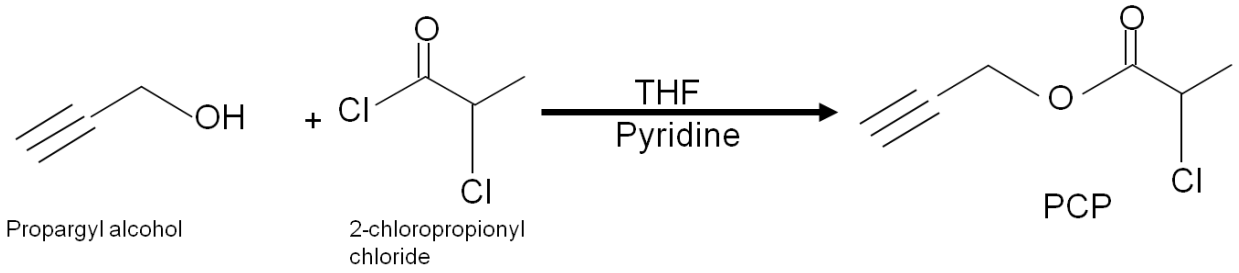


**Figure 2-3 (a):**Synthesis route for the ATRP initiator Propargyl 2-chloropropionate (PCP)

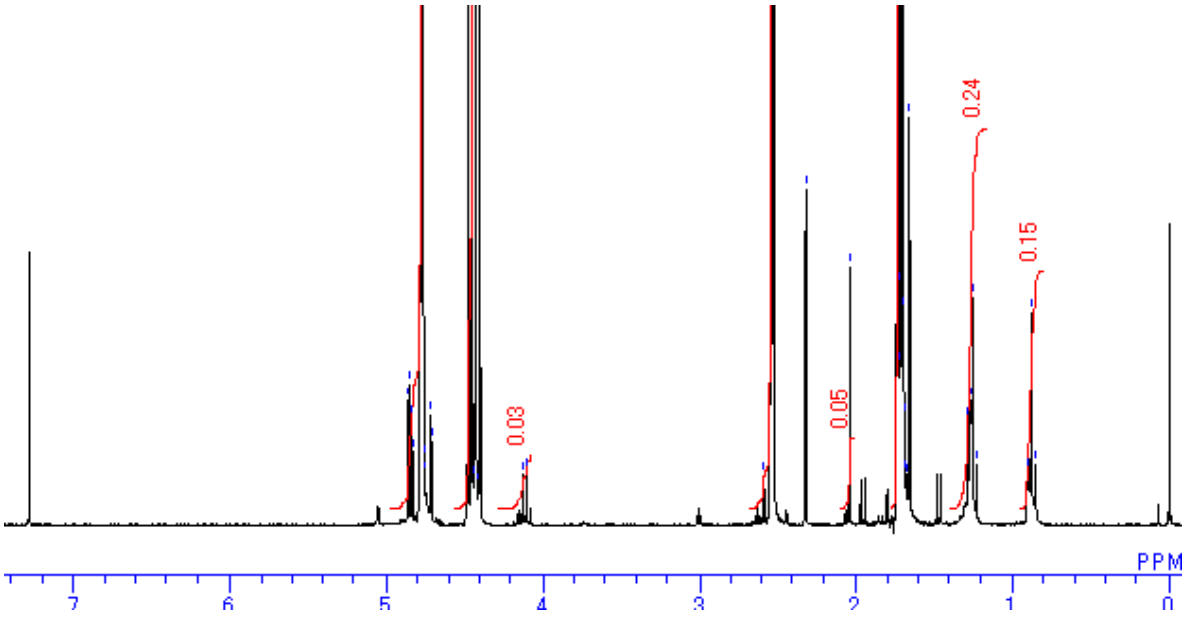


**Figure 2-3 (b):** NMR spectrum of Propargyl 2 chloropropionate (PCP)

### 2.2.2. Synthesis procedure of the ATRP initiator.

Propargyl 2-chloropropionate (PCP) was used as a free ATRP initiator. PCP was synthesized by an esterification reaction of propargyl alcohol with 2-chloropropionyl chloride in presence of dry trimethyl amine and THF (Figure 2-3 (a)). A typical procedure was as follow.

Air was removed from a 250 ml round –bottom flask by freeze/pump/thaw cycle and the flask was charged with trimethyl amine (1.98ml), propargyl alcohol (1.98 ml) and dry THF (40 ml). The reaction mixture was cooled to 0 $^{o}$C in an ice-water bath. 2-chloropropionyl chloride (3.37 ml) was added dropwise over a period of 1hour under continuous magnetic stirring. Then the mixture was stirred at 0 $^{o}$C for 1 hour and at room temperature whole night. The mixture was diluted with n-hexane (equivalent amount of THF volume) and washed with 10% HCl solution, $NaHCO_3$, brine and miliQ water. To remove water from the mixture, dried $MgSO_4$ was added and kept it over night. After removing $MgSO_4$ by filtration, the filtrate was concentrated and then further purified by silica gel column chromatography using a mixture of n-hexane: ethyl acetate = 9:1 as the eluent. Then the solvent was removed by rotary evaporator and residue was distilled under reduced pressure. A colorless liquid was obtained with 74% yield. $^{1}$H NMR (Figure 2-3 (b)) ($CDCl_3$, δ, ppm): 4.86 (2H, -C*H*$_2$O-), 4.42 (H, -C*H*Cl-), 2.53 (H, -C≡C*H*), and 1.695 (3H, -C*H*$_3$).

### 2.2.3 ATRP of NIPA in bulk solution and on surface of ATRP initiator layer.

Scheme 2-4 shows the preparation of PNIPA brushes on silicon surface. Formation of self-assembled monolayer was discussed above. The polymerization was carried out as follows: A Schlenk tube was charged with NIPA (1.65 gm,) as a monomer. 3ml dimethylsulfoxide (DMSO) was added with monomer inside glove box. The solution was degassed by three consecutive freeze/pump/thaw cycles and backfilled with nitrogen gas (procedure repeated three times). Then the tube was again charged with copper chloride (3.6 mg,), $Me_6$TREN (10.03 µl,) and PCP (3.6 µl). A silicon substrate with self-assembled monolayer was inserted into the solution of the tube very carefully under a nitrogen atmosphere. The tube was then sealed with stopper by using aboratory film paper. The grafting process was carried out at 20 $^{o}$C with continuous shaking by a shaker (Model: EYELA, NTS-4000) at different pre-planned time. After desired time period

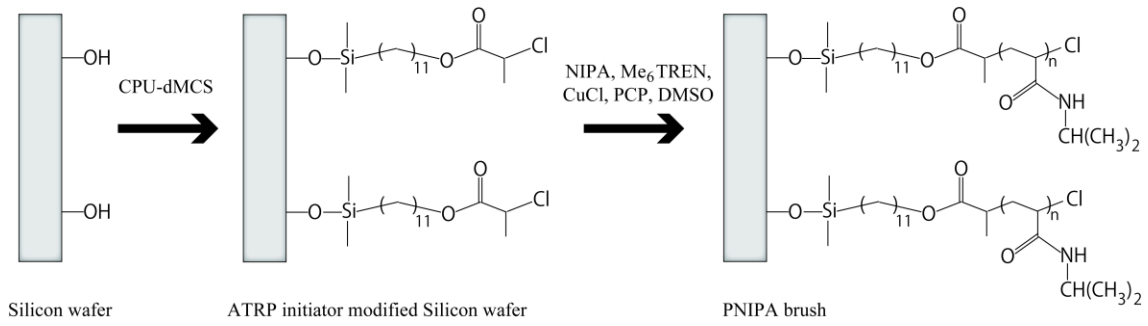


**Figure 2-4:** Schematic procedure for preparation of PNIPA brush on silicon wafer

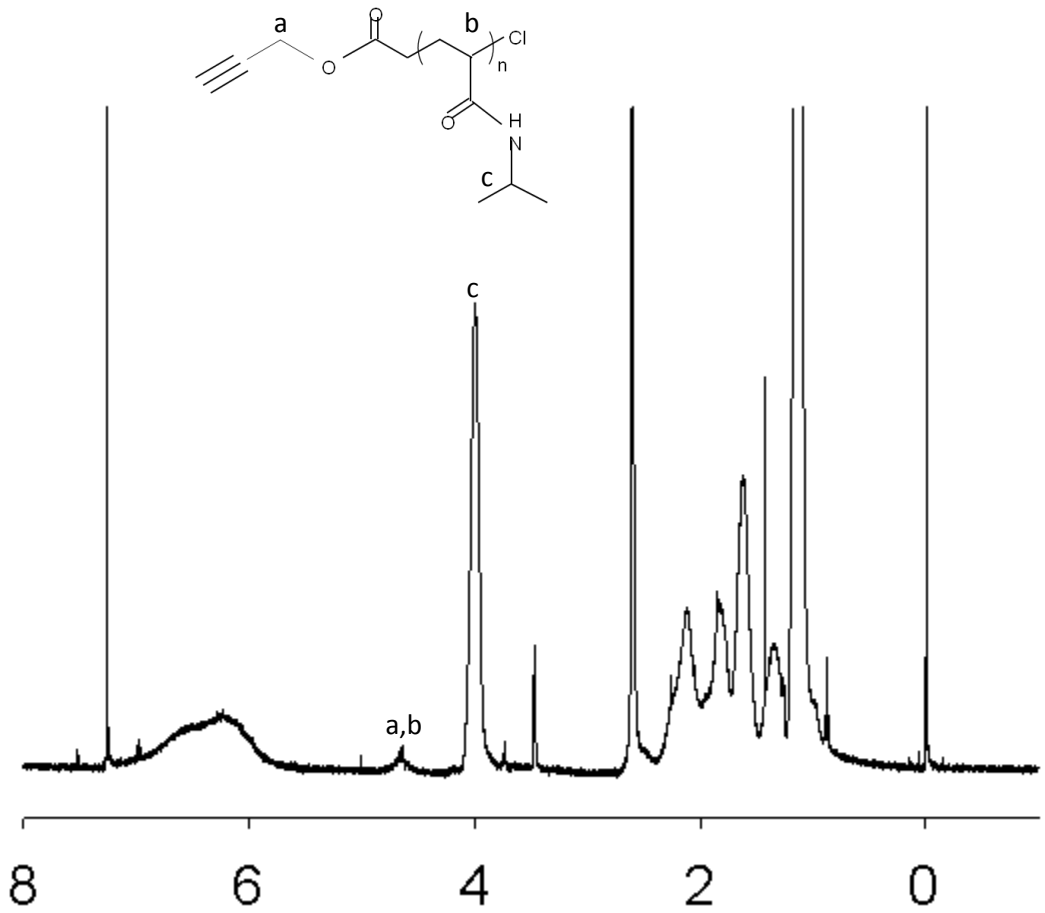


**Figure 2-5:** $^{1}H$ NMR spectrum of Poly(*N*-isopropylacrylamide) (PNIPA)

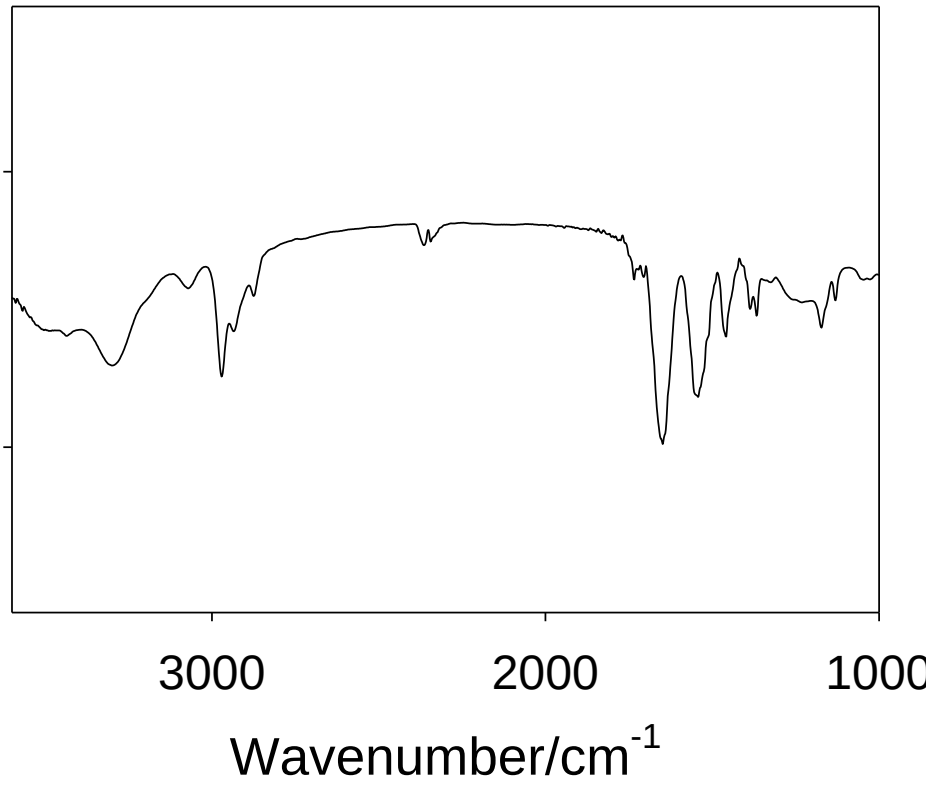


**Figure 2-6:** FT-IR spectra of PNIPA-Cl cast film.

the tube was exposed to air to terminate the polymerization. The collected eluents were concentrated and precipitated into an excess of hexane. Monomer conversions were observed by $^1$H NMR based on integration areas. At resonance peak 4.0 ppm was considered as NIPA monomer and PNIPA, the integration factor was assented to 1 and the resonance peak 6.0-6.4 ppm (vinyl portion of NIPA) as monomer. By GPC analysis number average molecular weight, $M_n$ and molecular weight distribution, $M_w/M_n$, were obtained. Thickness of the grafted membrane were measured by a multimode, Nanoscope IIIa controller (Digital Instruments, Santa Barbara, CA) equipped with an atomic head of 100×100 $\mu m^2$ scan range. Measurements were done in the air by contact mode using a commercially manufactured V-shaped silicon nitride ($Si_3N_4$) cantilever with gold on the back for laser beam reflection (Nanopics 2100, NPX2100). Air bubble contact angle measurements were made with a Data Physics telescopic goniometer with a Hamilton syringe with a flat-tipped needle. Water was used as the probe liquid.

## 2.3. RESULT AND DISCUSSION.

ATRP of NIPA on the silicon surface was accomplished in presence of a free initiator, CuCl/$Me_6$TREN system, and DMSO as a solvent, because the polymerization without the free initiator will give free polymers with $M_n$ values independent of monomer conversion and high molecular weight distribution ($M_w/M_n$ > 3). During the polymerization without a free initiator, the concentration of the $Cu^{II}$ complex produced from the reaction at the substrate surface is too low to reversibly deactivate $P^{\cdot}$, which is the propagating radical produced by the halogen atom (X) transfer from P-X to $Cu^{I}$ complex, with a sufficiently high rate. Thus, during polymerization reaction a minimum amount of deactivator is required to control the surface initiator of ATRP. On the other hand, the additional initiator would increase and adjust the concentration of $Cu^{II}$ complex as in a free ATRP system. Alternatively, the adjustment of the $Cu^{II}$ concentration could be made by directly adding an appropriate amount of $Cu^{II}$ complex. Another advantage of the addition of the free initiator is that it produces free polymers, which can be used for the measurement of molecular weight and molecular weight distribution of the graft chains, because the graft chains have nearly the same molecular weight and molecular weight distribution as the

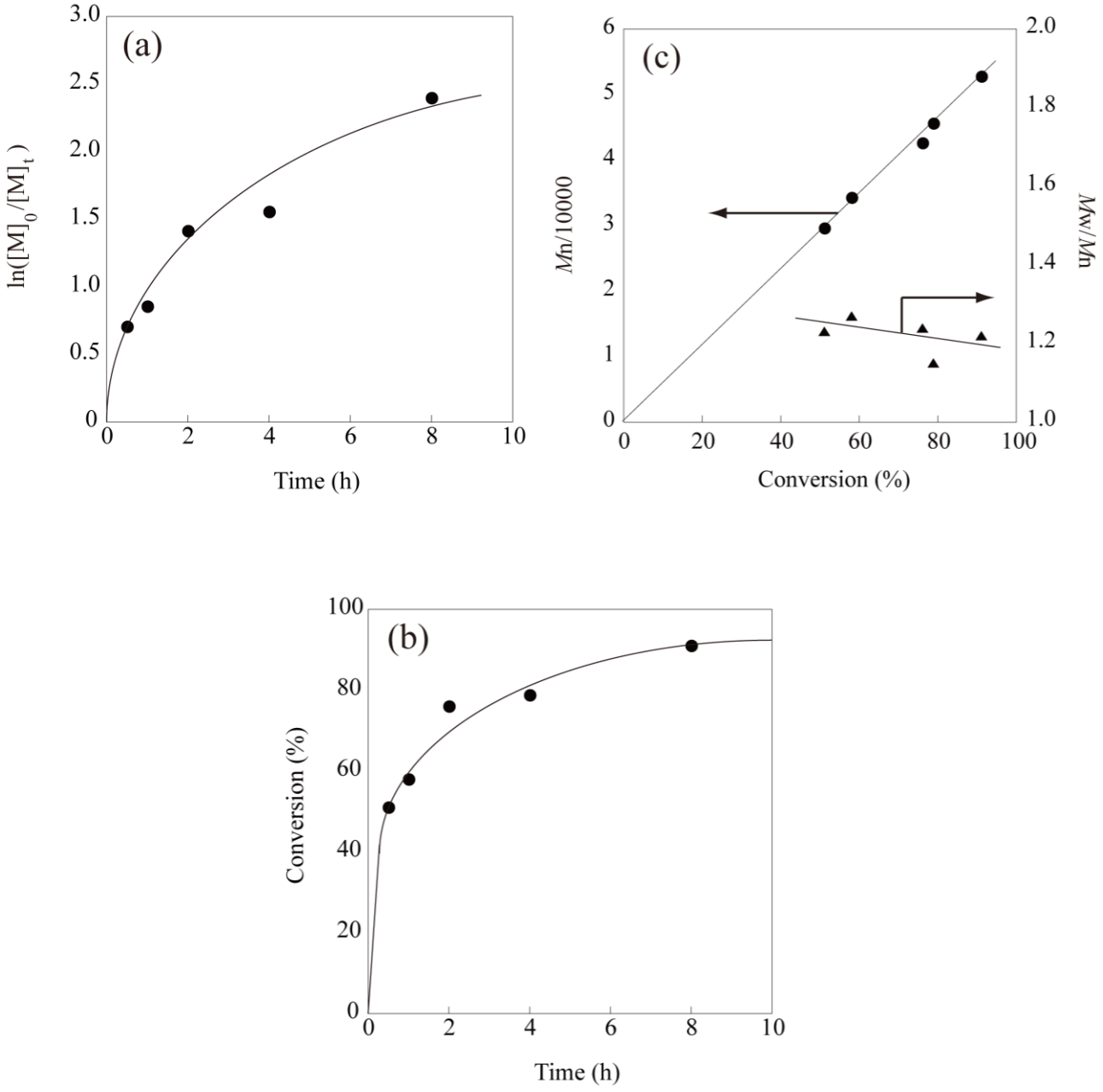


**Figure 2-7:** (a) First order kinetic plot for ATRP of NIPA in DMSO at 20°C. (b) Monomer conversion vs time curve for ATRP of NIPA in DMSO at 20°C. (c) Dependence of molecular weight and polydispersity on conversion.

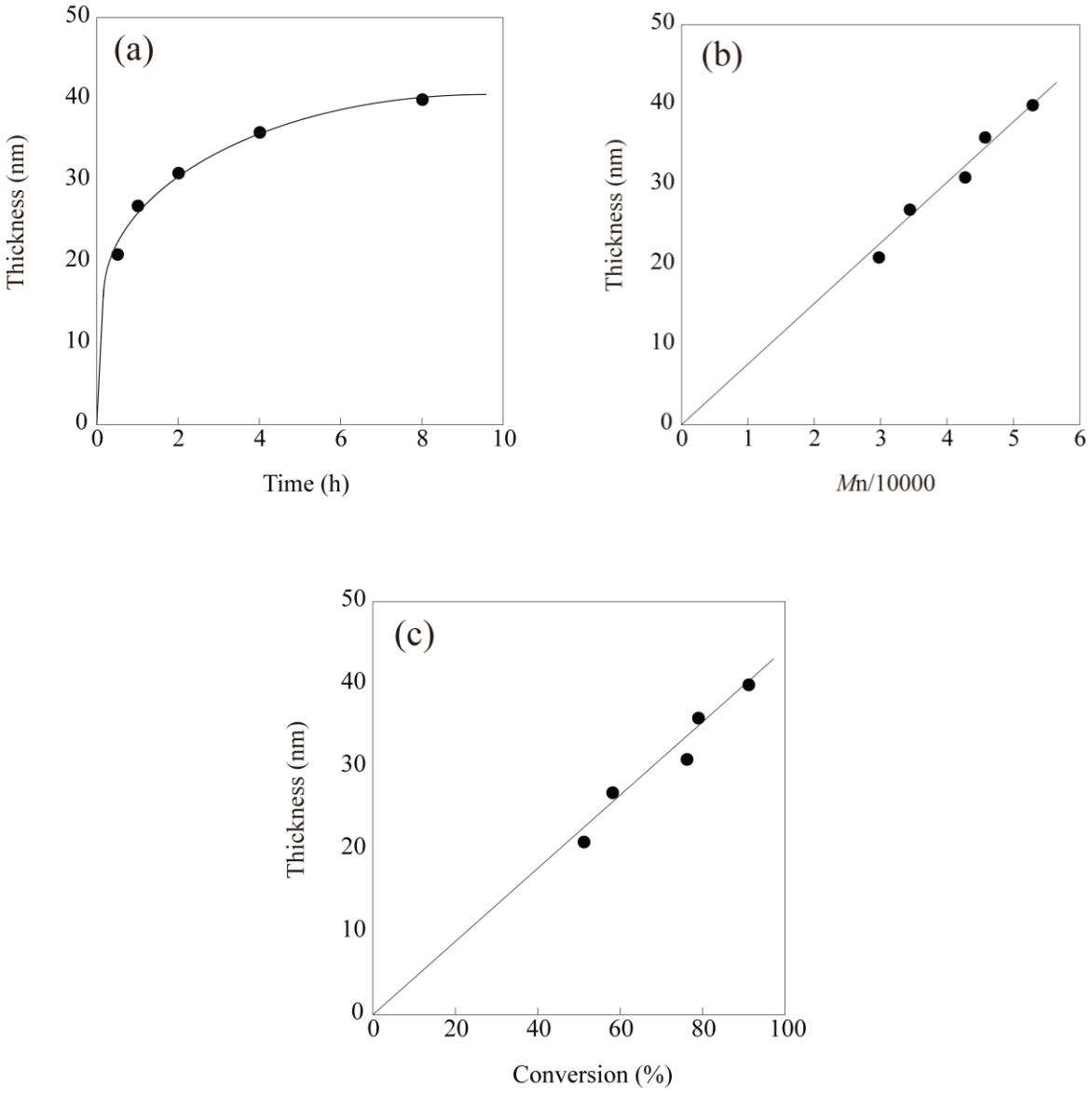


**Figure 2-8:** (a) Thickness of PNIPA brush vs time. (b) Thickness of PNIPA brush vs molecular weight of PNIPA. (c) Thickness of PNIPA brush vs monomer conversion.

free polymers. We performed polymerization reaction by varying polymerization time from 30 minutes to 8 hours keeping the temperature constant at 20 $^{o}$C.

The kinetic plot in Figure 2-7 for reaction that was carried out in DMSO shows curvature, which usually indicates (1) the presence of termination reactions caused by the increase in the amount of $CuCl_2$, (2) the deactivation of CuCl by the commingling of oxygen, or (3) the increase in the reaction kinetics by heat of reaction. If the curvature of the kinetic plot is caused by the case of (1), some tailing could be seen in the molecular weight peak in the GPC chromatogram, suggesting small amounts of dead chains. As, however, our obtained GPC chromatograms were symmetric curves, this concern will be swept aside. Since the final solutions turn to bluish tinge, the curvature of the kinetic plot could be due to a progressive reduction of the concentration of the available catalyst, i.e. by (2). The increase in the reaction kinetics by heat of reaction may be also important factor. The conversion approaches to 100 % with time (Figure 2-7 (b)). The molecular weight data are plotted in Figure 2-7 (c) molecular weights increased lineally, passing through the origin. The molecular weight distributions, which are relatively low, slightly decrease but nearly constant of approximately 1.2 with the conversion (Figure 2-7 (c)). These indicate that the number of polymer chains kept constant during the polymerization and the polymerization process is controlled with a negligible contribution of transfer and termination reactions. As the number of initiator is larger in solution polymerization than that of surface polymerization, termination could be less important in solution polymerization. Polymer growth is limited to a thin layer near surface and polymerization from the surface should be homogeneous. By repeated rinsing the membranes with solvents, we confirmed that the polymer chains were not physically adsorbed onto the membranes. The thickness of the polymer membranes, which were determined by AFM Nanopics imaging across the scratch boundary, is plotted against the polymerization time in Figure 2-8 (a). The layer thickness increased with polymerization time. As the molecular weight of the polymer grafted on the substrate should be correlated to that of the free polymer produced in the solution, the thickness was plotted against $M_n$ of the free polymer. The relationship between the thickness of the polymer layer grown from the surface and the $M_n$ of the free polymer chains is plotted in Figure 2-8 (b). A linear increase in the thickness with chain length was observed, indicating the chain growth from the surface is a controlled process with a degree of living character to it and that the thickness of the membrane,

which corresponds to the chain length, can be easily manipulated. The living nature was also probed by examining the relation between conversion and the thickness (Figure 2-8 (c)). These observations demonstrate that the growth of the polymer chains in the solution and from the surface is a living or controlled process.

From the data in Figure 2-8 (b), graft density, $\sigma$, can be determined from the molecular weight of the polymer chain, $M_n$, and the corresponding membrane thickness, $L$, by the equation,[14]

$$\sigma = L\rho N_A/M_n$$

where $\rho$ is the mass density of PNIPA (1.042 g/cm$^3$) and $N_A$ is Avogadro's number. The values of $\sigma$ for all samples are listed in Table I.

Table I. Values of graft density of the

| Reaction time (h) | 0.5 | 1 | 2 | 4 | 8 |
|---|---|---|---|---|---|
| $\sigma$ (chain/nm$^2$) | 0.45 | 0.5 | 0.46 | 0.5 | 0.48 |

The graft densities varied within a range from 0.45 to 0.5 chain/nm$^2$, where polymer chains behave as extended brushes, meaning that polymer chains are highly extended states regardless of the polymerization time.

To determine the behavior of thermo-sensitive wettability of the PNIPA brushes, contact angle must be one of the effective analytical methods. Static contact angle of air bubble under the polymer brushes of different samples as a function of temperature is shown in Figure 2-9. In the case of all five samples with different thickness, trend of the curve is almost the same. With

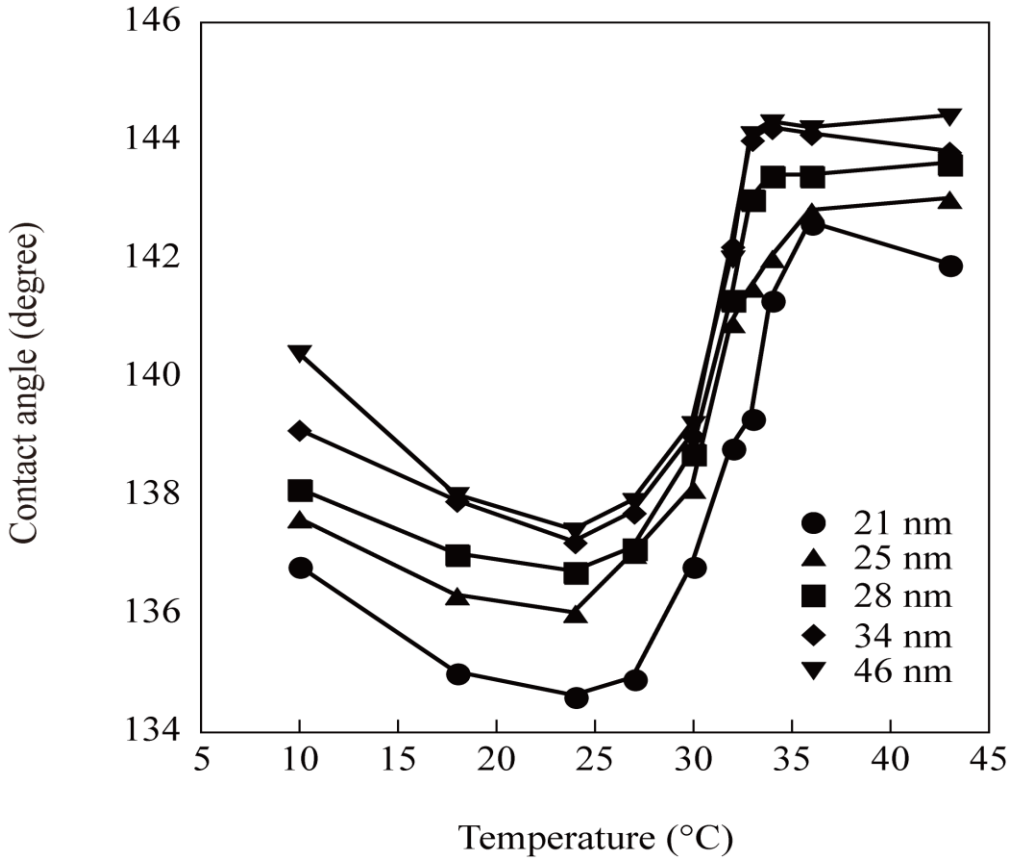


**Figure 2-9:** Contact angles of air bubble under PNIPA brushes with different thickness in water as a function of temperature.

increasing temperature, the contact angles of air bubble under the polymer brush samples gradually decrease up to around LCST. From around LCST, the values of the contact angles start to increase dramatically and become constant over 40 $^{o}$C. But in the case of typical PNIPA gels, with increasing temperature, the contact angle of air bubble moderately decreases bellow LCST and rapidly decrease at around LCST, followed by a slight decrease at the higher temperature.[15] Thus, it may indicate that, the morphology of the PNIPA brush surface differs from that of typical PNIPA gel surface. Moreover, the terminal chloride group of the polymer chain may affect the surface property of the high-density polymer brushes. To have a clear explanation about the matter, a more detail analysis needs to be carried out.

## 2.4. CONCLUSION.

A detailed explanation about the influence of reaction time variation on surface initiated polymerization of PNIPA on silicon surface is discussed. PNIPA polymer is strongly bonded on the surface of silicon wafer and is able to extent on it even at strong condition without loss of chain. The polymerization was carried out in a controlled way as affirmed the narrow molecular weight distributions of the grafted PNIPA chain. We also found a very interesting thermo-sensitivity of the PNIPA grafted membrane, which is antithetic to that of typical PNIPA gel. Additionally, the procedure is very simple to implement as the necessary reagents are readily available and no complicated synthesis is required.

**References and Notes.**


[1] Heskins, M.; Guillet, J. E. *J. Macromol. Sci., Chem.* **A2**, 1441-1455 (1968).

[2] Schild, H. G. *Prog. Polym. Sci.* **17**, 163-249 (1992).

[3] Chen, G.; Hoffman, A. S. *Nature (London)*, **373**, 49-52 (1995).

[4] Hay, D. N. T.; Rickert, P. G.; Seifert, S.; Firestone, M. A. *J. Am. Chem. Soc.*, ***126,*** 2290-2291 (2004).

[5] Xiang, G.; Norbert, K.; Heather, S. *Langmuir*, **25**, 10271-10278 (2009).

[6] Dai, X.; Zhou, F. ; Khan, N. ; Huck, W. T.S. ; Kaminski, C. F. *Langmuir*, **24**, 13182-13185 (2008).

[7]Zhou, F.; Huck, W. T. S. *Phys. Chem. Chem. Phys.*, **8**, 3815-3823 ( 2006).

[8] Pyun, J.; Kowalewski, T.; Matyjaszewski, K. *Macromol. Rapid Commun.*, **24**, 1043-1059 (2003).

[9] Mandal, T. K.; Fleming, M. S.; Walt, D. R. *Nano Lett.*, **2**, 3-7 (2002).

[10] Sill, K.; Emrick, T. *Chem. Mater.*, **16**, 1240-1243 (2004).

[11] Kickelbick, G.; Holzinger, D.; Brick, C.; Trimmel, G.; Moons, E. *Chem. Mater.*, **14**, 4382-4389 (2002).

[12] Vestal, C. R.; Zhang, Z. J. *J. Am. Chem. Soc.*, **124**, 14312-14313 (2002).

[13] Kim, J.-B.; Bruening, M. L.; Baker, G. L. *J Am. Chem. Soc.*, **122**, 7616-7617 (2000).

[14] Tsujii, Y.; Ohno, K.; Yamamoto, S.; Goto, A.; Fukuda, T. *Adv. Polym. Sci*. **197**, 1-45 (2006).

[15] Suzuki, A., Kobiki, Y., *Jpn. J. Appl. Phys.*, **38**, 2910-2916 (1999).

# Chapter 3

## Dominant influence of the terminal molecule of PNIPA grafted membrane obtained by Atomic Transfer Radical Polymerization

**Abstract.**

Poly(N-isopropylacrylamide) (PNIPA) brushes on silicon substrate was constructed and precisely controlled molecular weight and polydispersity index. Molecular behavior on the PNIPA grafted surface was observed by using captive bubble contact angle method. Here we found a very interesting phenomena of high density PNIPA grafted membrane with a terminal chloride molecule. The contact angle of high density PNIPA-Cl increased sharply while the temperature raises above 32 $^{o}$C. But in case of PNIPA gel surface the contact angle result decrease sharply while the temperature reaches above LCST. To identify the behind this abnormal behavior of PNIPA-Cl grafted membrane, we changed the terminal chloride molecule of PNIPA chain to less electronegative azide (-$N_3$) as well as carboxylic acid (-COOH). Finally we found that terminal molecule of high density PNIPA grafted membrane has a supirior power on the change the wettability of PNIPA membrane in water with changing the temperature.

### 3.1. Introduction.

Temperature responsive polymers have an appropriate meaning to define switchable surface properties when grafted on solid surfaces. This is because, by changing the temperature, its ease to alteration of the conformation of grafted polymer. These surface properties can also precedence to more complex phenomena, such as controlled movement of small particles on polymer-bearing surfaces; topography and adhesion facilitate movement including surface patterning and protective coating.[1-3] This surface has its tunable properties in response to environmental changes such as temperature, pH, wettability, adhesion, topography and humidity. Surface-initiated polymerization attached with atom transfer radical polymerization (ATRP) is one of the most well controlled living radical polymerization. It has been recognized as a versatile method for generating ultrathin film of surface grafted polymer brushes with well defined thickness and architecture. An example of this type of smart material is a Poly(*N*-isopropylacrylamide) (PNIPA), which has a lower critical solution temperature (LCST) at ~32$^{o}$C in water, between room temperature and physiological temperature.[4-7] Below the LCST, water is a good solvent and the PNIPA is hydrated and follow a random coil conformation. But water acts as a poor solvent and the PNIPA is dehydrated and collapsed into a globular conformation at above LCST. [8] If grafting density of polymer chains on solid surface is adequately high, polymer chains are constrain to stretch away from the surface to avoid overlap. This arrangement of solution polymer is called as "Polymer brushes". [9] The structure of polymer brushes is technologically important and is a matter of much scientific interest.

To obtain macroscopic properties of a given polymer brush, the measurement of contact angle is one of the most efficient way, and is governed by both the chemical composition and the geometrical microstructure of the surface. During measuring the contact angle underneath PNIPA grafted membrane, air bubble is attached with the surface of the polymer membrane by adhesive force. At the beginning of the adhesion process, an adhesive is essential to be in a liquid state to form a deep contact with the solid surface. Therefore, wetting is usually the first stage in adhesion [10]. For the case of adhesion in an aqueous environment, the liquid act as an aqueous solution whereas the fluid stimulates the adhesive. Wetting on the rough surface may consider either of two regimes: homogenous wetting [11] or heterogeneous wetting [12]. In

homogeneous wetting, liquid completely penetrates into the roughness grooves, whereas air is trapped underneath the liquid, inside the rough groves at heterogeneous wetting. The transition between these regimes plays an important role in the hydrophilicity and hydrophobicity [13].

It is well known that many polymer brushes on solid surfaces composed by different monomer undergo a volume phase transition from hydrophobic state to hydrophilic state in response to infinitesimal changes in temperature, pH, solvent composition, and hydrostatic pressure [14-18]. The volume phase transition is very important because of its technological importance for applications to actuators and drug delivery system [19]. Up to now, many investigations have been carried out to examine the phase transition of PNIPA as a function of temperature, pH or hydrostatic pressure [20-22]. But the phase transition of polymer brash, considering the hydrophilic and hydrophobic properties, no systematic study about the mechanism or reason has been reported.

This paper deals with synthesized high-density polymer brushes of PNIPA on silicon surface by the "grafting from" method and measured the static contact angle of sessile air bubbles in water on PNIPA grafted membrane surfaces. Here we observed that PNIPA membrane showed an unexpected phase transition behavior at temperature near LCST. To clarify this surprising behavior, we converted the terminal Chlorine group of the PNIPA brush chain by less electronegative Azide group and checked the wettability. Then we also converted the electronegative Azide to more hydrophobic carboxyl acid group and studied the effect of terminal end molecule on the wettability of the PNIPA brush surfaces. We also checked the phase transition of PNIPA grafted membranes under different pH solutions.

### 3.2. Experimental section.

#### 3.2.1. Materials.

Tetrahydrofuran (THF) (Kishida Chemical Co, Ltd.) and di-methylformaldehyde (DMF) (Kishida Chemical Co, Ltd.) were distilled from calcium hydride. Sodium Azide ($NaN_3$) (99.9%) (Sigma Aldrich) and 4-ethanoic benzoic acid (99.5%) (AB Chem. Inc.) were used as received. Deuterated solvents, dimethylsulfoxide-$d_6$ (*d*-DMSO) and deuterium oxide ($D_2O$), for $^1H$ NMR

and FT-IR analyses, were used as received. Water was purified using a Direct-Q UV water purification system (Millipore Corp.) and used in all experiments. All other chemicals used in this study were purchased at the highest purity and used as received. A silicon wafer with a crystalline orientation of 100 and one polished side was purchased from Toshiba Semiconductor Company.

### 3.2.2. Synthesis of *PNIPA-$N_3$*.

*PNIPA-Cl* (8.5 g), DMF (30 ml), and $NaN_3$ (325 mg, 5 mmol) were added in a 50 ml round-bottom flask. The reaction mixture was allowed to stir at 45 °c for 48 h. Then the DMF was removed at reduced pressure and the remaining portion was diluted with THF. The concentrated solution was precipitated into an excess of anhydrous hexane. The sediments were redissolved in THF, and passed through a neutral alumina column to remove residual sodium salts. The obtained product was dried overnight in a vacuum dryer for 24 h (yield: 85%, $M_n$ = 7400, $M_w/M_n$ = 1.12). Successful synthesis of PNIPA-$N_3$ was confirmed from $^1$H NMR data (Figure 3-1) and FT-IT observation (Figure 3-2).

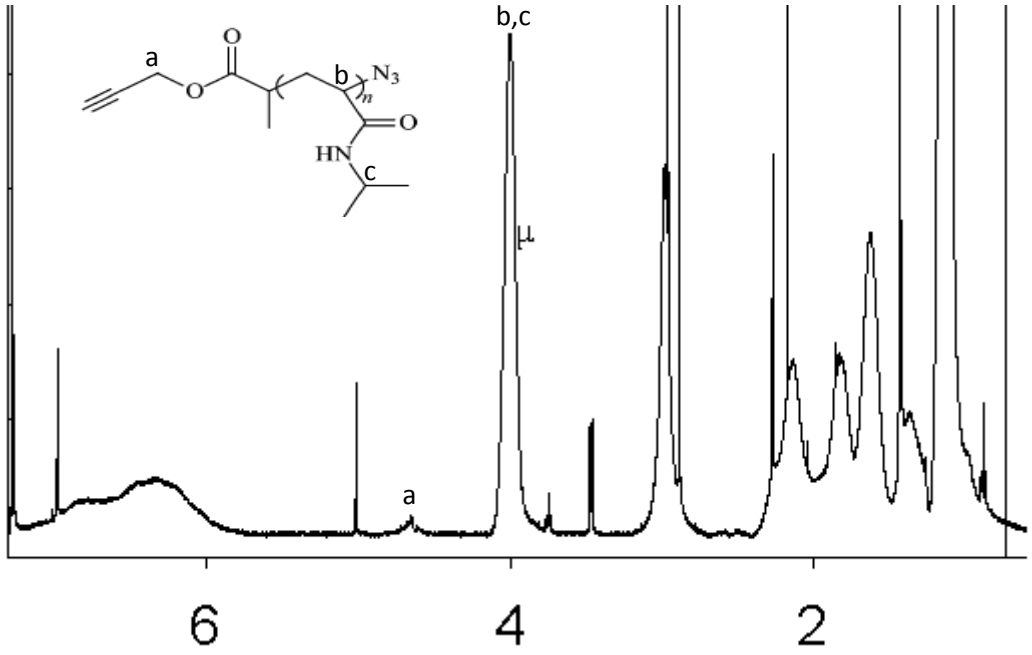


**Figure 3-1:** $^{1}H$ NMR spectrum of azide terminated Poly(*N*-isopropylacrylamide) (PNIPA-$N_3$)

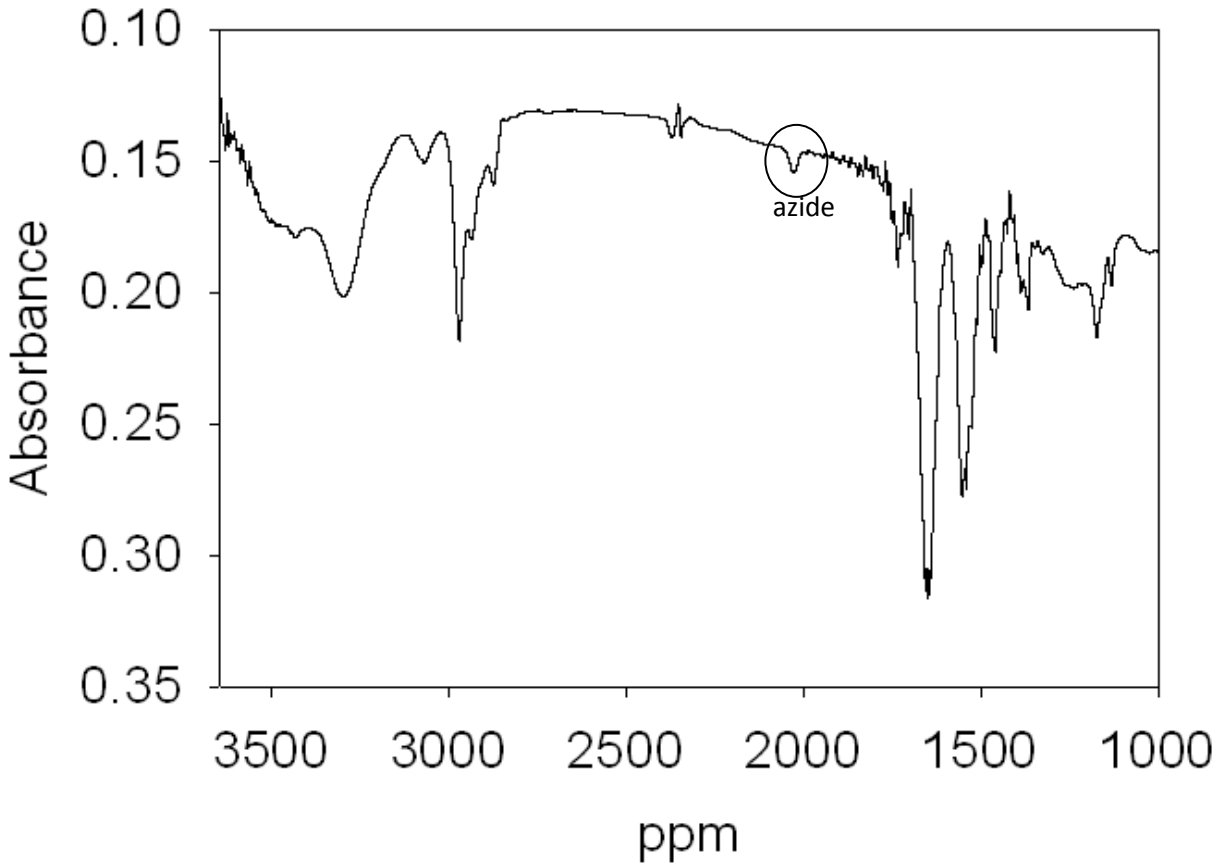


**Figure 3-2:** FT-IR spectra of PNIPA-$N_3$ cast film.

### 3.2.3. Synthesis of *PNIPA-COOH*.

PNIPA-$N_3$ (20.0 mg, 0.0655 mmol) and 4-ethanoic benzoic acid (173 mg, 1.31 mmol) were dissolved in dry DMF (0.3 mL) and to this were added L-ascorbic acid (23.1 mg, 0.131 mmol) in DMF (0.131 mL) and $CuSO_4.5H_2O$ (16.4 mg, 0.0655 mmol) in DMF (0.262 mL), and the reaction mixture was stirred at ambient temperature. After 12 h, L-ascorbic acid (23.1 mg, 0.131 mmol) in DMF (0.131 mL) and $CuSO_4.5H_2O$ (16.4 mg, 0.0655 mmol) in DMF (0.262 mL) were added again to the reaction mixture, and the reaction mixture was again stirred at room temperature for 9 h. The obtained polymer was then precipitated into a large amount of methanol and collected by centrifugation. The resulting polymer was dissolved in a small amount of DMF containing LiCl and the solution was poured into a large amount of hexane. This purification cycle was repeated three times. The obtained product was dried overnight in a vacuum dryer. (73% yield). Complete conversion of PNIPA-$N_3$ to PNIPA-COOH was confirmed by the FT-IR spectrum (Figure 3-4)which showed the disappearance of the azide signal of PNIPA-$N_3$. According to the $^1$H-NMR data (Figure 3-3) of 4-ethanoic benzoic acid, proton peak for aromatic portion is appeared at 7.6 ppm. After converting PNIPA-COOH, we have found that integration ration of that position has increased which proves the presence of aromatic group at that position.

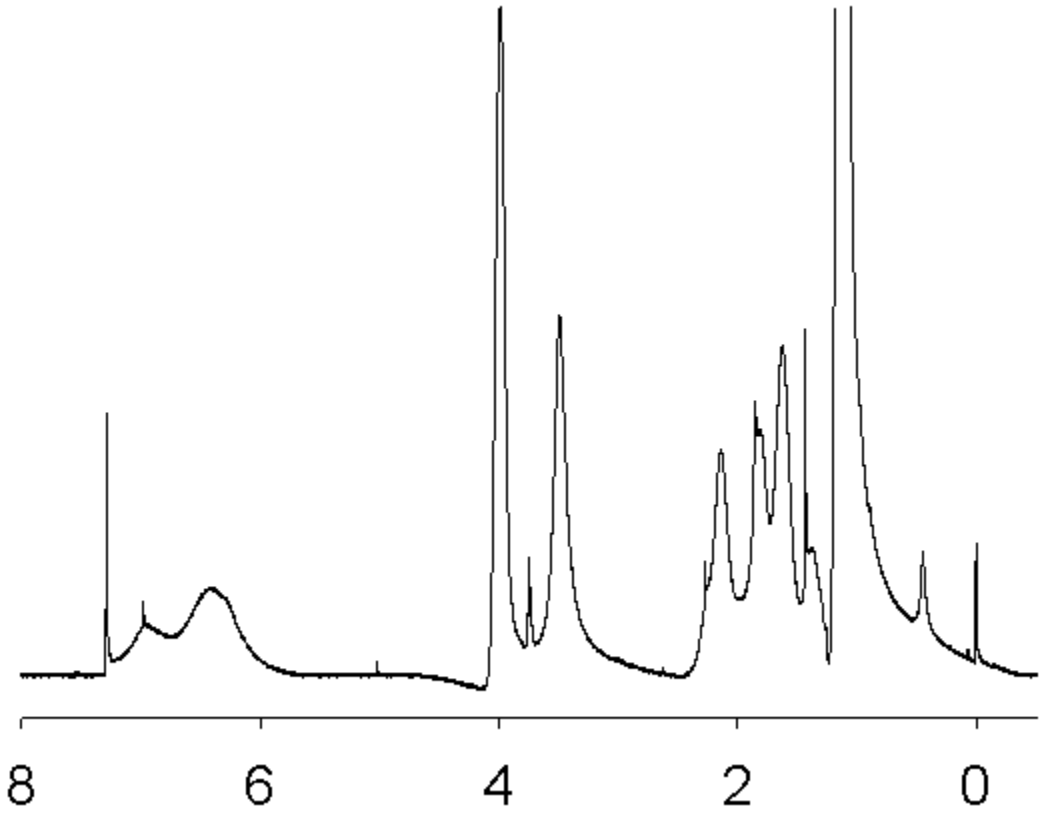


**Figure 3-3:** $^{1}H$ NMR spectrum of acid terminated Poly(*N*-isopropylacrylamide) (PNIP-COOH)

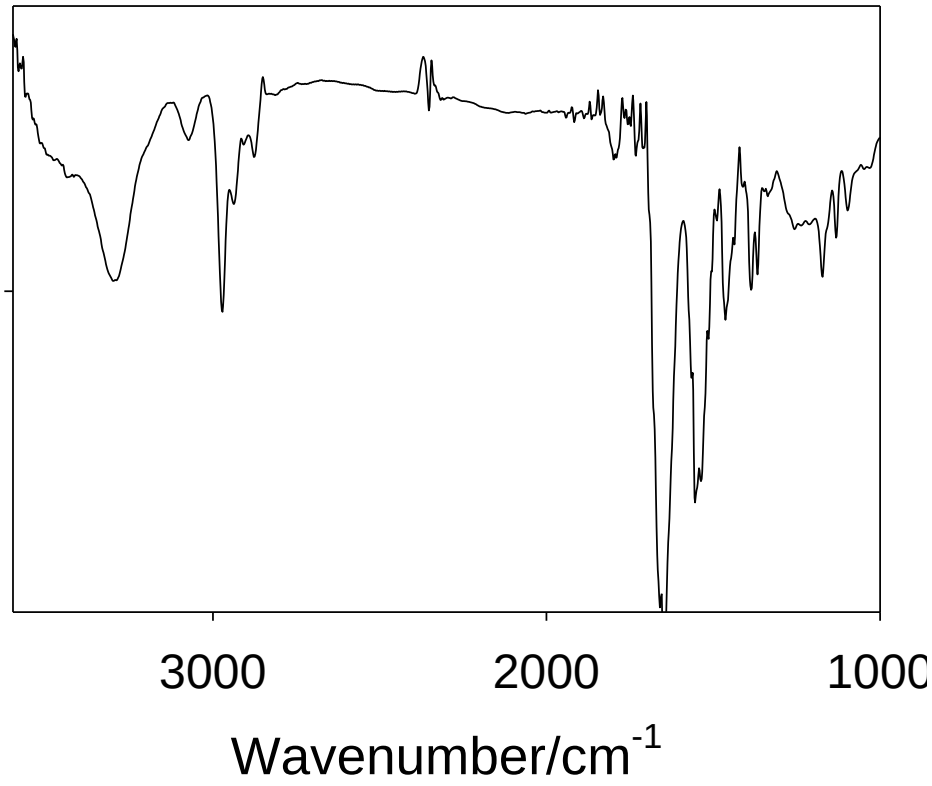


**Figure 3-4:** FT-IR spectra of PNIPA-COOH cast film

### 3.3. Results and discussion.

ATRP technique has been used to synthesize homo polymer brushes to the surface tethering by grafting from method. [23-27] PNIPA brush on silicon surface was synthesized by ATRP in presence of a free initiator, CuCl/$Me_6$TREN system, and DMF as a solvent. The covalent attachment of the initiator onto the silicon substrate was accomplished in a single step. We synthesize the polymer brushes on silicon surface by varying polymerization time from 0.5h to 8h keeping the temperature constant at 20 $^oC$. The end of this polymer chain is capped with an active halide atom that can be reinitiated to replace by other atoms. During polymerization monomer conversion and polymer molecular weight were determined at different stages. By GPC analysis number average molecular weight, $M_n$ and molecular weight distribution, $M_w/M_n$ was obtained. The surface thermo-sensitivities of the PNIPA grafted membranes were determined by captive air bubble method. Measurement of contact angle using captive air bubble technique is a flexible technique in consideration of hydrophilicity/hydrophobicity of water attracting polymeric substrate. An air bubble was trapped underneath the polymer grafted membranes in water and equilibrated until the chemical potential of water vapor in the vapor-saturated air bubble equalized that of liquid water. Achieving an equilibrated contact angle of the air bubble took more than 30m depending on the water temperature. Then the equilibrated contact of the air bubble was recorded after waiting an adequate amount of time. Figure 3-5 (a) shows the static contact angle θ, at different temperature for five different polymer brush samples with different chain length. Here, θ indicates the mean contact angle of θ's at some separate locations on the respective sample. Here we can see that the contact angle of all the grafted membranes slightly decrease with increasing temperature, where the decrement of θ is not observed while crossing the phase transition temperature. The contact angle suddenly starts to increase sharply at temperature ~32 $^oC$ and follows up to 40 $^oC$ and then become constant. Although the net change of contact angle is not so large, but these surfaces show a remarkable temperature-dependant morphology change that shows very much unlike properties than conventional PNIPA gel surface. In case of conventional PNIPA gel, θ slightly decreases at low temperature, and rapidly decreases at around LCST, followed by a slight decrease at higher

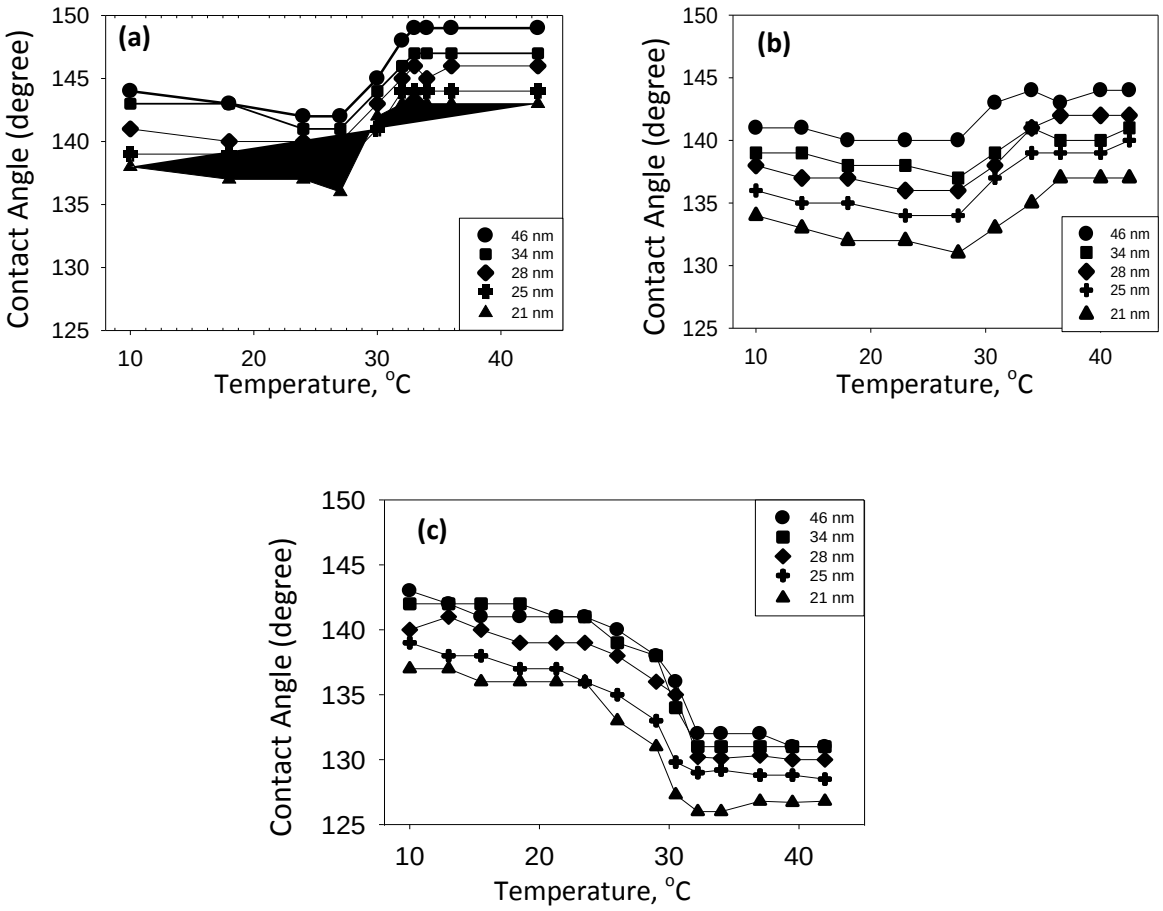


Figure 3-5. Contact Angle of air bubble underneath PNIPA grafted membranes in water as a function of temperature, (a) PNIPA-Cl, (b) PNIPA- $N_3$ and (c) PNIPA-COOH. Thickness (which were determined by AFM Nanopics imaging across the scratch boundary) of the five different samples are 46 nm, 34 nm, 28 nm, 25 nm, 21 nm and the graft density of these samples are 0.48, 0.5, 0.46, 0.5 and 0.45 chain/ $nm^2$ respectively.

temperature. [28] Electro-negativity of terminally capped chloride molecule may be responsible for this conflicting behavior shown by PNIPA-Cl grafted membrane than conventional PNIPA gel. So the effects of the terminal atom of the polymer chain on the wettability of the grafted chain should discuss to analyze the experimental results. As PNIPA brush is chemically stable, the change of wettability of the PNIPA brush surface occurs only by the exchange of water with surrounding environment and by the change of the temperature [29].

It is well known that the power of a chloride atom in a molecule to attract electrons to itself is higher than an azide molecule. So the electro-negativity of azide atom is lesser than that of chloride. So we modified the terminal chloride group by less electronegative azide ($-N_3$) group and checked the wettability. But in case of azide modified grafted film, hardly any difference is observed in the contact angle of the film (Fig: 3-5 (b)). The contact angle gradually decreased with increasing temperature up to 27 $^{o}$C, and then while the temperature reached at LCST, the contact angle increase sharply as shown in previous PNIPA-Cl system. In case of PNIPA-$N_3$, an increasing the contact angle after crossing the LCST, is not so steep comparing with PNIPA-Cl. Since the value of contact angle of the PNIPA-$N_3$ grafted membrane has been reduced comparing to PNIPA-Cl system, it can be said that the modification of end group from chloride to azide reduce the hydrophilicity of the polymer surface. This phenomenon of grafted membrane reveals that terminal molecule of PNIPA brush surface has an effect on the wettability of grafted film. Modification of chloride to azide group makes the surface more hydrophobic. But our concern mainly focused on the unexpected behavior of PNIPA grafted membrane at temperature near LCST. PNIPA-$N_3$ also shows similar types of trend with PNIPA-Cl at temperature near LCST. To find more significant effect of the terminal molecule, we modified the azide molecule of PNIPA chain to more hydrophobic carboxylic acid. When the carboxyl groups are attached to long alkyl chains, the hydrogen bonds are particularly stable. Hydrogen bonds between the acid and the anion are known to be much stronger than those between the unionized molecules. So carboxylic acid has more hydrophobic characteristics than those of chloride and azide molecule. Figure 3-5 (c) shows the static contact angle of PNIPA-COOH grafted membrane at different temperature. Comparing with PNIPA-Cl and PNIPA-$N_3$, the curves of all five PNIPA-COOH samples showed absolutely different trend near LCTS due to different surface properties. With increasing temperature, contact angle of the PNIPA-COOH

grafted membrane decreases at low temperature, and rapidly decreases at around 31 $^{o}$C, followed by a slight decrease at higher temperature. It should be noted that contact angle of the PNIPA-COOH rapidly but continuously changes at the transition temperature, which is opposite with the chloride and azide terminated grafted membrane. PNIPA-COOH has higher degree of freedom than PNIPA-Cl and PNIPA-$N_3$, therefore it is easy for PNIPA-COOH to expand energy with raise of the temperature. This result of the contact angles of air bubble follows with the contact angle result of usually observed PNIPA gel. In case of PNIPA-COOH, the sessile air bubble accumulates the surface at the border of the contact at LCST, which might be a reason of decreasing the value contact angle.

### 3.3.1. pH responsive contact angle.

The contact angle of PNIPA brush was measured under the aqueous buffer solution with different pH values. Phosphate buffer with different pH strength was prepared, the concentration of the buffer solutions were kept constant at 0.01 mol $L^{-1}$ and ionic strength of the solution was adjusted to 0.15 mol $L^{-1}$ by the addition of NaCl. The PNIPA-COOH modified substrate was immersed in the define buffer solution, kept it for 30 minutes to become equilibrate and then measured air bubble contact angle. The pH value was varied from 2 to 10 and back again from 10 to 2. For each pH value, four spots were measured with the method for contact angle measurements as described above. Figure 3-6 shows the contact angle of PNIPA-COOH membrane as a function of the temperature under different pH solution. Here we see that the PNIPA-COOH grafted membranes also have phase transition under pH solution near the LCST of PNIPA. PNIPA-COOH chain conformation doesn't have any significant change at temperature region 10 to 28 $^{o}$C, but the value of contact angle dropped rapidly while it crossed LCST of PNIPA. In this case decrease of the contact angle may be ascribed to the decrease in the surface tension with the temperature rise. The value of contact angle for all samples become constant at temperature above 33 $^{o}$C, which means that chain conformation of PNIPA-COOH doesn't have any change even also at higher temperature. But at higher temperature the grafted membrane become hydrophobic comparing with at lower temperature. From the figure 3-6, it is also clear that PNIPA-COOH brush membranes become hydrophilic with the increase of pH at all temperature.

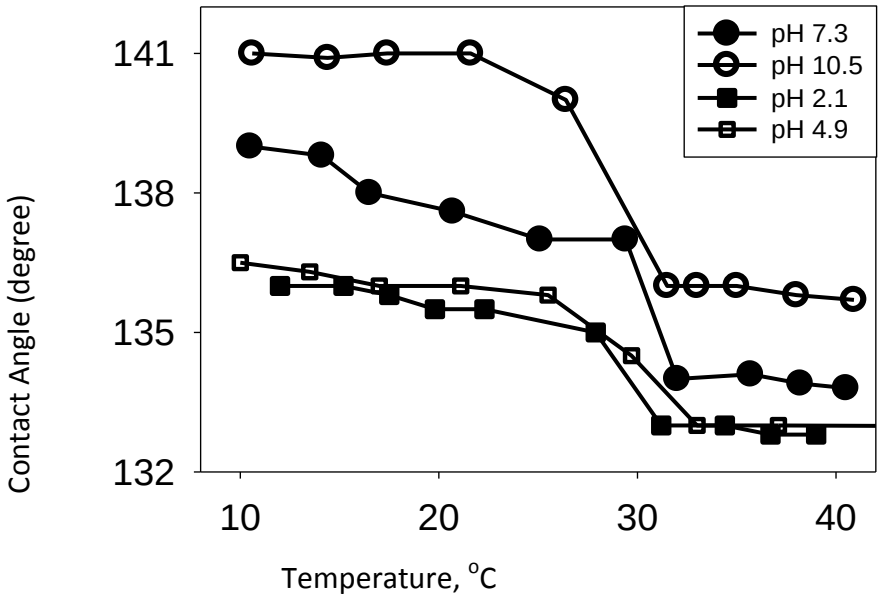


Figure 3-6. Contact angle of air bubble underneath PNIPA-COOH grafted membranes under different buffer solution as a function of temperature.

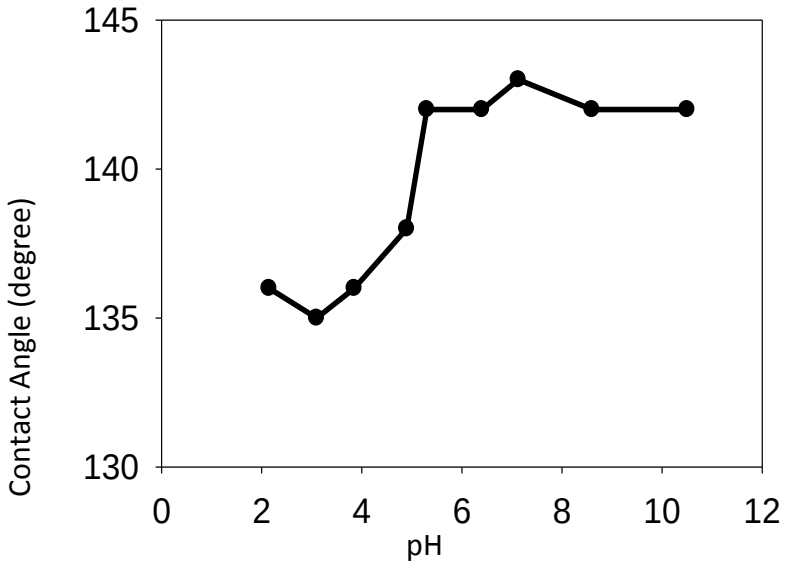


Figure 3-7. Contact angle of air bubble underneath PNIPA-COOH grafted membrane in buffer solution. Thickness of the polymer brush is 46 nm and graft density is 0.48 chain/nm$^2$

Figure 3-7 shows equilibrium contact angles of air bubble resulting at 23 $^{o}$C underneath the PNIPA-COOH grafted membrane composed of molecular weight ($M_n$) with 52000 and graft density of approximately 0.48 chain/nm$^2$. At pH levels lower than 4, the value of contact angle was almost constant and almost independent of pH. This may be happen because most of the PNIPA-COOH molecules exist as un-ionized carboxyl groups at low pH, and the grafted membrane behaves as a neutral network. As the pH was increased at around 5, the value of contact angle was increased. This is because, with the increase of the pH, the number of ionized carboxyl (carboxylate) groups on the network also increased, causing the grafted membrane hydrophilic. At higher pH the contact angle become constant meaning that PNIPA-COOH grafted membrane is also independent at higher pH. Most of the carboxylate groups formed sodium salt combined with the sodium ion of the buffer solution. So it's clear that the contact angle of the grafted membrane depends on the charge density of carboxyl groups at buffer solution. At pH less than 5, brush surfaces are less ionized results the increase of positive charge on the brush surfaces, which cause the lower value of contact angle. At around $pK_a$ value of PNIPA-COOH, the inverse scenario may be assigned. Almost all carboxylate groups are ionized and make the surface hydrophilic. The charges are completely compensated at higher pH (above 7) that result a charge neutral and pH independent surface. So the contact angle become constant at the pH above 7. This variation of hydrophobicity on the grafted membrane can only be understood in terms of the microenvironment of the monolayers, specifically the positions of the PNIPA chain with respect to the terminal ester groups of PNIPA-COOH chains.

### 3.4. Conclusion.

High density polymer brush on silicon substrate was synthesized seccessfully. In water, high density grafted membrane of PNIPA-Cl do not follow all properties of usually observed PNIPA gel. Surface roughness do not have any influence on the wettability of PNIPA-Cl grafted membrane. Terminal molecule of PNIPA-Cl chain can be positioned on the surface or can be hidden at the vicinity of the surface. Converted of terminal molecule of PNIPA grafted chain reveals that the terminal molecule of the PNIPA grafted chain can be positioned on the surface even at collapsed state.

**References and Notes.**

(1) S.A. Prokhorova, A. Kopytsev, A. Ramakrishnan, H. Zhang, J. Rühe, "Can polymer brushes induce motion of nano-objects?", *Nanotechnology* **2003**, 14, 1098. (1) Storey, R.F.; Hickey, T.P. *Polymer* **1994**, *35*, 830.

(2) S.A. Prokhorova, A. Kopytsev, A. Ramakrishnan, H. Zhang, J. Rühe,

"Polymer substrates as a medium for motion of nano objects", manuscript.

(3) *E. Manias, M. Rackaiti, T.M.D. Foley*, K. Efimenko, J. Genzer, *Polymer Preprints* **2005** , *46(2)*, 12

(4) Heskins, M.; Guillet, J. E. *J. Macromol. Sci., Chem* A2, **1968,** 1441-1455.

(5) Schild, H. G. *Prog. Polym. Sci.* 17, **1992,** 163-249.

(6) Chen, G.; Hoffman, A. S. *Nature (London)*, 373, **1995,** 49-52.

(7) Hay, D. N. T.; Rickert, P. G.; Seifert, S.; Firestone, M. A. *J. Am. Chem. Soc.*, *126***, 2004,** 2290-2291.

(8) Heskins, M.; Guillet, J. E.; James, E. *J. Macromol. Sci., Chem.* **1968**, *A2*, 1441.

(9) Zhao, B.; Brittain, W. J. *Prog. Polym. Sci.* **2000**, *25*, 677.

(10) Abraham Marmur, *Langmuir* **2004,** *20*, 1317-1320

(11) Wenzel, R. N. *Ind. Eng. Chem.* **1936**, *28*, 988-994.

(12) Cassie, A. B. D.; Baxter, S. *Trans. Faraday Soc.* **1944**, *40*, 546-551.

(13) Marmur, A. *Langmuir* **2003**, *19*, 8343-8348.

(14) Hirotsu, S.; Hirokawa, Y.; Tanaka, T. J Chem Phys **1987**, 87, 1392.

(15) Tanaka, T. Sci Am **1981**, 244, 110.

(16) Amiya, T.; Hirokawa, Y.; Hirose, Y.; Li, Y.; Tanaka, T. J ChemPhys **1987**, 86, 2375.

(17) Kato, E. J Chem Phys **1997**, 106, 3792.

(18) Kato, E. J Chem Phys **2000**, 113, 1310.

(19) Okano, T. Adv Polym Sci **1993**, 110, 179.

(20) A.W. Adamson; *Physical chemistry of Surface* (john Wiley & sons, New York, 1990) 5th ed.

(21) D. Y. Kwok, T. Gietzelt, K. Grundke, H.J. jacobasch and A. W. Neumann: Langmuir 13, **1997,** 2880.

(22) S. Balamurugan, Sergio Mendez, Sreelatha S. Balamurugan, Michael J. O'Brien II, and Gabriel P. Lo´pez, *Langmuir* **2003,** *19*, 2545-2549

(23) Kim, J.-B.; Bruening, M. L.; Baker, G. L. *J. Am. Chem. Soc.* **2000**, *122*, 7616.

(24) Shah, R. R.; Merreceyes, D.; Husemann, M.; Rees, I.; Abbott, N. L.; Hawker, C. J.; Hedrick, J. L. *Macromolecules* **2000**, *33*, 597.

(25) Jones, D. M.; Brown, A. A.; Huck, W. T. S. *Langmuir* **2002**, *18*, 1265.

(26) Zhao, B.; Brittain, W. J. *Macromolecules* **2000**, *33*, 8813.

(27) Bo¨rner, H. G.; Duran, D.; Matyjaszewski, K.; da Silva, M.; Sheiko,

(28) Atsushi S. and Yasuhiro K. , Jpn. J. Appl Phys. 38, **1999,** 2910-2916

(29) Takato N., Mineo H., Hideya K.i, Keiichi M., Masayuki T., and Takashi .Physical review, **54,** 1663-1668

# Chapter 4

## Precise Synthesis and Physicochemical Properties of High-Density Polymer Brushes designed with Poly(N-isopropylacrylamide

**Abstract**.

A high density polymer brush of poly(*N*-isopropylacrylamide) (PNIPA) was precisely prepared following carefully selected procedures, which included selecting the underlying substrate, preparing its surface, and grafting PNIPA on the substrate. As a result, the graft density and the dried thickness of the brush reached more than 0.5 chains/nm$^2$ and 200 nm, respectively, for the best combination of each procedure. This high density polymer brush showed gradual collapse with increasing temperature in water, which must be attributed to both the low swelling and the low shrinking abilities of the brush that result from the physically constrained state of the polymers. The contact angle of the air bubbles underneath the high-density polymer brush also gradually decreased up to around 25 °C in water with increasing temperature, which indicate that the hydrophilicity of the surface decreases as it does in typical PNIPA grafted membranes and gels. Starting at the lower critical solution temperature of free PNIPA in water, approximately 32 °C, the value of the contact angle started to increase dramatically, and it became constant when the solution temperature exceeded 40 $^{o}$C. Ultimately, the surface exhibited a mostly hydrophilic nature at higher temperatures. The temperature-dependent contact angles can be interpreted by assuming that the terminally chlorinated alkyl groups of the elongated PNIPAs can be positioned on the surfaces or hidden in the vicinity of the membranes, depending on the temperature of the solution.

## 4.1. **Introduction.**

Stimuli-sensitive polymers have received constant attention as building blocks for the fabrication of smart soft materials[1-3] with various forms, such as dispersed colloidal aggregations,[4-5] grafted membranes,[6] and gels.[7,8] When exposed to small alterations in the environment, such as temperature, pH, solvent composition, and ionic strength, smart soft materials can dramatically transform their shape and size.( The term "smart" here means that the soft materials are sensitive to changes in the environment.) Smart soft materials have received a great deal of interest for their manifold applications, including drug delivery systems,[9-13] sensors,[14] on-off switches,[15] artificial muscles,[16] and catalysts.[17]

The anticipated physicochemical properties of smart soft materials in many cases conform to the inherent physicochemical properties of the stimuli-sensitive polymers used. For example, if a certain polymer is sensitive to environmental temperature and exhibits a coil-globule transition at a given temperature, the gel composed of this thermo-sensitive polymer is expected to show a drastic volume change at a similar transition temperature. [18] However, there can be a difference between the two due to intermolecular cooperation between the polymers in the gel. Cooperation occurs mainly as a result of the enhancement of interactions between the polymers. Soft materials that are less affected by interactions, such as a weakly cross-linked polymer gel, may exhibit slightly different properties, but the variances are predictable. As a result of recent advancements in synthetic technology, however, highly ordered soft materials can be fabricated, and their physicochemical properties are strongly influenced by molecular interactions.[19-21] In particular, we are interested in recent progress in controlled or living radical polymerizations, [22-25] which can be applied in various smart soft materials with ordered architectures. Such organized smart soft materials are complex, which is unexpected given the properties of the component polymer in the diluted solution[26] and have potential in both basic and applied research.

In this work, we present the precise preparation of a high-density brush of poly(*N*-isopropylacrylamide) (PNIPA) by atom transfer radical polymerization (ATRP) and its physicochemical properties, which are distinct from those of past sparsely grafted PNIPA membranes and roughly prepared PNIPA brushes. PNIPA is a representative thermo-sensitive

polymer that exhibits a lower critical solution temperature (LCST) in water with a temperature around 32 °C. This thermo-sensitive behavior has been modified for a variety of purposes. For example, when using a PNIPA-grafted membrane to control cell adhesion,[27] the change in the wettability of the outer surface of the membrane is critical to the expected physicochemical properties of this membrane. For the preparation of cell sheets, the surface must be hydrophobic around the cultivation temperature, i.e., 37 °C, and hydrophilic below the LCST. As a result, the cell sheets cultured at 37 °C that are useful for tissue engineering are safely isolated from the membranes below the LCST. The thermo-sensitive behavior of PNIPA-grafted membranes has been reported in many studies.[12,27-31] However, our precisely prepared high-density brush composed of highly ordered PNIPA exhibits an unexpected change, especially in the wettability results, due to temperature change: whereas the hydrophilicity of the surface decreased with an increase in temperature from 10 °C to 25 °C, the surface regained hydrophilicity with a further increase in temperature and became mostly hydrophilic at higher temperatures. This temperature-dependent contact angle may be understood by assuming that the terminally chlorinated alkyl groups of the elongated PNIPAs can be positioned on the surfaces or hidden in the vicinity of the membranes, depending on the temperature. Here, we describe the preparation procedure and the various physicochemical properties of the high-density brush composed of PNIPA and discuss the cause of the unexpected surface wettability change of the brush.

## 4.2. Experimental Section.

### 4.2.1. Materials.

Ethyl 2-chloropropionate (ECP) (Wako Pure Chemical Industries, Ltd., 96%), copper (I) chloride (beads, 99.99%), and dimethylsulfoxide (DMSO) (anhydrous, 99.9%), 10% HCl aqueous solution (Wako Pure Chemical Industries, Ltd.), platinum (0)-1,3-divinyl-1, 1,3,3-tetramethyldisiloxane 0.10 M in xylene (Karstedt Catalyst) (Sigma-Aldrich Co.), and 0.2 M ethylenediaminetetraacetic acid disodium solution (EDTA solution) (Kishida Chemical Co, Ltd.) were used as supplied. Tetrahydrofuran (THF) (Kishida Chemical Co, Ltd.) and toluene (Kishida Chemical Co, Ltd.) were distilled from calcium hydride. NIPA (Kohjin) was recrystallized twice from toluene-hexane mixed solvent and dried under a vacuum prior to use. Tris[2-(dimethylamino)ethyl]amine ($Me_6$TREN) was obtained as a gift from Mitsubishi Chemical Co. and distilled at 110 °C with 5 mmHg. Deuterated solvents, dimethylsulfoxide-$d_6$ (*d*-DMSO) and deuterium oxide ($D_2O$), for $^1$H NMR and FT-IR analyses, were used as received. Water was purified using a Direct-Q UV water purification system (Millipore Corp.) and used in all experiments. All other chemicals used in this study were purchased at the highest purity and used as received. A silicon wafer with a crystalline orientation of 100 and one polished side was purchased from Toshiba Semiconductor Company.

### 4.2.2. Sample Synthesis.

#### 4.2.2.1.Preparation of [11-(2-chloro)propionyloxy]undecyl-dimethylchlorosilane (CPU-dMCS) as Surface-Attachable ATRP Initiator.

The surface-attachable ATRP initiator ([11-(2-chloro)propionyloxy]undecyl-dimethylchlorosilane, CPU-dMCS), was synthesized by the hydrosilylation of 10-undecen-1-yl 2-chloropropionate with dimethylchlorosilane in the presence of Karsted catalyst (Figure 4-1).[32,33] First, the synthesis of 10-undecen-1-yl 2-chloropropionate is described below. Triethylamine (4.88 g, 48.2 mmol), 10-undecen-1-ol (6.81 g, 40.0 mmol), and dry tetrahydrofuran (45 mL) were mixed for 10 min in an ice bath followed by dropwise addition of 2-chloro-propionyl chloride (5.08 g, 40.0 mmol) over 5 min. The mixture was stirred at 0 ° for 2

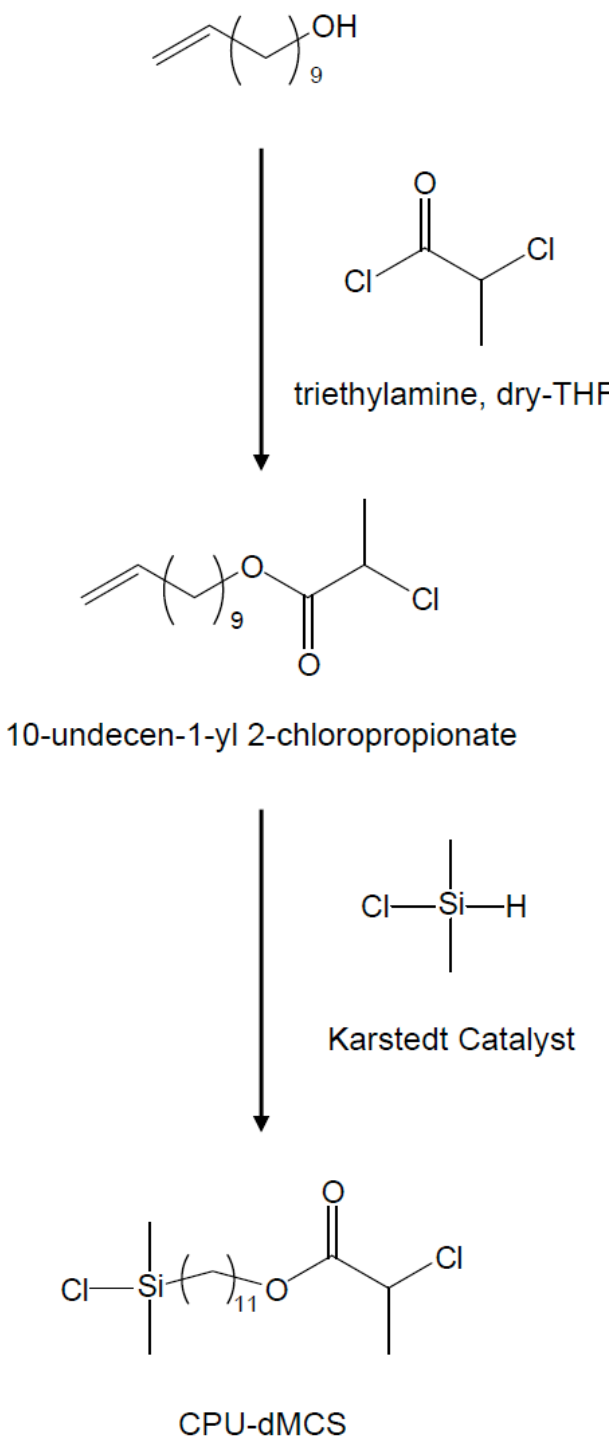


Figure 4-1. Synthetic route of CPU-dMCS.

hr and at room temperature for 12 hr and then diluted with hexane (100 ml) and washed with 10% HCl aqueous solution, sodium bicarbonate water, and purified water. The organic phase was dried with calcium sulfate. The crude compound was purified by column chromatography with hexane/ethyl acetate mixed solvent (25/1 v/v) as an eluent. After the solvent was removed under reduced pressure, 7.72 g (74%) of 10-undecen-1-yl 2-chloropropionate as a colorless oil was obtained. Next, 10-undecen-1-yl 2 chloropropionate (0.67 g, 2.57 mmol), dimethylchlorosilane (1.21 g, 12.81 mmol), and Kaestedt catalyst (10.0 $\mu$L) were added to a dry flask. The mixture was stirred at room temperature for 12 hr while the reaction was monitored by $^1$H NMR. After the excess reagent was removed under reduced pressure, 0.83 g (91%) of the surface-attachable ATRP initiator as a colorless oil was obtained.

$^1$H NMR (□□[ppm], 270MHz, $CDCl_3$): 0.401 (6H, s, -Si-$CH_3$), 0.832 (2H, t, -Si-$CH_2$-), 1.19-1.48 (16H, m, -$CH_2$-), 1.57-1.75 (5H, m, -COO-$CH_2$-C$\underline{H}_2$-, C$\underline{H}_3$-CHCl-), 4.17 (2H, t, -COO-C$\underline{H}_2$-), 4.35 (1H, q, $CH_3$-C$\underline{H}$Cl-), 0.030 (6H, s, $CH_3$-Si-O-Si-), 0.127 (2H, t, -Si-O-Si-$CH_2$-)

#### 4.2.2.2. Preparation of [11-(2-methyl)propionyloxy]undecyl-dimethylchlorosilane (MPU-dMCS) as an ATRP-Inactive Alkyldimethylsilane Derivative.

A dimethylchlorosilane derivative with a similar chemical structure to CPU-dMCS ([11-(2-methyl)propionyloxy]undecyl-dimethylchlorosilane, MPU-dMCS) was synthesized by hydrosilylating 10-undecen-1-yl 2- methylpropionate with dimethylchlorosilane in the presence of Karsted catalyst (Figure 4-2).[32,33] The preparation of 10-undecen-1-yl 2-methylpropionate conforms to that of 10-undecen-1-yl 2-chloropropionate as follows. Triethylamine (4.88 g, 48.2 mmol), 10-undecen-1-ol (6.81 g, 40.0 mmol), and dry tetrahydrofuran (45 mL) were mixed for 10 min in an ice bath followed by the dropwise addition of 2-methylpropionyl chloride (4.26 g, 40.0 mmol) over 5 min. The mixture was stirred at 0 ° for 2 hr and at room temperature for 12 hr; then, it was diluted with hexane (100 ml) and washed with 10% HCl aqueous solution, sodium bicarbonate water, and purified water. The organic phase was dried with calcium sulfate. The crude compound was purified by column

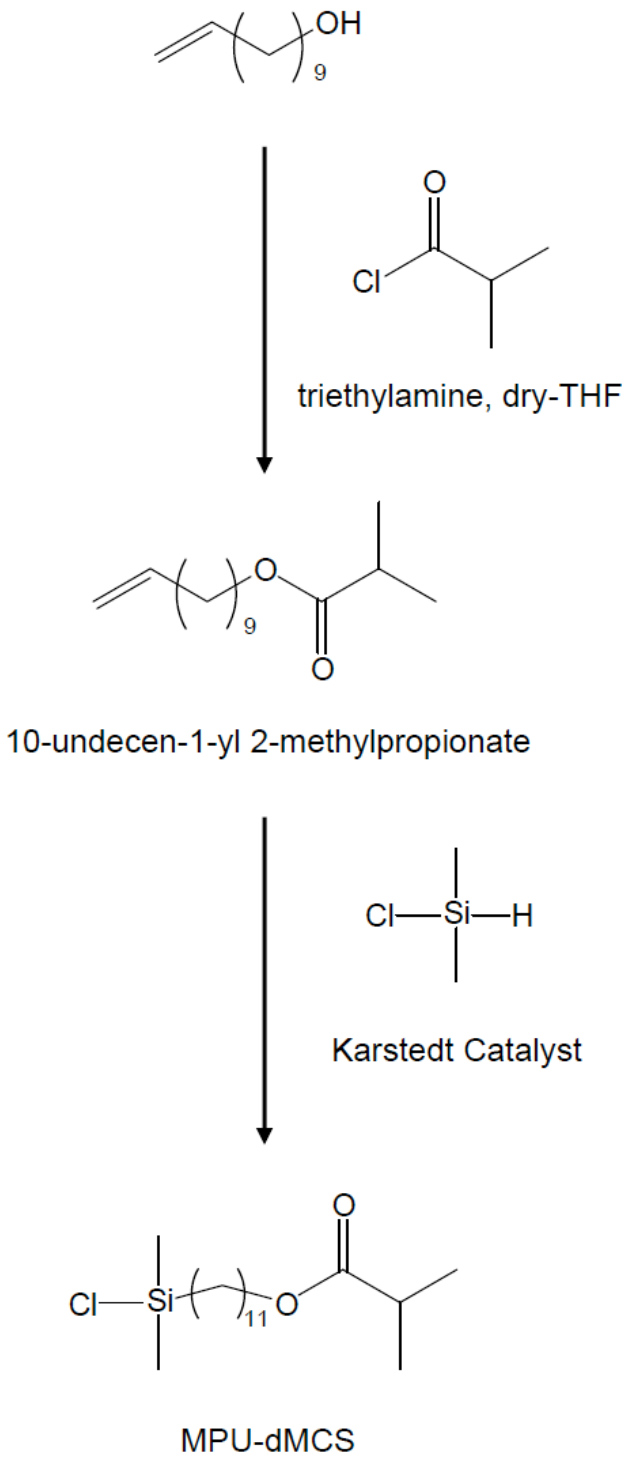


Figure 4-2. Synthetic route of MPU-dMCS.

chromatography with hexane/ethyl acetate mixed solvent (25/1 v/v) as an eluent. After the solvent was removed under reduced pressure, 8.85 g (92%) of 10-undecen-1-yl 2-methylpropionate as a colorless oil was obtained. The preparation of MPU-dMCS conforms to that of CPU-dMCS as follows10-undecen-1-yl 2 chloropropionate (0.62 g, 2.57 mmol), dimethylchlorosilane (1.21 g, 12.81 mmol), and Kaestedt catalyst (10.0 $\mu$L) were added to a dry flask. The mixture was stirred at room temperature for 12 hr while the reaction was monitored by $^1$H NMR. After the excess reagent was removed under reduced pressure, 0.65 g (76%) of the dimethylchlorosilane as a colorless oil was obtained (Figure 4-3).

$^1$H NMR (□□[ppm], 270MHz, $CDCl_3$): 0.394 (6H, s, -Si-$CH_3$), 0.810 (2H, t, -Si-$CH_2$-), 1.15 (6H, d, C$\underline{H}_3$-CH-), 1.21-1.48(12H, m, -$CH_2$-), 1.52-1.69(2H, m, -COO-$CH_2$- C$\underline{H}_2$-), 2.53 (1H, m, $CH_3$-C$\underline{H}$-), 4.05 (2H, t, -COO-C$\underline{H}_2$-), 0.022 (6H, s, $CH_3$-Si-O-Si-), 0.119 (2H, t, -Si-O-Si-$CH_2$-)

### 4.2.2.3. Preparation of ATRP Initiator-Deposited Silicon Wafer.

A CPU-dMCS and/or MPU-dMCS-functionalized surface was prepared according to the literature[32,33] with small modifications. A silicon wafer was cut into 1.0 × 1.5 cm pieces and placed in a UV/ozone treatment chamber (UV253S, Filgen) filled with pure oxygen to clean the surface for 30 min. The freshly cleaned silicon wafers were placed into anhydrous toluene containing the CPU-dMCS and/or MPU-dMCS (with a total concentration of 5.08 mM). The silicon wafers were allowed to stand in this solution for 84 hrs at 60 °C. The resultant samples were isolated, ultrasonically cleaned by dry toluene, rinsed sequentially with toluene and ethanol, and dried in a $N_2$ stream. The samples were stored at room temperature in a dried, $N_2$-filled glove box when not used in the following reactions.

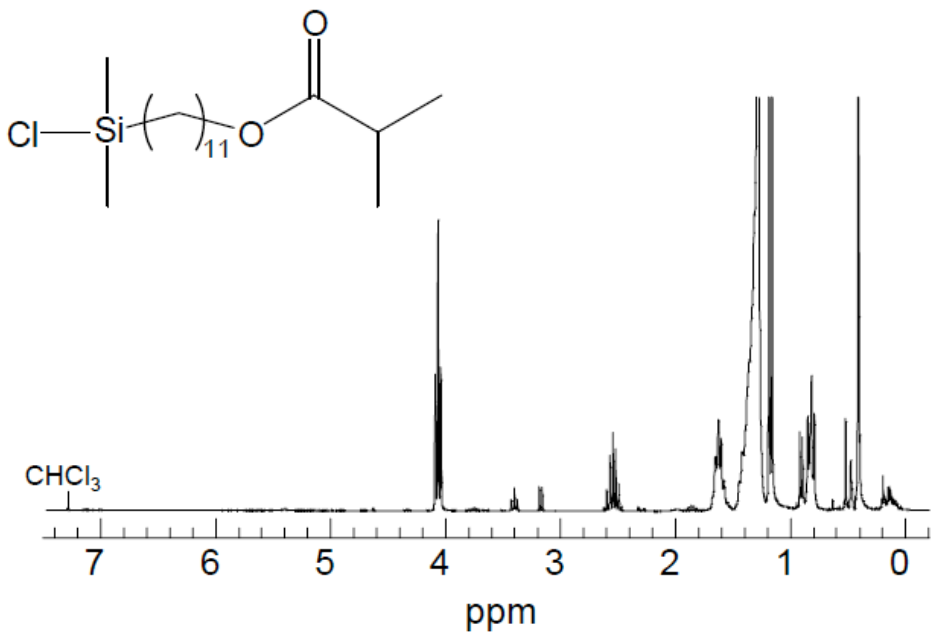


Figure 4-3. $^{1}H$ NMR spectrum of MPU-dMCS in $CDC1_3$.

#### 4.2.2.4.General Procedure for Synthesis of Grafted PNIPA from ATRP Initiator-Modified Silicon Wafers.

In a typical experiment ([NIPA] : [ECP] : [CuCl] : [$Me_6$TREN] = 1000 : 1 : 1 : 1), a 10-mL stoppered test tube was loaded with NIPA (3.39 g, 30 mmol) and 3.40 g of DMSO as the solvent. The solution was sealed with a three-way stopcock and cycled three times between argon gas and a vacuum to remove the oxygen. ECP (4.1 mg, 0.03 mmol) as a free initiator, CuCl (3.0 mg, 0.03 mmol) with $Me_6$TREN (6.9 mg, 0.03 mmol) as a catalyst, and the initiator-modified silicon wafer were then added to the solution in a glove box. The sealed test tube was placed into a water bath with a temperature of 20 °C, and polymerization occurred. A small amount of hydroquinone was added to the test tube to stop the polymerization after a predetermined time. The newly formed polymer grafted membrane was washed with ethanol with sonication for 1 minute and rinsed with the EDTA solution, distilled water, ethanol to remove unreacted species, the catalyst, and free polymers and dried under a $N_2$ stream. The resultant polymer solution was used to determine the monomer conversion by $^1$H NMR in *d*-DMSO and to examine the average polymer molecular weight and polydispersity index (PDI) by gel permeation chromatography (GPC).

### 4.2.3. Characterization.

#### 4.2.3.1. *XPS Analysis of monolayer.*

Chemically grafted monolayers were characterized by X-ray photoelectron spectroscopy (XPS) using an ESCA-3300 (Shimadzu) with an Mg K□ X-ray at 10 mA and 30 kV over 16 scans. All binding energies were referenced to Si 2p at 99.5 eV.

#### 4.2.3.2. *AFM Analysis of Monolayer and Polymer Brush.*

The thicknesses of the dried membranes were measured by Nanopics 2100 (SII NanoTechnology) with a NPX1CTP003 cantilever (SII NanoTechnology). Surface images of the CPU-dMCS and/or MPU-dMCS-functionalized silicon wafers and the polymer grafted membranes grown on the silicon wafers were obtained using an SPA400/SPI3800N system (Seiko Instrument) with a silicon cantilever (SI-DF20) in AFM mode. The thicknesses and the

roughness of the swollen polymer grafted membranes were also measured by the same apparatus at different temperatures.

#### 4.2.3.3. Equilibrium Contact Angle Measurements.

Contact angle measurements were made with FACE CA-XP (Kyowa Interface Science) using a sessile water droplet in air and captive air bubble within a water-filled temperature controlled cell by a circulating water bath (LAUDA E-200) (Figure 4-4). A static contact angle, $\theta$, of a water droplet (ca. 1 $\mu$L) on the surfaces of the CPU-dMCS- and/or MPU-dMCS-functionalized silicon wafers was determined 5 times to obtain a reliable average value by the sessile drop method at 20 °C. In the captive air bubble method, the polymer grafted membranes were immersed face-down in Millipore water to attain an equilibrium swollen state in the temperature controlled cell for 30 min before bringing the air bubble into contact with the surfaces of the membranes. As a result, an air bubble (ca. 3 $\mu$L) was trapped underneath the polymer grafted membranes in water and equilibrated until the chemical potential of water vapor in the vapor-saturated air bubble equaled that of liquid water.[34] Achieving an equilibrated contact angle of the air bubble took more than 30 minutes depending on the water temperature. Then, the equilibrated contact angle of the air bubble was recorded after waiting an adequate amount of time. The reported values are averages of 5 measurements from different areas of the sample surface.

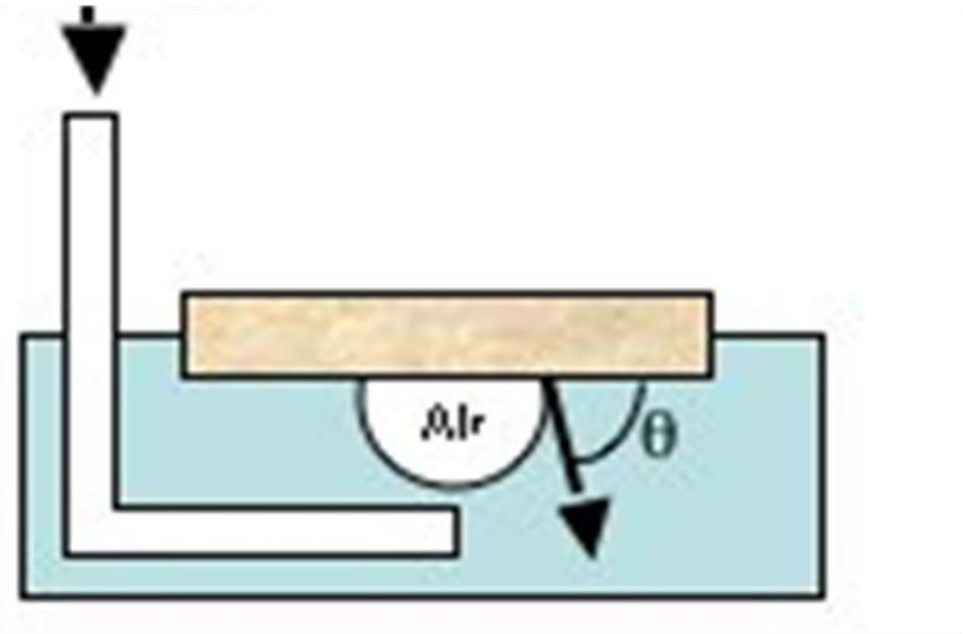


Figure 4-4. Schematic illustration of Captive bubble method under various temperatures.

#### 4.2.3.4.Gel Permeation Chromatography (GPC).

Average polymer molecular weights and PDIs were determined by the GPC system. A GPC measurement was performed using GL-7410 HPLC (GL Science), KD-804 and KD-805 columns (Shodex) and a GL-7454 refractive index detector (GL Science) maintained at 20 °C. For PNIPA analysis, narrow-disperse polymethacrylate standards were used for calibration. The eluent was DMF: chloroform 50: 50 (v/v) mixed solvent including 5 mM of LiCl at a flow rate of 1.0 mL $min^{-1}$. The samples for analysis were prepared by directly diluting a given amount of the reaction mixture in the eluent for GPC to obtain a polymer concentration of about 1 wt%.

#### 4.2.3.5. $^{1}$H NMR spectroscopy.

Conversions for polymerizations were estimated by $^{1}$H NMR spectroscopy. $^{1}$H NMR spectra were measured on JNM-GSX270 or JNM-A400 spectrometers with samples dissolved in *d*-DMSO. The direct analysis of the polymer from the unpurified reaction mixture should give more representative values of the polydispersities and the conversions. Thus, the reaction mixtures were diluted by *d*-DMSO to obtain solute concentrations of about 1 wt% and used for $^{1}$H NMR analysis.

#### 4.2.3.6. Fourier Transform Infrared Spectroscopy (FT-IR).

Transmission IR spectra of the polymer grafted membranes on the silicon substrates were measured using an FTS 6000 FT-IR spectrometer with a HgCdTe semiconductor (MCT) detector (Bio-Rad Laboratories). For dried polymer grafted membranes on the silicon substrates, the samples were placed in the chamber of the spectrometer in a nitrogen atmosphere. A surface cleaned bare silicon wafer was used as a blank sample to obtain differential spectra (Figure 4-5). For the water swollen polymer grafted membrane on the silicon substrate, the dried sample was placed between two $CaF_2$ rectangular plates (22 × 41 mm, thickness 4 mm) with a 6-$\mu$m thick

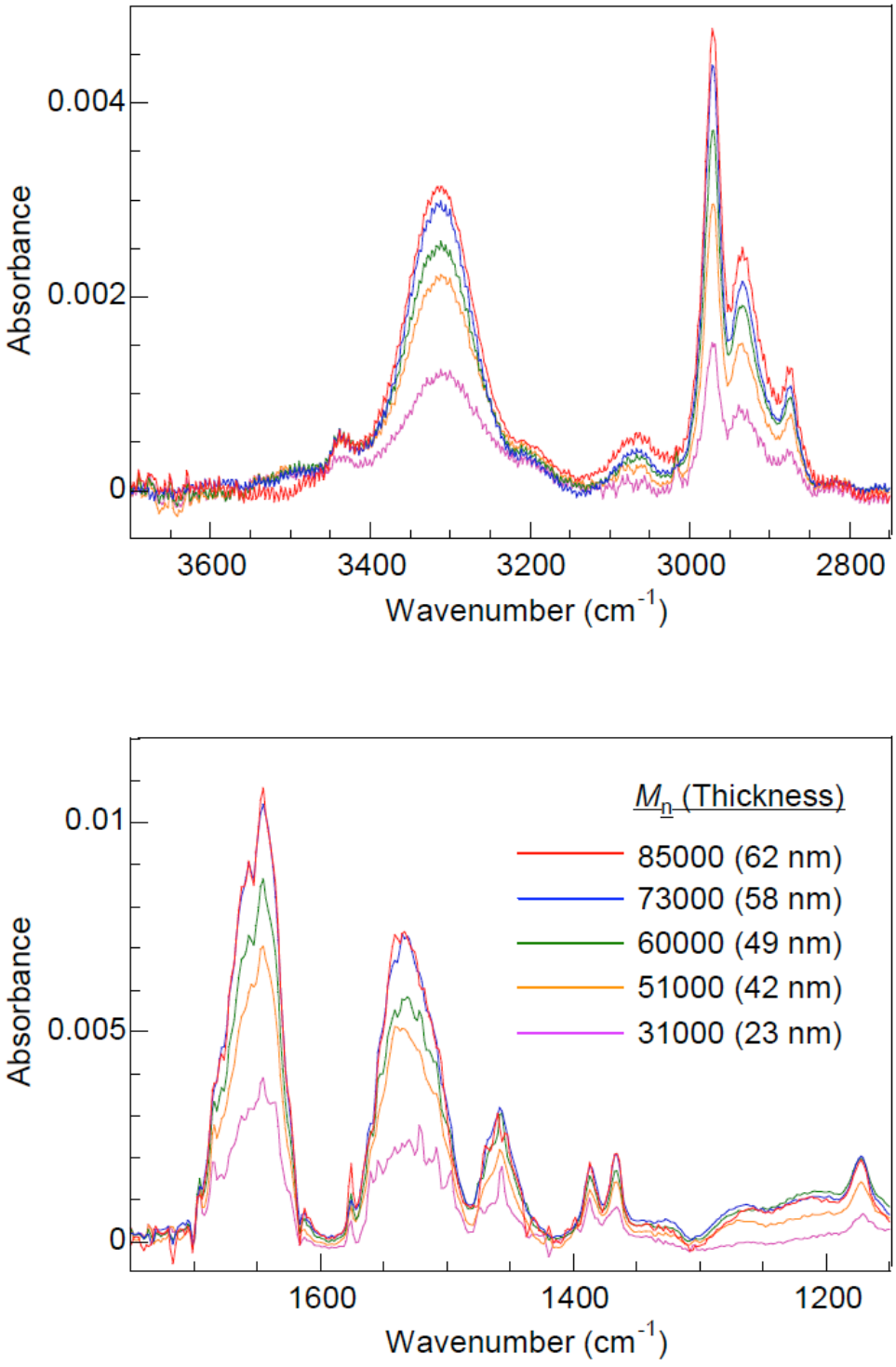


Figure 4-5. FT-IR spectra of dried PNIPA grafted membranes with different $M_n$. a) 3700 – 2750 $cm^{-i}$, b) i750 – ii50 $cm^{-i}$.

Mylar film. Afte $D_2O$ was injected into the cell, the cell was attached to a metal cell holder and a temperature controlled jacket with a circulating water bath (LAUDA E-200) and placed in the chamber of the spectrometer under a nitrogen atmosphere. An electronic thermometer (AS ONE TM-300) with a precision of ±0.1 °C continuously monitored the temperature of the cell. A total of 128 scans were accumulated for each spectrum at a 4-$cm^{-1}$ spectral resolution at a given temperature. Data analyses of the IR spectra, such as curve fitting, baseline subtraction, and waveform separation, were performed with Origin 6.0 (Origin Lab), Resolutions Pro (Varian) and SPNIA, which was supplied by Prof. Katsumoto.

### 4.3. Results and Discussion.

When fabricating a high-density brush composed of PNIPA, it is important to choose the appropriate surface conditions for attaching PNIPA to one end and the preparatory procedure to obtain a high-density brush. In this study, we used a silicon wafer as an underlying substrate because of its flatness, smoothness, and the ease with which its surface chemicals can be modified. Because the ATRP method was applied to obtain PNIPA in a well-controlled polymerization method, the surface of the silicon wafer was initially modified by an ATRP initiator with various surface densities. Then, low-dispersity PNIPA chains were grown by ATRP in a variety of reaction conditions from the surface bound initiator. Here, we explain each step used to make the high-density brush composed of PNIPA and present several of its physicochemical properties.

#### 4.3.1. Preparation of Silicon Surface Modified with ATRP Initiator.

A number of different chemical structures of surface silanized membranes composed of organosilanes on a silicon wafer, especially for di- and tri-hydrolyzable organosilanes, can be produced depending on the reaction conditions because these organosilanes can react not only with Si-OH groups on the surface oxide layer of a silicon wafer but also with each other in the silanized membranes obtained.[35] Mono-hydrolyzable organosilanes are attractive in terms of the reproducibility of surface structures of silanized membranes on a silicon wafer.[35-36] However, because the reactions of the alkyldimethylsilane derivatives with only one hydrolyzable group at the solution-solid interface are very slow in the later stages of the reaction, long reaction times

are necessary to achieve maximum bonding density. Based on our previous results, the reaction continues over days and is not complete within 1 or 2 days. Some reports using carefully optimized conditions showed that densely packed monolayers with alkyldimethylsilane derivatives were highly hydrophobic, with water contact angles of about 110 $^{o}$C.[35-36] In contrast, however, the value of the contact angle of the water drop for our monolayer composed of MPU-dMCS reached about 87 °. This difference is not due to kinetic limitations but is inherent to the pretreatment of a silicon wafer surface and the reaction conditions with the alkyldimethylsilane derivatives. A bare silicon surface is usually covered by a native oxide layer with a thickness of 2 – 10 Å.[37] To obtain a surface of the oxide layer saturated with OH groups, the standard RCA treatment developed by Radio Corporation of America should be used. Meanwhile, UV/ozone cleaning eliminates organic contaminants but does not affect the oxide layer; thus the surface of the oxide layer that we used in this study was not fully saturated with OH groups.[38] Moreover, because the presence of a base for the surface modification of organosilanes is required to achieve a high surface density, our systems probably did not reach densely packed states. [35] Even so, our resultant monolayers meet the requirement to fabricate the high-density polymer brushes due to the larger steric hindrance of polymer chains.

The surface density of silanols on hydroxylated silica covering the surface of a silicon wafer is 4.6 Si-OH groups / nm$^{2,}$ and approximately 60% of the groups can react with alkyldimethylsilanes with one hydrolyzable group.[35,39,40] As a result, the cross-sectional area of the alkyldimethylsilyl groups in the densely packed monolayer was 32 – 38 Å$^2$, which is a lower density than that of self-assembled alkyltri-hydrolyzable-silanes derived monolayers on a silicon wafer (~ 20 Å$^2$).[36] At the same time, because the cross sectional area of typical acrylate polymers that have a substantially stretched form in the brush state at the solid surface is ~ 200 Å$^2$,[41] i.e., only 1 of 5 or 6 alkyldimethylsilane derivatives, which act as ATRP initiators bound to the surface, is expected to initiate polymerization for the densely packed monolayers. Thus, we do not need to use densely packed monolayers composed of ATRP initiative alkyldimethylsilane derivatives to generate densely packed, i.e., high-density, polymer brushes.

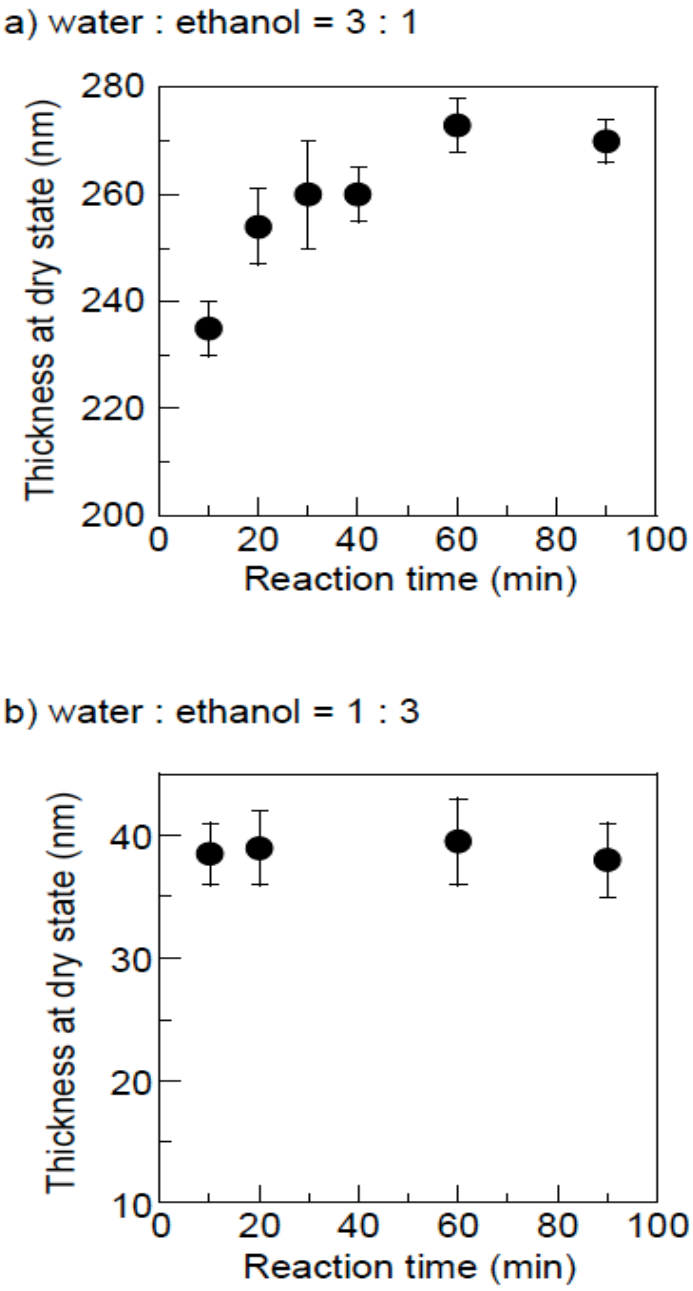


Figure 4-6. The film thickness of dried PNIPA grafted membrane as a function of reaction time. Polymerization conditions: [NIPA] = 2.0 M, [CuBr] = 10 mM, [PMDETA] = 50 mM, water:ethanol = a) 3:1, b) 1:3 (vol/vol), at room temperature

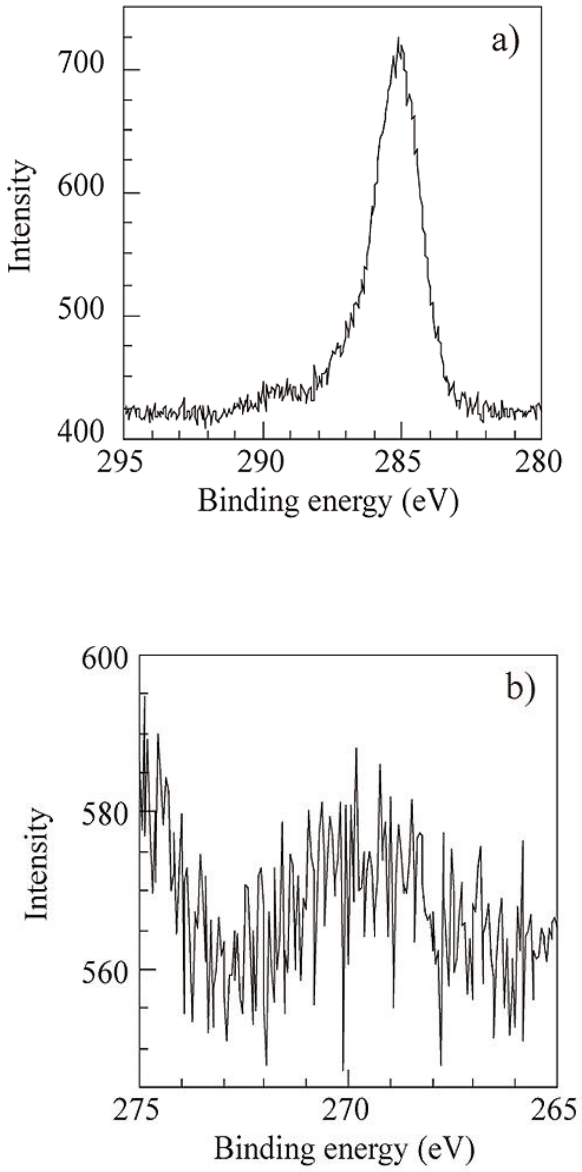


Figure 4-1-1: XPS data of (a) C 1S and (b) Cl 2S of CPU- d MCS modified silicon wafer.

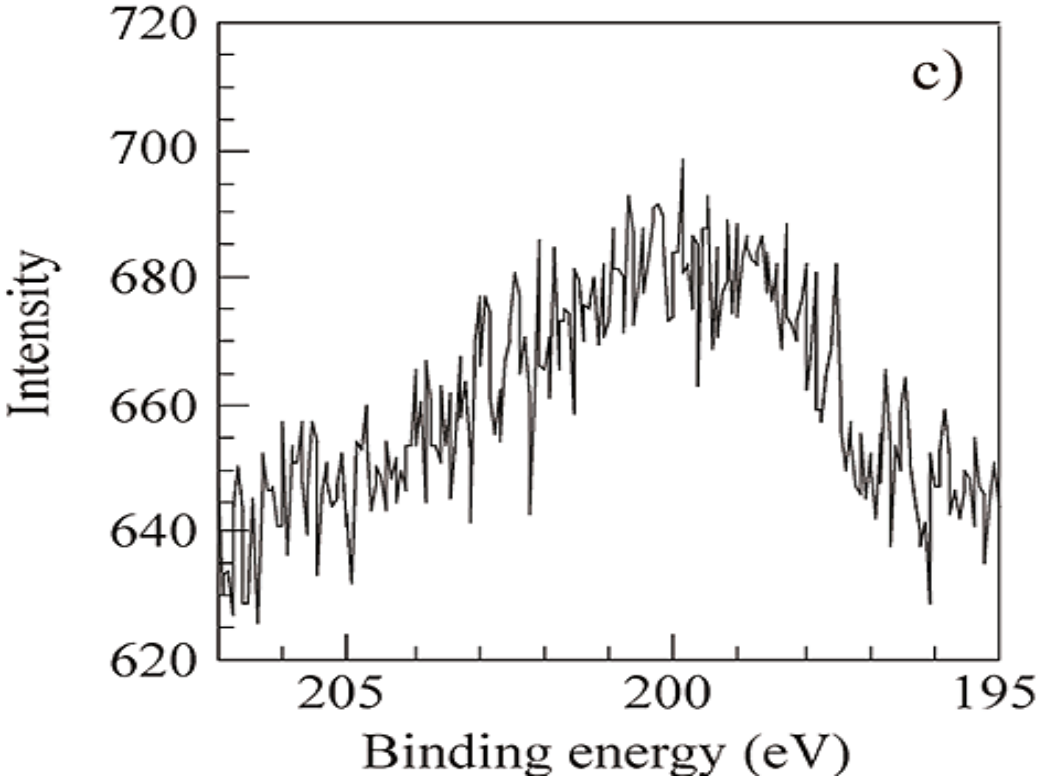


Figure 4-1-2: XPS data of (c) Cl 2P of CPU-d MCS modified silicon wafer.

The successful deposition of CPU-dMCS that acts as an ATRP initiator was verified by XPS. Figure 4-1-1 (a), 4-1-1 (b), and 4-1-2 (c) show XPS data of a) C 1s, b) Cl 2s, and c) Cl 2p, respectively, for the CPU-dMCS monolayer prepared by immersion into the CPU-dMCS toluene solution for 84 hours at 60 °C. The asymmetric C 1s peak is composed of three components as follows: 1) a small peak around 288.5 eV corresponding to unsaturated carbon in the carbonyl group, 2) a band around 285.6 eV due to a carbon adjoining the carbonyl group and carbon in the $–OCH_2$ group, and 3) a band at around 284.7 eV attributed to saturated carbon in the alkyl chain,[42] which proves the immobilization of CPU-dMCS on a silicon wafer (Figure 4-1-1a). Initiator immobilization is also apparent from the appearance of chlorine peaks in the XPS data (figure 4-1-1b and figure 4-1-2c). We used CPU-dMCS and MPU-dMCS, which has no reactive site, with vinyl monomers to make mixed monolayers to control the polymer density. CPU-dMCS and MPU-dMCS are both alkyldimethylsilane derivatives with a long alkyl chain and one hydrolyzable group. Since these derivatives are similar in chemical structure, homogeneously mixed membranes must be formed on the surface of a silicon wafer depending on the composition in the precursor solution. We formed mixed monolayers on a silicon wafer using stock solutions ranging from 0% to 100% of CPU-dMCS. Figure 4-1-3(a) shows the change in the water contact angle for the mixed monolayers prepared by immersion into the various CPU-dMCS/MPU-dMCS mixed toluene solutions for 84 hours at 60 °C. The water contact angles on the monolayers monotonically decreased with the amount of CPU-dMCS in the precursor solutions. The increase in the composition of CPU-dMCS in the monolayers on a silicon wafer was confirmed by the decrease in the contact angle because CPU-dMCS ha a slightly more hydrophilic character than MPU-dMCS. The contact angle measurement implies that the ratios of CPU-dMCS and MPU-dMCS in the monolayers are at least similar to the ratios in the stock solutions.

The Cassie equation is an empirical expression that relates the macroscopic contact angle of a pure fluid on an atomically smooth, but chemically heterogeneous, solid surface,

$$\cos\theta = f_1\cos\theta_1 + f_2\cos\theta_2 \qquad (1)$$

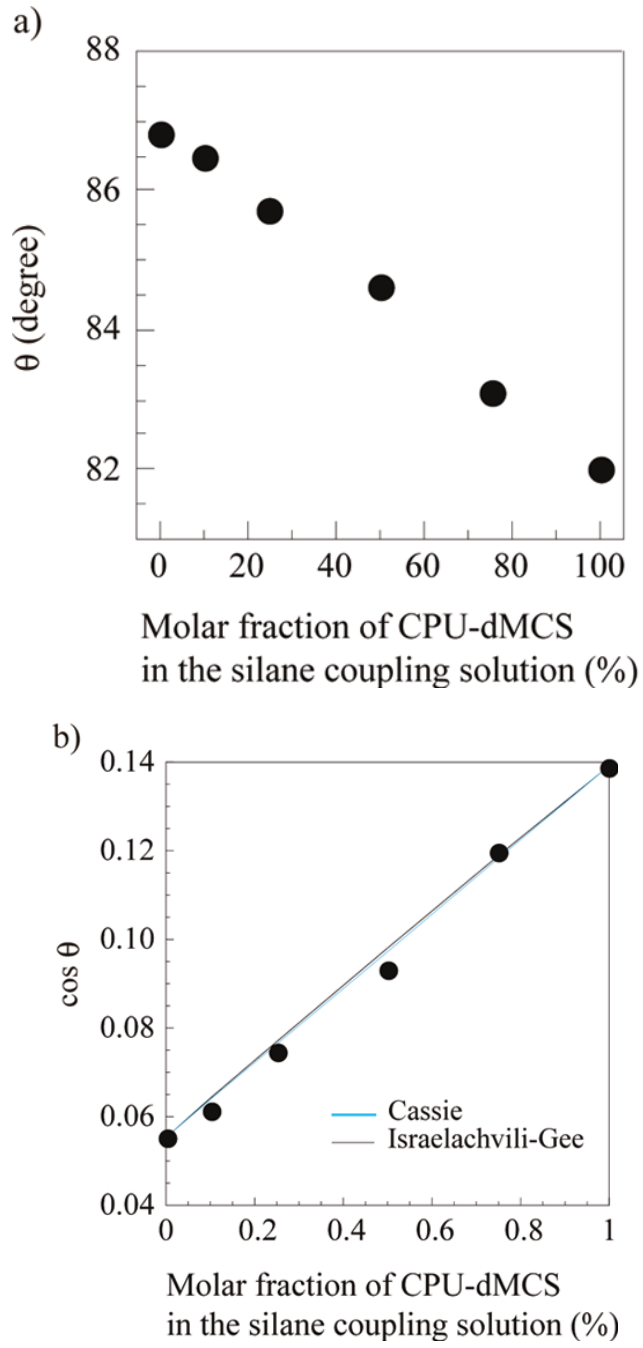


Figure 4-1-3(a) Static contact angle of water on CPU-dMCS/MPUdMCS modified silicon wafer at 20 $^{o}$C as a function of molar fraction of CPU-dMCS in silane coupling reaction solution. (b) Experimental result in part a compared with two theoretical treatments, the Cassie equation and the Israelachvili-Gee equation

where $f_i$ is the area fraction of component i and $\theta_i$ is the contact angle of the fluid on a surface of pure i.[43] When the size of the domains, composed of each component, approaches molecular dimensions, the Israelachvili-Gee equation should be used.[44]

$$(1 + \cos\theta)^2 = f_1(1 + \cos\theta_1)^2 + f_2(1 + \cos\theta_2)^2 \qquad (2)$$

In Figure 4-1-3 (b), the simulation results using both the Cassie equation and the Israelachvili-Gee equation for the water contact angles are compared with the experimental data. Because there is no difference between the two simulation results due to the small change in $\theta_1$ and $\theta_2$, good agreement is seen between each simulation result and the experimental results. Thus, we can apply either equation to analyze a chemically heterogeneous system with a small change between the contact angles of the fluid on each surface of pure i. This conclusion must be applicable to any contact angle measurement method, such as the captive bubble method.

### 4.3.2. ATRP of NIPA for Preparation of Grafted Membrane.

The best approach to the synthesis of a well-defined high-density brush is the "grafting from method" using a surface bound initiator.[45-47] The surface initiated ATRP of NIPA onto a silicon wafer and Au-deposited mica has been reported, but in many cases, the authors do not give molecular weight and polydispersity data. [48-59] Judging by our additional examinations, many cases of surface-initiated ATRP of NIPA on a flattened surface such as silicon, the thickness of the grafted PNIPA membranes cannot be well-controlled according to the living polymerization system (Figure 4-6). Moreover, the densities of the grafted PNIPA membranes are in diluted or semi-diluted regions, and as a result, the intermolecular interaction between grafted polymers is not significant due to the poor choice of the polymerization systems. However, ATRP is attractive because it can provide good control over predictable polymer molecular weight, PDI and end groups as long as the conditions are suitable. The appropriate selection of experimental conditions, such as initiators, catalysts, solvents, and temperatures for ATRP, results in polymers with high conversions, low PDIs, and defined average polymer molecular weights. So far, ATRPs of acrylamide derivatives have been attempted with several conditions, but these attempts were fraught with difficulty in many cases.[60,61] Catalyst inactivation, low values of ATRP equilibrium constants, and displacement of the terminal halide have been recognized as complicating factors during polymerization. However, recent research has induced solution

approaches for ATRP of acrylamide derivatives.[62,63] Some researchers believe that Cu salts tend towards the polymer chain ends and stabilize the radicals. This stabilization retards the deactivation step in ATRP and produces an unacceptably high concentration of radicals that leads to spontaneous termination reactions. These results were attributed to the occurrence of slow deactivation in conjunction with fast activation and to the loss of bromine end groups through a cyclization reaction involving nucleophilic Br displacement by the penultimate amide nitrogen. The use of Cl instead of Br should decrease the risk of nucleophilic substitution of the halogen from the dormant chain end. When linear amines or bipyridine based ligands were employed, acrylamide derivatives were not polymerized controlled by ATRP. The combination of a chloropropionate functionalized initiator and $Me_6$TREN as the ligand was found to be an effective system for the ATRP of acrylamide derivatives.[62-64] Consequently, using alkyl chlorides rather than bromides as initiators in conjunction with $Me_6$TREN as a ligand improved control. Moreover, DMSO was chosen as the solvent for ATRP of NIPA on the premise that a solvent with the electron-pair donating property could interact with the amide groups of NIPA and thus reduce their interaction with both the catalyst and the propagating chain end. In addition, DMSO is a good solvent for PNIPA over a very wide range of temperatures. The success of the ATRP of NIPA in pure water has been reported recently, but we did not choose the water reaction system because of the high sensitivity of the PNIPA configuration in an aqueous solution.[65] Thus, we used CPU-dMCS as a surface-modified initiator, CuCl/$Me_6$TREN as a catalytic system, and DMSO as a solvent.

To form a PNIPA brush from the surface bound initiator, ECP was added as a free initiator in the reaction solution to control the polymerization process. Without the free initiator, the concentration of $Cu^{II}$ complex produced from the reaction at the surface becomes too low to deactivate the active chain ends of polymers with a sufficiently high rate. The concentration of $Cu^{II}$ complex can be raised and automatically adjusted by adding the free initiator.[24] Furthermore, we can obtain information about the polymerization product, such as the average polymer molecular weight and PDI in the brush, by observing those of the free polymer because good agreement in the number average molecular weight ($M_n$) and PDI between the graft and free polymers has been confirmed by several research groups.

The ATRP in this condition provides high conversion, reaching about 81 % in 10 h, but the first-order kinetic plot shows noticeable curvature (Figure 4-1-4 (a)). However, the GPC traces were reasonably symmetrical with no shoulders and tailing even at higher conversions (Figure 4-1-4 (b)). Moreover, $M_n$ increased linearly with conversion, and the PDI remained low throughout the polymerization (Figure 4-1-4 (c)), which indicates that the growing centers were not lost during the reaction. Thus, the apparent curvature of the plot in Figure 4-1-4 (a) is attributed to a progressive reduction of the concentration of the available catalyst rather than chain termination. $M_n$ obtained by GPC was comparable to the target molecular weight at each time point, wich also demonstrates that the initiator is efficient. Additionally, the PDI decreased from 1.34 to 1.21 with increasing conversion, which also proves the living process.[23]

The thicknesses of the dried polymer grafted membranes ($L_d$) on the silicon wafers were determined by AFM imaging across the boundary of a scratched and an unscratched region. An almost linear relationship between the brush thickness and the molecular weight can be seen in Figure 4-1-4 (d). These data demonstrate that chain growth from the surface of the substrate is also a controlled process in keeping with the nature of this ATRP reaction in solution. In this condition, $L_d$ can be grown to over 60 nm. The value of $R_{RMS}$ for sample No. 5', which is the thickest membrane in this series, is 0.60 nm over 25 $\mu m^2$ using the AFM (Fig. 4-1-5), which shows that the surface is very smooth. To obtain a thicker dried grafted membrane with the same graft density, we tried to raise the ratio of NIPA to initiator because the theoretical $M_n$ for an ideal ATRP reaction can be increased by increasing the ratio. Figure 4 show the results for the ATRP of NIPA depending on the ratio of NIPA to initiator. The experimentally obtained $M_n$ is also very consistent with the theoretical value of $M_n$, and the PDI remains narrow even at higher molecular weights (Figure 4-1-6 (a)). A linear increase in the thickness up to over 200 nm with chain length was observed (Figure 4-1-6 (b)), which indicates that the chain growth from the surface is a controlled process with a degree of living character to it and that the thickness of the membrane, which corresponds to the chain length, can be easily manipulated. As above, we have shown that the ATRP of NIPA using the combination of ECP as an initiator and CuCl/$Me_6$TREN as a catalytic

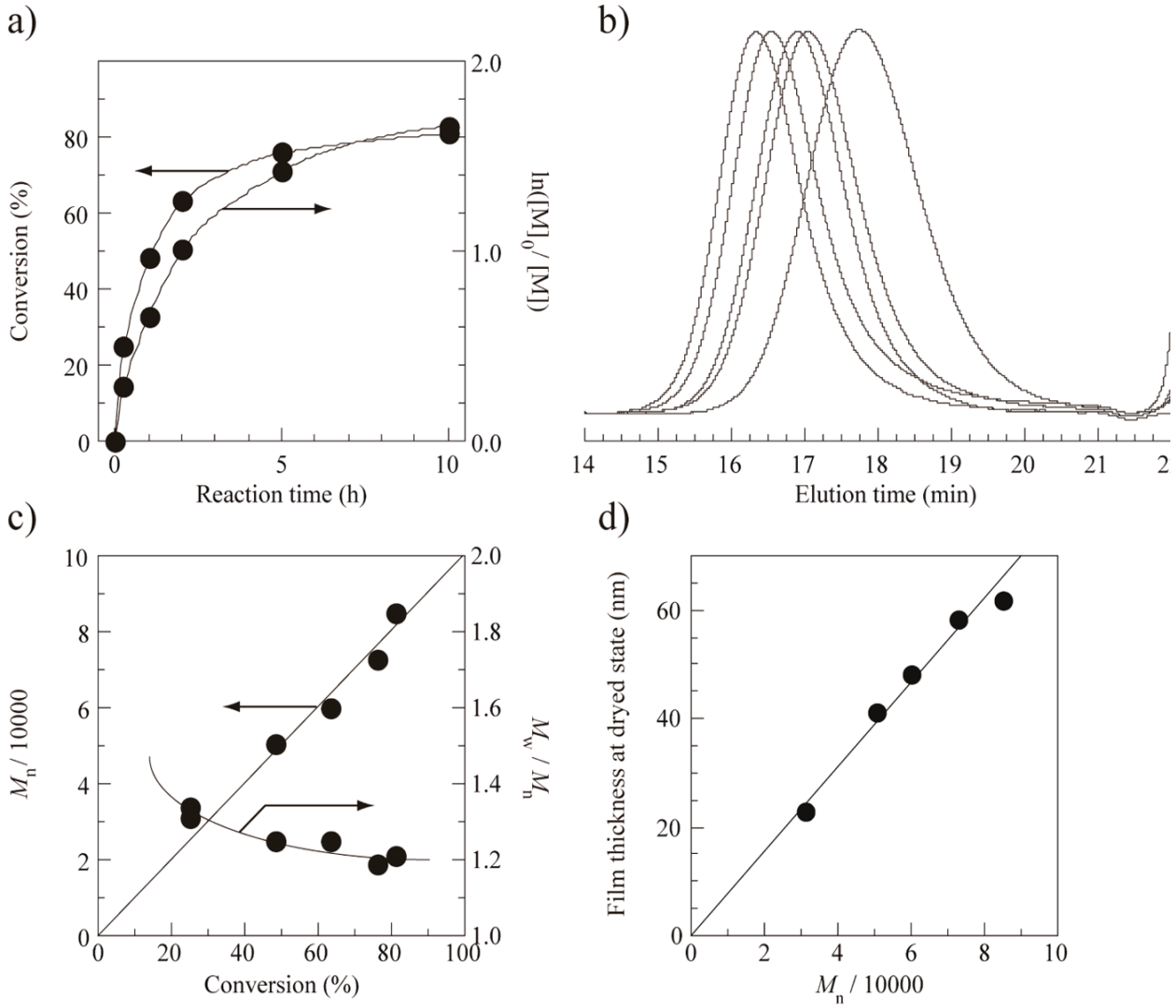


Figure 4-1-4. (a)Monomer conversion and kinetic plot with polymerization time during ATRP of NIPA. (b) Evolution of GPC traces with polymerization time during ATRP of NIPA. (c) Number-average molecular weight, $M_n$, and polydispersity index ($M_w/M_n$) versus conversion plots. The straight line corresponds to the theoretical $M_n$ versus conversion, (d) Plots of dried thickness of polymer grafted membrane versus $M_n$

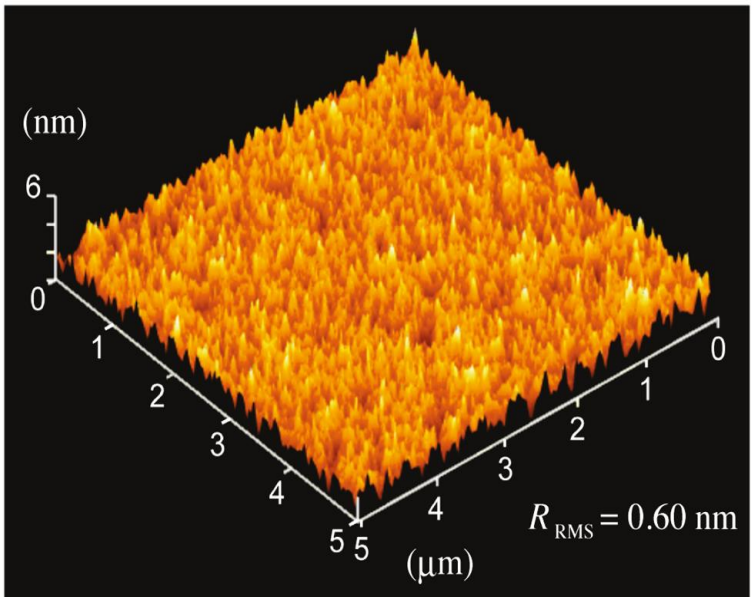


Figure 4-1-5: AFM image of densely grafted dried PNIPA membrane, sample no. 5`.

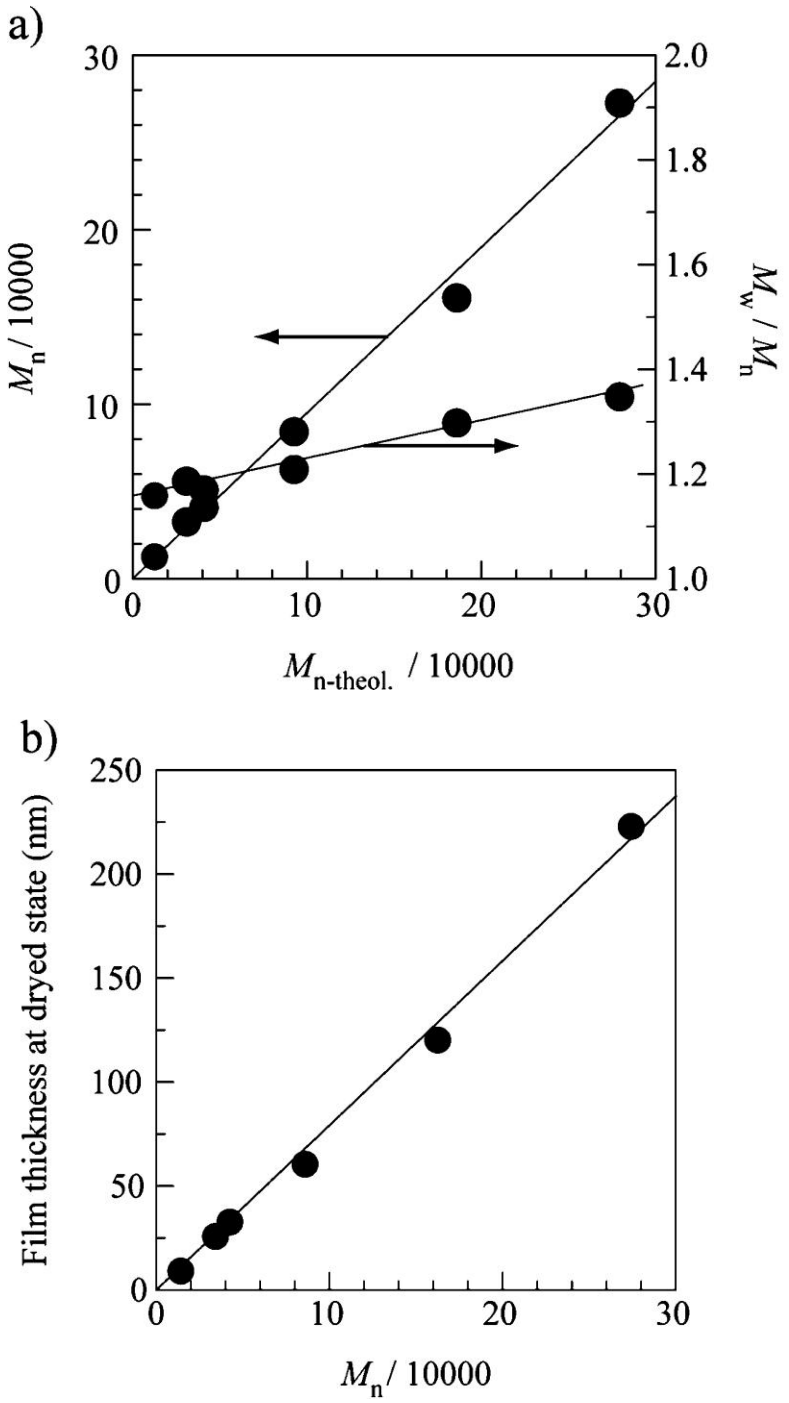


Figure 4-1-6 (a) Number-average molecular weight, $M_n$, and polydispersity index ($M_w/M_n$) versus theoretical $M_n$ plots. (b) Plots of dried thickness of polymer grafted membrane versus $M_n$.

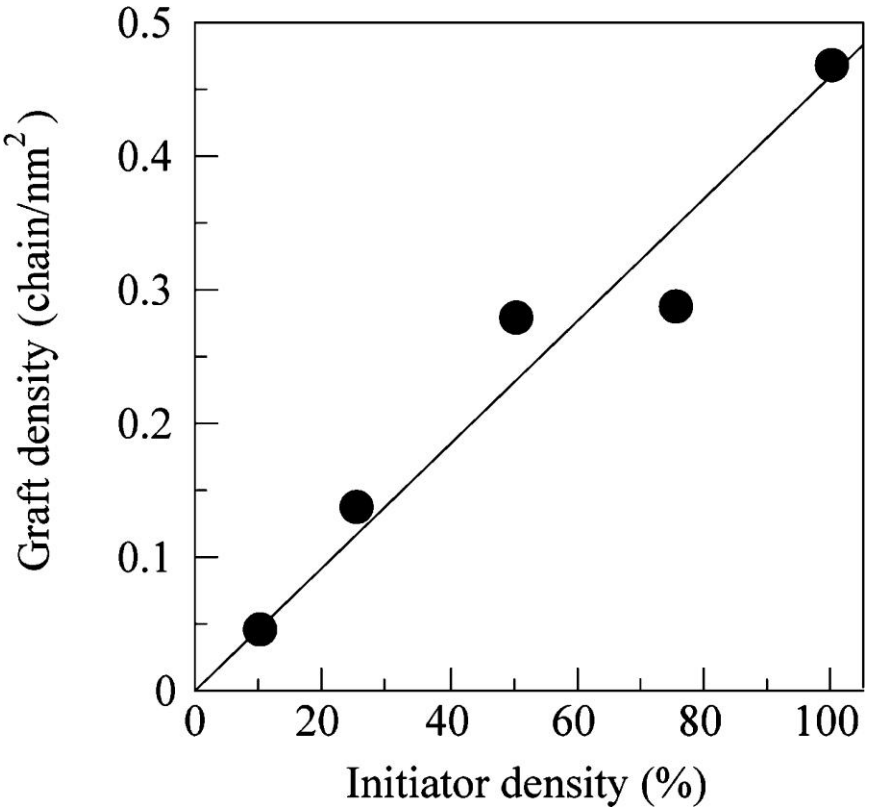


Figure 4-1-8. Graft density of PNIPA versus initiator density estimated from the ratio of CPU-dMCS and MPU-dMCS in the stock solutions.

system in DMSO at 20 °C was successful in producing narrow disperse PNIPA with high conversion and good molecular weight control.

From the slope of the line in Figure 4-1-5 (d) and 4-1-6 (b), the graft density $\sigma$ can be estimated by the following equation.[66]

$$\sigma = L_d \rho N_A / M_n \qquad (3)$$

where $\sigma$ is the mass density of PNIPA (1.042 g/cm$^3$) and $N_A$ is Avogadro's number. The graft densities are virtually constant around 0.5 chain/nm$^2$: the cross sectional area of the grafted PNIPA is ~ 200 Å$^2$. For comparison, we calculated the contour lengths of the directionally fully stretched PNIPA chains ($L_c$) using a C-C bond length of 1.54 Å and a ∠CCC of 110.5 ° based on $M_w$ and show the result with the experimentally obtained values of $L_d$ (Figure 4-1-7).[67] For any samples, the thickness in the dry state is more than 25% of the fully stretched polymer chain length ($L_d/L_c$), which indicates that the polymers are directionally extended perpendicular to the surface of the substrate compared with their unperturbed dimensions.[45-46] This result shows that PNIPA chains in these dried membranes are directionally extended states with an extremely high graft density regardless of the molecular weight. When we used the CPU-dMCS/MPU-dMCS mixed monolayer on the silicon wafers shown above, the graft density of PNIPA is also controlled by the initiator density (Figure 4-1-8). If the alkyldimethylsilane derivatives formed densely packed states, the graft density of PNIPA could be constant above ca. 20% of the initiator density. However, the graft density of PNIPA is proportional to the initiator density, which also suggests that the alkyldimethylsilane derivative modified substrates did not reach the densely packed state. As above, we successfully demonstrated that the ATRP of NIPA at the initiator modified silicon surfaces could be conducted in a well-controlled manner, which resulted in PNIPA grafted membranes with tunable polymer thickness and density.

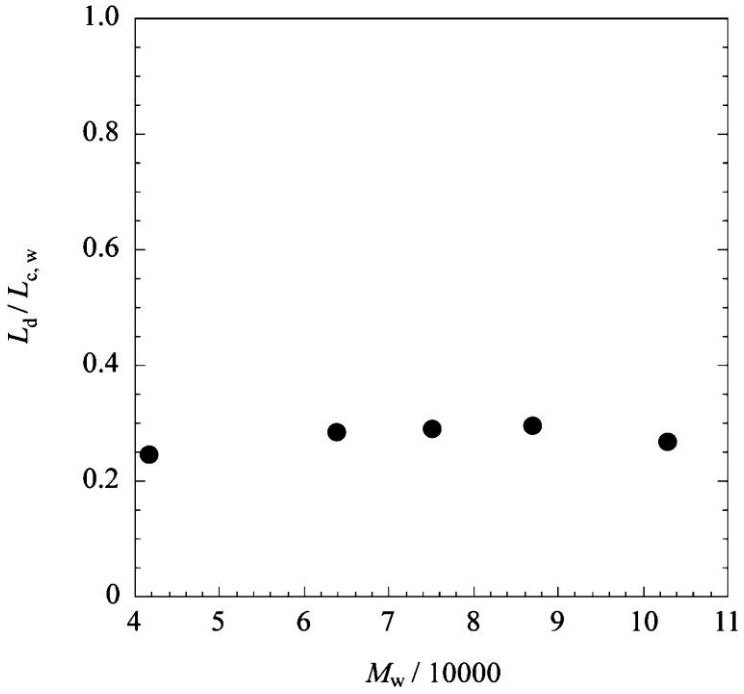


Figure 4-1-7. Plots of $L_d/L_{c,w}$ versus weight-average molecular weight, $M_w$

### 4.3.3. Change in Thickness of High-Density Grafted Membrane of PNIPA in Water with Changing Temperature.

Figure 4-1-9 shows the change in the thickness of the high-density grafted membrane of PNIPA with $L_d$ of 121 nm (sample No. 10') in water with changing temperature. Polymer chains grafted on a flat substrate at one end with an extremely high graft density can be stretched further in good solvents. The greatest value of $L_s/L_c$ of 0.47, where $L_s$ is the thickness of the grafted membrane in a solvent, indicates that the graft chains in this membrane in water at 19 °C are in a highly extended state: PNIPA chains in the membranes under this condition form so-called "high density brushes". Even at the fully collapsed state in water at 36 °C, the value of $L_s/L_c$ is 0.32, which indicates that the polymer chains are in a more extended state than the dried state. This observation suggests that the interaction between the PNIPA chains and water molecules in the membrane is significant even in the fully collapsed state. In addition, the gradual collapse of the PNIPA-grafted membrane was assessed by measuring its thickness by AFM in water with increasing temperature. Theoretical predictions suggested that the collapse of surface-tethered polymer brushes accompanying the solubility transition proceed continuously over a much broader range as the solvent quality decreases, which is distinct from the behavior of free flexible chains adopting random coil conformations in solution. The change in the thickness of our high-density brush in water is amenable to the theory.

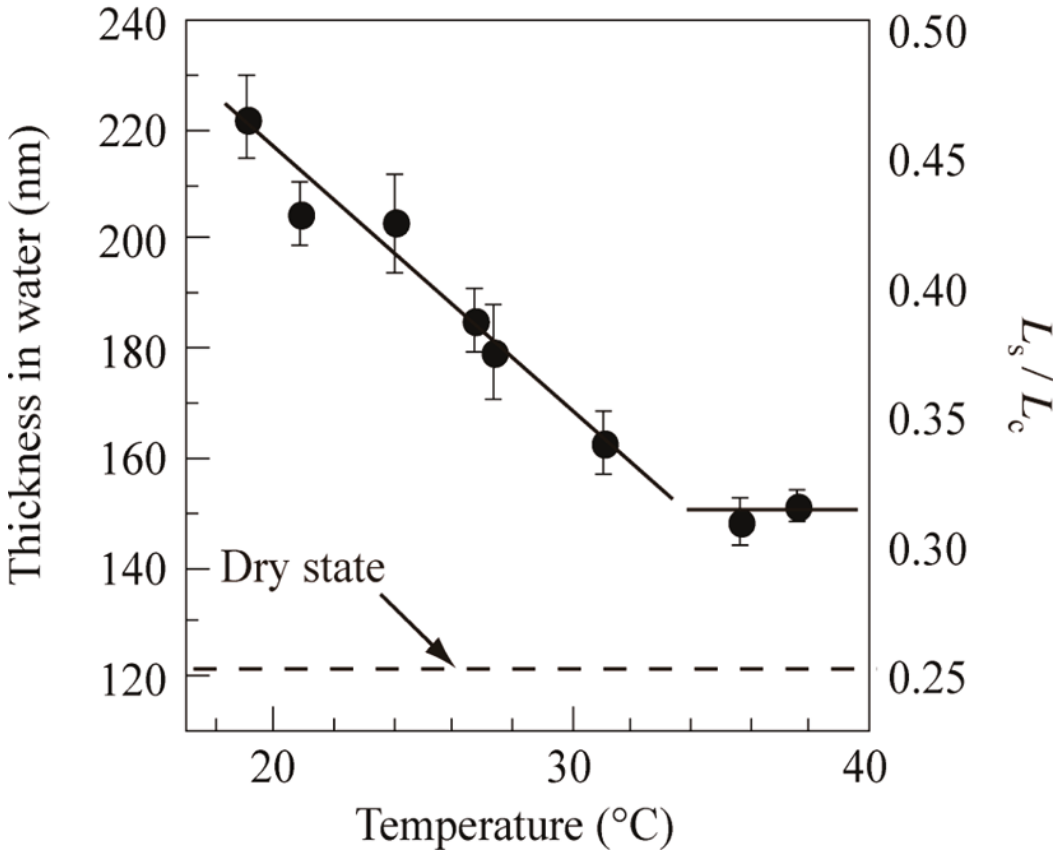


Figure 4-1-9. Thickness of high density grafted membrane of PNIPA (sample No.10`) as a function of temperature in water

### 4.3.4. FT-IR to Observe Molecular Behavior of PNIPA in Grafted Membrane under Water.

To observe the molecular behavior of the polymer chains in the membranes, we measured the FT-IR spectra of the grafted membranes in water at several temperatures. FT-IR observation is a powerful method to elucidate interaction information at the molecular level. In our intended system, the vibrations of amide groups in PNIPA chains are highly sensitive to changes in the conformation of the polymer chains and in the interaction with solvent molecules.[69] In this study, we used $D_2O$ as a solvent instead of $H_2O$ because the bending vibration band of $H_2O$ observed around 1600 $cm^{-1}$ overlaps the amide I band, whereas that of $D_2O$ appears around 1200 $cm^{-1}$. During the change in temperature across the LCST for the PNIPA linear polymer in a solution state, an isosbetic point can be observed at 1637 $cm^{-1}$ (Figure 4-7). Isosbetic behavior means that there exist two absorption peaks that have a constant position, and only the intensities of these peaks change. There are various views on the assignment of these peaks.[69-72] Maeda et al. state that the lower wavenumber peak observed around 1625 $cm^{-1}$ may be assigned to the C=O group that is bound to water molecules, and the higher one observed around 1650 $cm^{-1}$ may be the C=O group interacting with the neighboring N-H group via hydrogen bonding. [69] On the other hand, Katsumoto et al. propose that the peak at around 1625 $cm^{-1}$ is mainly due to a stretching

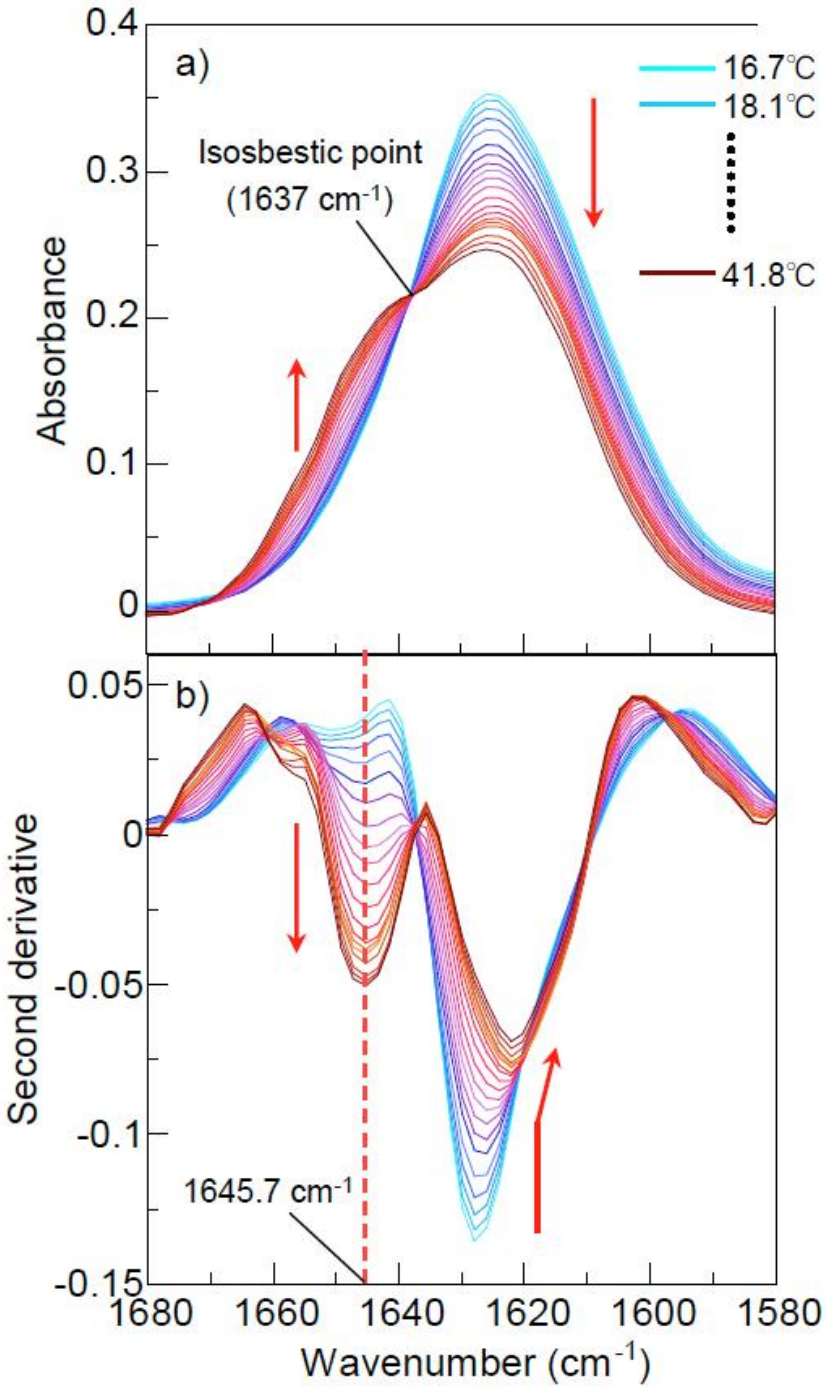


Figure 4-7. a) FT-IR spectra and b) second derivatives in Amide I region of linear PNIPA in $D_2O$ measured at various temperatures.

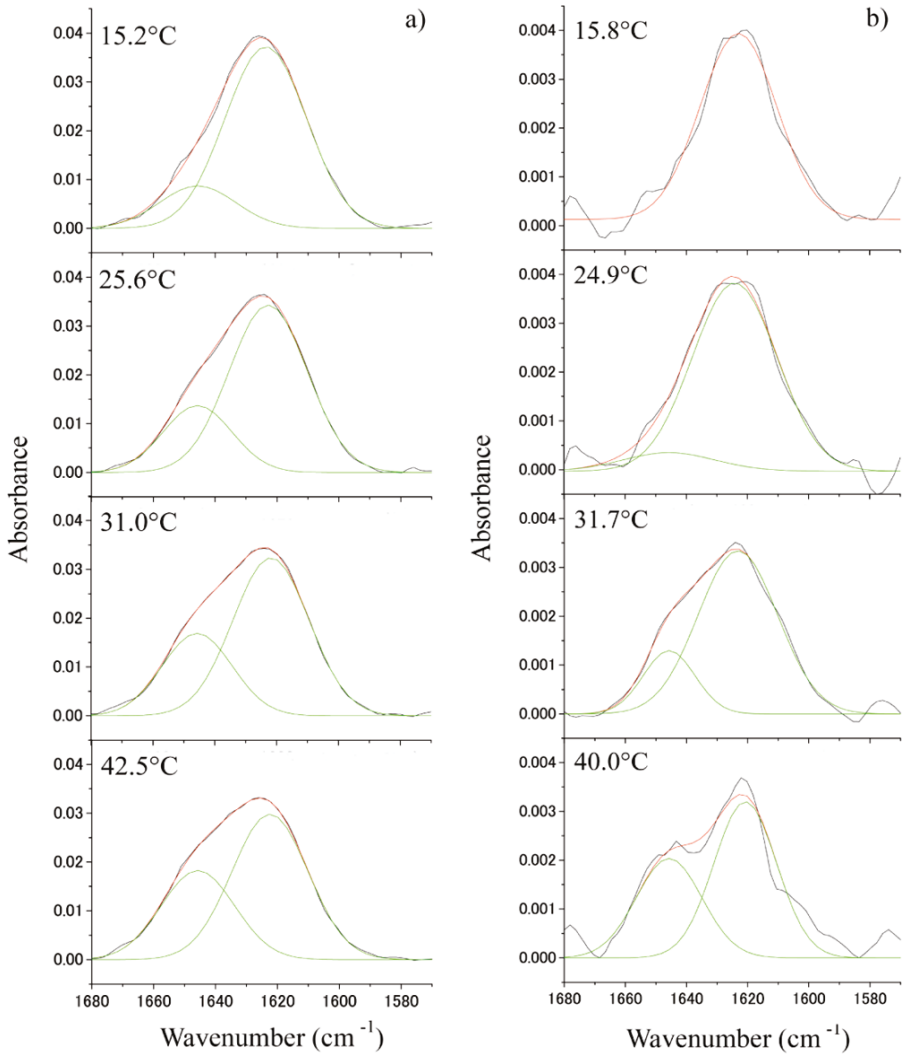


Figure 4-1-10: IR absorption spectra in amide I region for PNIPA grafted membranes with different graft densities at several temperatures. Black line: baseline subtracted amide I band, red line: curve fitted peak, green line: best fitted single Gaussian component. (a) $\sigma = 0.48$ chains/nm$^2$; (b) $\sigma = 0.06$ chains/nm$^2$.

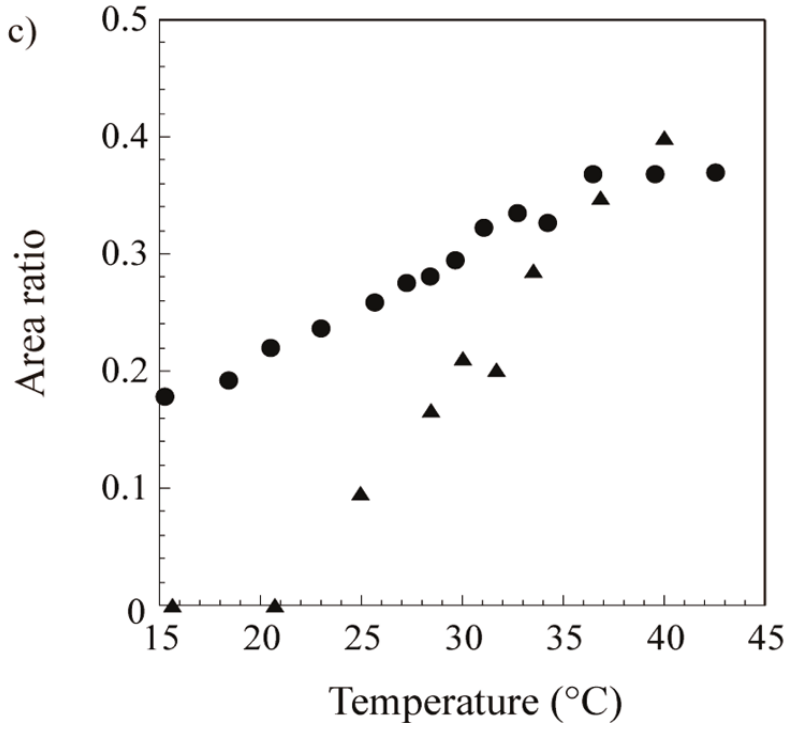


Figure 4-1-10 (c): Area ratio for the two components in amide I band versus temperature. The area ratio is calculated as follows: the area ratio= area of 1650 $cm^{-1}$ component/total area of amide I band.

vibration of the C=O group forming a strong hydrogen bond with the neighboring N-H group, while the peak at around 1650 $cm^{-1}$ may be due to the free C=O group.[70] Maeda et al. suppose that PNIPA chains form hydrogen bonding between the amide groups above the LCST, whereas Katsumoto et al. suggest that the hydrogen bonding between the amide groups formed below the LCST is broken above the LCST. Other groups' results using $^{1}$H-NMR and UV resonance Raman spectra show that the C=O group forms hydrogen bonds with two water molecules lower than the LCST, while the C=O group interacts with only one water molecule on average above the LCST.[71] As described above, there is still room for this argument, but their common view shows that the interaction between the C=O group of the polymer chains and water molecules can be changed drastically in the vicinity of the LCST. Therefore, to investigate the molecular situation of the PNIPA chains in the grafted membranes, we observed the change in the absorption peaks around the vibrations of amide groups in PNIPA resulting from temperature change. Figure 4-1-10 (a) shows the amide I band of a high-density polymer brush with a graft density of 0.48 chains/$nm^2$ composed of PNIPA with an $M_n$ of 187000 and $M_w/M_n$ of 1.40 measured in $D_2O$ as a result of temperature changes. As the temperature increased from 15.2 °C to 42.5 °C, the amide I band of PNIPA showed a change in waveform. The amide I band could be separated into two components centered at 1625 $cm^{-1}$ and 1650 $cm^{-1}$ at any temperature. The intensity of the peak at 1625 $cm^{-1}$ decreased with temperature, while that at 1650 $cm^{-1}$ increased. On the other hand, the amide I band of a grafted PNIPA membrane with a graft density of 0.06 chains/$nm^2$ and composed of PNIPA with $M_n$ of 187000 and $M_w/M_n$ of 1.41 measured in $D_2O$ at 15.8 °C consists of a single Gaussian component centered at 1625 $cm^{-1}$ (Figure 4-1-10-(b)). The second component centered at 1650 $cm^{-1}$ appeared as the temperature increased. This behavior is nearly identical to that of the amide I band of linear PNIPA in a solution state. Figure 4-1-10 (c) shows the temperature-dependent area ratio of these components for each sample. For the lower-density PNIPA grafted membrane, the peak at 1650 $cm^{-1}$, which does not appear when the solution temperature is below 20 °C, intensifies abruptly as the temperature increases. This increase suggests that the PNIPA chains exhibit a coil-globule-like transition similar to the transition shown by linear PNIPA in a solution (Figure 4-8). At the same time, for the densely grafted PNIPA chains on the silicon substrate, the peak at 1650 $cm^{-1}$ accounted for about 18%of the total area of the spectram shown in the Figure 4-1-10 (a) at 15.2 °C, which means that

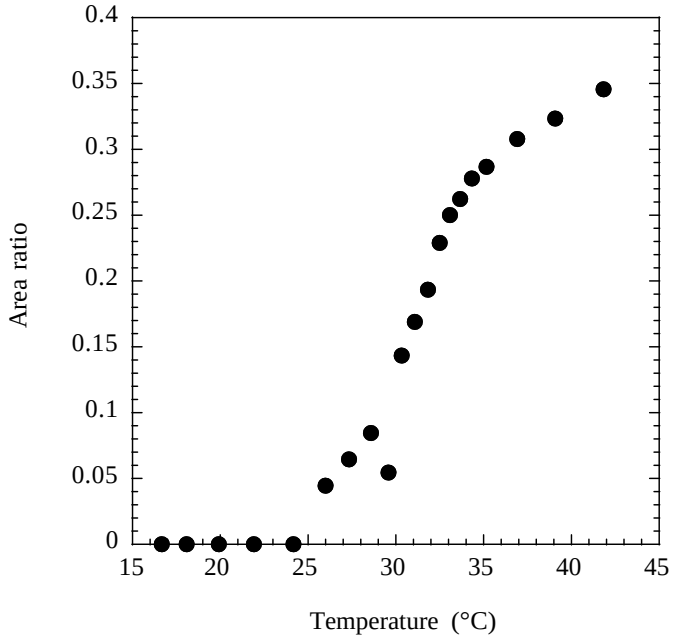


Figure 4-8. Evolution of area ratio of high wavenumber component of Amide I band of linear PNIPA in $D_2O$ as a function of temperature.

the PNIPA chains partly behave like a collapsed state at a sufficiently low temperature. As above, the PNIPA chains in the high-density brush are in a physically constrained state and cannot fully interact with water molecules. As a result, perhaps, the thickness of the membrane changed continuously over a much broader range with changes in temperature.

### 4.3.5. Contact Angle of Air Bubble underneath PNIPA Grafted Membranes under Water.

Through FT-IR observation, we can understand changes in the molecular behaviors of PNIPA on the inside of the grafted membranes, while the molecular behaviors on the surface can be examined by contact angle measurements. The surface thermo-sensitivities of the PNIPA grafted membranes were assessed by the captive air bubble method. Generally, the hydrophilicity/hydrophobicity of material surfaces can be determined by the sessile drop method. To examine the hydrophilicity of water-soluble polymer grafted membranes and hydrogels, however, applying the sessile drop method is inappropriate because of the continuous change in the conformation and swollen state of polymers due to the strong interaction between the polymers and water molecules in addition to the evaporation of water. In contrast, the contact angle measurement using a captive air bubble is a versatile and reproducible technique to quantify the extent of hydrophilicity/hydrophobicity of water-attracting polymeric substrates in contact with water. Figure 4-1-11 (a) shows equilibrium contact angles of an air bubble resulting from temperature changes underneath the PNIPA grafted membranes composed of different molecular weights but with the same graft density of approximately 0.5 chains/nm$^2$ in water. These changes in the contact angles of air bubbles disagree with the past results for polymer grafted membranes composed of PNIPA.[73] For example, at 11 °C when the brush is swollen with water, the contact angle of the air bubble underneath the membrane composed of PNIPA with 52000 in $M_n$ is about 141 °. The contact angle decreased with an increase in temperature up to 24 °C as shown in previous systems but then jumped up to 137 ° around 30 °C. Although the net change of the contact angle is small, this temperature-dependent contact angle behavior has not been observed before. The PNIPA brushes, composed of different molecular weights but with nearly identical $\theta$ values of around 0.5 chains/nm$^2$, undergo a similar change, while the absolute values over all temperatures decrease as the molecular weight decreases. The reason for the

(a)

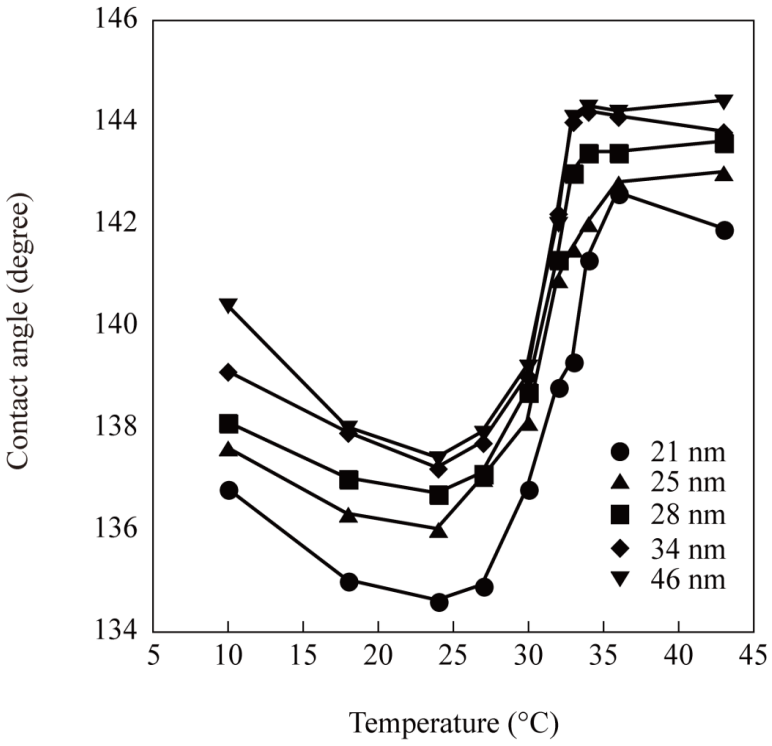


Figure 4-1-11 . Contact angle of air bubble underneath PNIPA grafted membranes in water, (a) for the same high density PNIPA brushes with different molecular weight

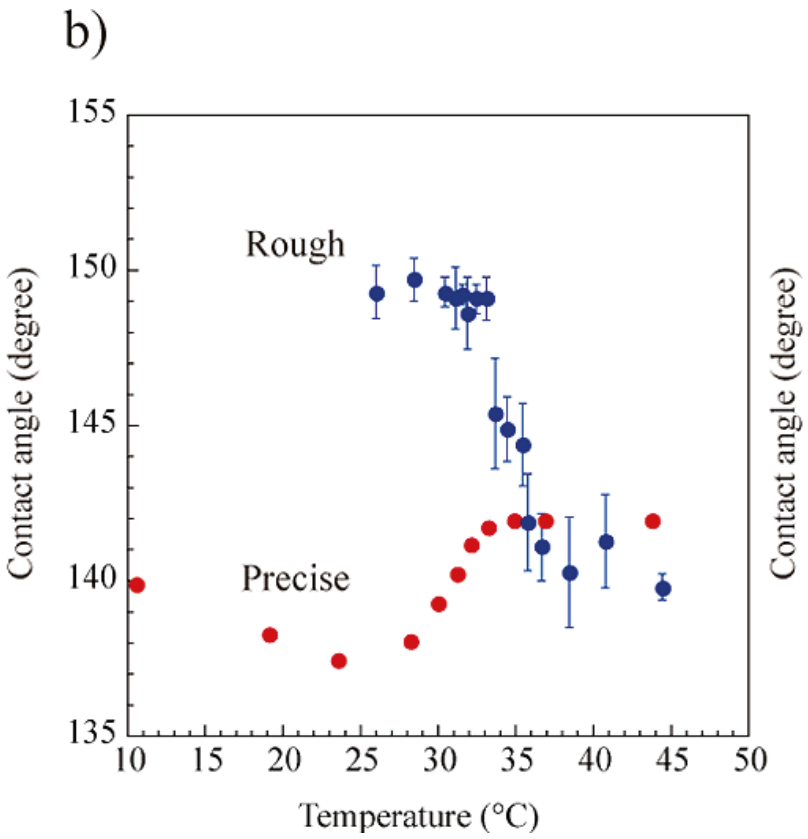


Figure 4-1-11. Contact angle of air bubble underneath PNIPA grafted membranes in water, (b) for the high density PNIPA brush with 85000 inMn shown in part a compared with the roughly prepared PNIPA grafted brush.

(c)

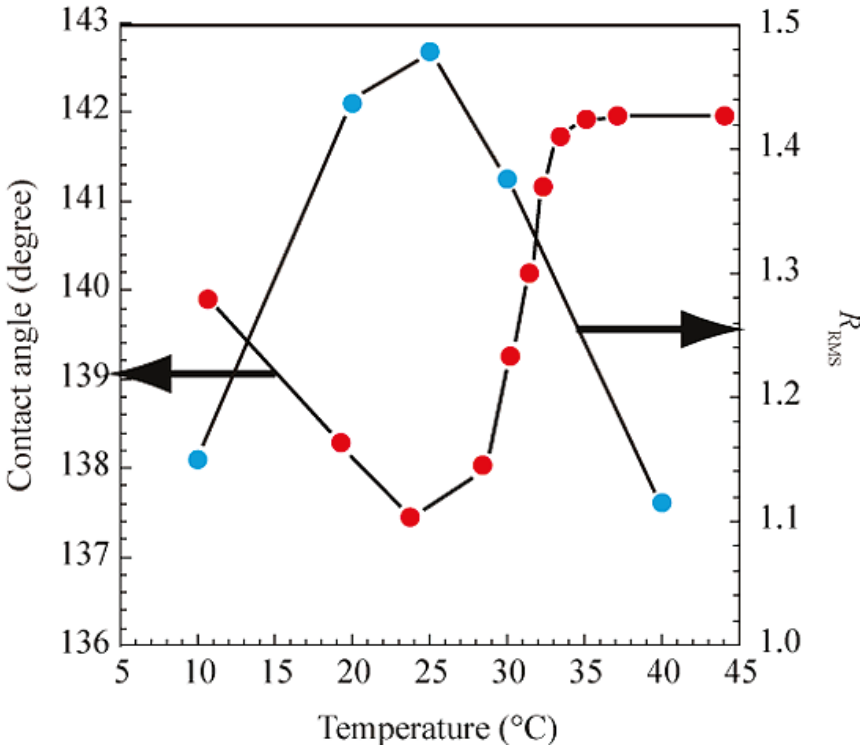


Figure 4-1-11. Contact angle of air bubble underneath PNIPA grafted membranes in water, (c) temperature dependent contact angle of air bubble underneath the high density PNIPA brush with 52000 in Mn shown in part a is compared to the change in the surface roughness with changing temperature.

decrease in $\theta$ with the molecular weight is not yet understood, but a similar change is also observed in other thermo-sensitive polymer brushes. The increase in the lateral expansion of the grafted polymers in response to an increased of the thickness may affect the contact angle.[74-75] Compared to roughly prepared PNIPA brushes, the contact angles for these precisely prepared high-density PNIPA brushes drop dramatically at lower temperatures while the ones at higher temperatures increase slightly.

Compared to roughly prepared PNIPA brushes the contact angles for these precisely prepared high-density PNIPAbrushes drop dramatically at lower temperatures while the ones at higher temperatures are almost same or increase only slightly Figure 4-1-11(b). From the FT-IR observation, the decrease in the contact angle of the air bubble for the high-density PNIPA brushes at lower temperatures may be partly attributed to the decrease in the hydration ability of the polymer chains even in the vicinity of the surfaces. The most important parameters controlling wettability are the surface roughness, the relative area contributions of the chemically different portions of the surface, and their respective surface energies. If the surface is composed of single component rough surface and the size of an air bubble is sufficiently larger than the roughness scale, the Wenzel equation, considering the roughness of a surface, can be applied in the following form:[43]

$$\cos\theta = r \cos \theta_{Y} \qquad (4)$$

where $r$ is the roughness factor, which is the ratio of the actual and projected surface areas, and $\theta_{Y}$ is the Young contact angle (i.e., the intrinsic contact angle as calculated from Young's equation[76]). The value of $r$ is always greater than 1. This equation states that the presence of roughness makes a hydrophilic surface more hydrophilic and a hydrophobic surface more hydrophobic than a flat surface with the same chemical composition. Since the values of $\theta$ in our system are larger than 90 ° at any temperature and the surfaces are categorized as hydrophilic surfaces, the increment in the roughness factor intensifies the values of $\theta$. To examine the change in the surface roughness of the precisely prepared high-density PNIPA brush, the values of $R_{RMS}$ for the samples in water were measured by AFM at different temperatures. Figure 9c shows the temperature-dependent change in $R_{RMS}$ for sample No. 5' and compares it with the equilibrium contact angles of air bubbles underneath the sample in water resulting from temperature changes.

The temperature dependence for the values of $R_{RMS}$ shows a maximum at about 25 °C, whereas the values of $\theta$ with changes in temperature show a minimum at about 25 °C. Considering that the fluctuation of the polymer densities in solution systems and gel systems increase near the LCST, the maximum value of $R_{RMS}$ at about 25 °C must be attributed to maximizing the fluctuation of polymer densities in the brush.[77-78] If we applied the Wenzel equation to explain the change in $\theta$ with the variation of $R_{RMS}$, the temperature dependence for the values of $\theta$ would also show a maximum at about 25 °C. However, just the opposite change occurred in our systems.

As the conformation of grafted polymers can change in the membrane due to temperature changes, the chemical composition on the surface of the membrane may also change because it is significantly influenced by the change in the interaction between polymers.[79] For this reason, we have to consider changes in chemical composition on the surface of the membrane with changes in temperature. If the surface is chemically heterogeneous with roughness, the Cassie equation is modified to account for the real contact areas between the bubble and the surface.[43] For a two-component surface, the roughness of both components of the surface can be considered by introducing the parameter $r_i$ to describe the respective ratios between the real area of the rough surface divided by the projected two-dimensional areas.[80]

$$\cos\theta = r_1 f_1 / (r_1 f_1 + r_2 f_2)\cos\theta_1 + r_2 f_2 / (r_1 f_1 + r_2 f_2)\cos\theta_2 \qquad (5)$$

The nature of the terminal groups of the elongated polymers significantly affects the contact angle of the surface of the PNIPA brushes. As the polymer chains are flexible even in the condensed brush state, the end groups of the grafted chains can move near the surfaces. The results for the temperature-dependent contact angles may be interpreted by assuming that the terminally chlorinated alkyl groups of the elongated polymers can be positioned on the surfaces or can be hidden in the vicinity of the membranes, depending on temperature. If the chemical compositions on the surfaces can be varied by changing the temperature and more than two components participate in the variation, the theoretical explanation should be more complicated due to a variety of factors. At present, because detailed experimental information on the chemical compositions of water surfaces as the temperature varies had not been available, we cannot verify the hypotheses. Moreover, because the displacement of the end groups to more

hydrophilic or hydrophobic groups can be achieved for this polymer, the contribution of end groups to this characteristic change in the contact angle must be elucidated. Studies to confirm these hypotheses are being performed.

## 4.4 Conclusions.

High-density thermo-sensitive PNIPA brushes can be successfully prepared under carefully controlled conditions. We have performed a systematic study of the physicochemical properties of the brushes. The gradual decrease in the thickness of the densely grafted brushes with temperature was assessed by AFM in water. In general, grafted membranes and gels have both high swelling and high shrinking abilities that result in abrupt changes in thickness. Meanwhile, comparing the fully collapsed thickness with the dried thickness, we observed a significant interaction between PNIPA chains and water molecules in the brush, even in the fully collapsed state in water at 36 °C. In addition, FT-IR data indicate that the PNIPA chains in the brush behave partially like a collapsed state even at a sufficiently low temperature, e.g., at 15.2 °C in water. As above, the PNIPA chains in the high-density brush are in a physically constrained state and cannot fully interact with water at low temperatures, but they can interact with a greater amount of water at high temperatures. As a result, the thickness of the brush changes continuously over a much broader range with changes in temperature. Furthermore, the contact angle of air bubble underneath the high-density polymer brush also gradually decreases up to around 25 °C in water, indicating that the hydrophilicity of the surface decreases like the typical PNIPA grafted membranes and gels. However, the value of the contact angle starts to increase dramatically from around the LCST of free PNIPA in water and becomes constant over 40 $^{o}$C. Eventually, the surface above 40 °C exhibits a more hydrophilic nature than that below the LCST. This temperature-dependent contact angle may be understood by assuming that the terminally chlorinated alkyl groups of the elongated PNIPAs can be positioned on the surfaces or hidden in the vicinity of the membranes, depending on the temperature.

**References and Notes.**

(1) Stuart, M. A. C.; Huck, W. T. S.; Genzer, J.; Muller, M.; Ober, C.; Stamm, M.; Sukhorukov, G. B.; Szleifer, I.; Tsukruk, V. V.; Urban, M.; Winnik, F.; Zauscher, S.; Luzinov, I.; Minko, S. Nat. Mater. 2010, 9 (2), 101–113.

(2) Ionov, L. J. Mater. Chem. 2010, 20 (17), 3382–3390.

(3) Liu, F.; Urban, M. W. Prog. Polym. Sci. 2010, 35 (1-2), 3–23.

(4) Luo, S. Z.; Xu, J.; Zhu, Z. Y.; Wu, C.; Liu, S. Y. J. Phys. Chem. B 2006, 110 (18), 9132–9139.

(5) He, Y. Y.; Lodge, T. P. Chem. Commun. 2007, 26, 2732–2734.

(6) Nagase, K.; Kobayashi, J.; Kikuchi, A. I.; Akiyama, Y.; Kanazawa, H.; Okano, T. Langmuir 2008, 24 (2), 511–517.

(7) Yoshida, R.; Uchida, K.; Kaneko, Y.; Sakai, K.; Kikuchi, A.; Sakurai, Y.; Okano, T. Nature 1995, 374 (6519), 240–242.

(8) Oya, T.; Enoki, T.; Grosberg, A. Y.; Masamune, S.; Sakiyama, T.; Takeoka, Y.; Tanaka, K.; Wang, G. Q.; Yilmaz, Y.; Feld, M. S.; Dasari, R.; Tanaka, T. Science 1999, 286 (5444), 1543–1545.

(9) Kim, S. W.; Bae, Y. H.; Okano, T. Pharm. Res. 1992, 9 (3), 283–290.

(10) Feil, H.; Bae, Y. H.; Feijen, J.; Kim, S. W. Macromolecules 1993, 26 (10), 2496–2500.

(11) Brannonpeppas, L.; Peppas, N. A. J. Controlled Release 1989, 8 (3), 267–274.

(12) Miura, M.; Cole, C. A.; Monji, N.; Hoffman, A. S. J. Biomater. Sci., Polym. Ed. 1994, 5 (6), 555–568.

(13) Hoffman, A. S. Adv. Drug Delivery Rev. 2002, 54 (1), 3–12.

(14) Nakayama, D.; Takeoka, Y.; Watanabe, M.; Kataoka, K. Angew. Chem., Int. Ed. 2003, 42 (35), 4197–4200.

(15) Stayton, P. S.; Shimoboji, T.; Long, C.; Chilkoti, A.; Chen, G. H.; Harris, J. M.; Hoffman, A. S. Nature 1995, 378 (6556), 472–474.

(16) Osada, Y.; Gong, J. P. Prog. Polym. Sci. 1993, 18 (2), 187–226.
(17) Wang, G. Q.; Kuroda, K.; Enoki, T.; Grosberg, A.; Masamune, S.; Oya, T.; Takeoka, Y.; Tanaka, T. Proc. Natl. Acad. Sci. U.S.A. 2000, 97 (18), 9861–9864.
(18) Hirokawa, Y.; Tanaka, T. J. Chem. Phys. 1984, 81 (12), 6379–6380.
(19) Alvarez-Lorenzo, C.; Guney, O.; Oya, T.; Sakai, Y.; Kobayashi, M.; Enoki, T.; Takeoka, Y.; Ishibashi, T.; Kuroda, K.; Tanaka, K.; Wang, G. Q.; Grosberg, A. Y.; Masamune, S.; Tanaka, T. Macromolecules 2000, 33 (23), 8693–8697.
(20) Takeoka, Y.; Honda, M.; Seki, T.; Ishii, M.; Nakamura, H. ACS Appl. Mater. Interfaces 2009, 1 (5), 982–986.
(21) Takeoka, Y.; Berker, A. N.; Du, R.; Enoki, T.; Grosberg, A.; Kardar, M.; Oya, T.; Tanaka, K.; Wang, G. Q.; Yu, X. H.; Tanaka, T. Phys. Rev. Lett. 1999, 82 (24), 4863–4865.
(22) Kato, M.; Kamigaito, M.; Sawamoto, M.; Higashimura,T. Macromolecules 1995, 28 (5), 1721–1723.
(23) Wang, J. S.; Matyjaszewski, K. Macromolecules 1995, 28 (23), 7901–7910.
(24) Ejaz, M.; Yamamoto, S.; Ohno, K.; Tsujii, Y.; Fukuda, T. Macromolecules 1998, 31 (17), 5934–5936.
(25) Ohno, K.; Morinaga, T.; Koh, K.; Tsujii, Y.; Fukuda, T. Macromolecules 2005, 38 (6), 2137–2142.
(26) de Gennes, P. G. Nobel Lecture, December 9. 1991.
(27) Okano, T.; Yamada, N.; Sakai, H.; Sakurai, Y. J. Biomed. Mater. Res. 1993, 27 (10), 1243–1251.
(28) Zhang, J.; Pelton, R.; Deng, Y. L. Langmuir 1995, 11 (6), 2301–2302.
(29) Nakamura, T.; Hattori, M.; Kawasaki, H.; Miyamoto, K.; Tokita, M.; Komai, T. Phys. Rev. E 1996, 54 (2), 1663–1668.
(30) Ito, Y.; Chen, G. P.; Guan, Y. Q.; Imanishi, Y. Langmuir 1997, 13

(10), 2756–2759.
(31) Liang, L.; Rieke, P. C.; Fryxell, G. E.; Liu, J.; Engehard, M. H.; Alford, K. L. J. Phys. Chem. B 2000, 104 (49), 11667–11673.
(32) Bao, Z. Y.; Bruening, M. L.; Baker, G. L. Macromolecules 2006, 39 (16), 5251–5258.
(33) Matyjaszewski, K.; Miller, P. J.; Shukla, N.; Immaraporn, B.; Gelman, A.; Luokala, B. B.; Siclovan, T. M.; Kickelbick, G.; Vallant, T.; Hoffmann, H.; Pakula, T. Macromolecules 1999, 32 (26), 8716–8724.
(34) Yamamoto, S.; Ejaz, M.; Tsujii, Y.; Fukuda, T. Macromolecules 2000, 33 (15), 5608–5612.
(35) Yamamoto, S.; Ejaz, M.; Tsujii, Y.; Matsumoto, M.; Fukuda, T. Macromolecules 2000, 33 (15), 5602–5607.
(36) Advincula, R.; Brittain, W. J.; Caster, K. C.;R€uhe, J., Ed., Polymer Brushes: Synthesis, Characterization, Applications; Wiley-VCH: Weinheim, Germany, 2004.
(37) Jones, D. M.; Smith, J. R.; Huck, W. T. S.; Alexander, C. Adv. Mater. 2002, 14 (16), 1130–1134.
(38) Balamurugan, S.; Mendez, S.; Balamurugan, S. S.; O'Brien, M. J.; Lopez, G. P. Langmuir 2003, 19 (7), 2545–2549.
(39) Kaholek, M.; Lee, W. K.; Ahn, S. J.; Ma, H. W.; Caster, K. C.; LaMattina, B.; Zauscher, S. Chem. Mater. 2004, 16 (19), 3688–3696.
(40) Tu, H. L.; Hong, L.; Anthony, S. M.; Braun, P. V.; Granick, S. Langmuir 2007, 23 (5), 2322–2325.
(41) Yim, H.; Kent, M. S.; Satija, S.; Mendez, S.; Balamurugan, S. S.; Balamurugan, S.; Lopez, G. P. Phys. Rev. E 2005, 72 (5).
(42) Liu, Y.; Klep, V.; Luzinov, I. J. Am. Chem. Soc. 2006, 128 (25), 8106–8107.
(43) Plunkett, K. N.; Zhu, X.; Moore, J. S.; Leckband, D. E. Langmuir

2006, 22 (9), 4259–4266.
L Macromolecules, Vol. XXX, No. XX, XXXX Suzuki et al.
(44) Lokuge, I.; Wang, X.; Bohn, P. W. Langmuir 2007, 23 (1), 305–311.
(45) He, Q.; Kuller, A.; Grunze, M.; Li, J. B. Langmuir 2007, 23 (7), 3981–3987.
(46) Schepelina, O.; Zharov, I. Langmuir 2007, 23 (25), 12704–12709.
(47) Mathieu, M.; Friebe, A.; Franzka, S.; Ulbricht, M.; Hartmann, N. Langmuir 2009, 25 (20), 12393–12398.
(48) Wang, S. Q.; Zhu, Y. X. Langmuir 2009, 25 (23), 13448–13455.
(49) Teodorescu, M.; Matyjaszewski, K. Macromolecules 1999, 32 (15), 4826–4831.
(50) Rademacher, J. T.; Baum, R.; Pallack, M. E.; Brittain, W. J.; Simonsick, W. J. Macromolecules 2000, 33 (2), 284–288.
(51) Bontempo, D.; Li, R. C.; Ly, T.; Brubaker, C. E.; Maynard, H. D. Chem. Commun. 2005, No. 37, 4702–4704.
(52) Xu, J.; Ye, J.; Liu, S. Y. Macromolecules 2007, 40 (25), 9103–9110.
(53) Masci, G.; Giacomelli, L.; Crescenzi, V. Macromol. Rapid Commun. 2004, 25 (4), 559–564.
(54) Millard, P.-E.;Mougin, N. C.;B€oker,A.;M€uller,A.H.E. Controlled/ Living Radical Polymerization: Progress in ATRP; Matyjaszewski, K., Ed.; ACS Symposum Series; American Chemical Society: Washington, DC, 2009; pp 127-137.
(55) Jonas, A. M.; Glinel, K.; Oren, R.; Nysten, B.; Huck, W. T. S. Macromolecules 2007, 40 (13), 4403–4405.
(56) Fadeev, A. Y.; McCarthy, T. J. Langmuir 2000, 16 (18), 7268–7274.
(57) Fadeev, A. Y.; McCarthy, T. J. Langmuir 1999, 15 (11), 3759–3766.
(58) Tong, Q. Y.; Gosele, U. M. Adv. Mater. 1999, 11 (17), 1409–1425.
(59) Donose,B.C.;Taran,E.;Vakarelski, I.U.; Shinto,H.;Higashitani,K. J. Colloid Interface Sci. 2006, 299 (1), 233–237.
(60) Armistea, Cg; Tyler, A. J.; Hambleto, Fh; Mitchell, S. A.; Hockey,

J. A. J. Phys. Chem. 1969, 73 (11), 3947–3953.
(61) Zhuravlev, L. T. Langmuir 1987, 3 (3), 316–318.
(62) Jones, D. M.; Brown, A. A.; Huck, W. T. S. Langmuir 2002, 18 (4), 1265–1269.
(63) Wang, X. J.; Tu, H. L.; Braun, P. V.; Bohn, P. W. Langmuir 2006, 22 (2), 817–823.
(64) Marmur, A. Soft Matter 2006, 2 (1), 12–17.
(65) Israelachvili, J. N.; Gee, M. L. Langmuir 1989, 5 (1), 288–289.
(66) Fukuda, T.: Tsujii, Y.; Ohno, K.; Macromolecular Engineering. Precise Synthesis, Materials Properties, Applications; Matyjaszewski, K., Gnanou, Y., Leibler, L., Eds.; Wiley-VCH: Weinheim, Germany, 2007.
(67) Shah, R. R.; Merreceyes, D.; Husemann, M.; Rees, I.; Abbott, N. L.; Hawker, C. J.; Hedrick, J. L. Macromolecules 2000, 33 (2), 597–605.
(68) Zhulina, E. B.; Borisov, O. V.; Pryamitsyn, V. A.; Birshtein, T. M. Macromolecules 1991, 24 (1), 140–149.
(69) Maeda, Y.; Higuchi, T.; Ikeda, I. Langmuir 2000, 16 (19), 7503–7509.
(70) Katsumoto, Y.; Tanaka, T.; Sato, H.; Ozaki, Y. J. Phys. Chem. A 2002, 106 (14), 3429–3435.
(71) Ahmed, Z.; Gooding, E. A.; Pimenov, K. V.; Wang, L. L.; Asher, S. A. J. Phys. Chem. B 2009, 113 (13), 4248–4256.
(72) Hu, T. J.; You, Y. Z.; Pan, C. Y.; Wu, C. J. Phys. Chem.B 2002, 106 (26), 6659–6662.
(73) Suzuki, A.; Kobiki, Y. Jpn. J. Appl. Phys., Part 1: Reg. Pap. Short Notes Rev. Pap. 1999, 38 (5A), 2910–2916.
(74) Takeoka, Y.; Watanabe, M. Langmuir 2002, 18 (16), 5977–5980.
(75) Jonas, A. M.; Hu, Z. J.; Glinel, K.; Huck, W. T. S. Nano Lett. 2008, 8 (11), 3819–3824.

(76) The Young equation, cos θ = (σsf - σsl)/σlf, was developed in the case of an ideal solid surface, which is defined as smooth, rigid, chemically homogeneous, insoluble, and nonreactive.
(77) Tanaka, T. Sci. Am. 1981, 244, 124–136.
(78) Laloyaux, X.; Mathy, B.; Nysten, B.; Jonas, A. M. Langmuir 2010, 26 (2), 838–847.
(79) Senshu, K.; Yamashita, S.; Ito, M.; Hirao, A.; Nakahama, S. Langmuir 1995, 11 (6), 2293–2300.
(80) Jcarn, M.; Brieler, F. J.; Kuemmel, M.; Grosso, D.; Linden, M. Chem. Mater. 2008, 20 (4), 1476–1483.

# Chapter 5

Stimuli responsive behavior of high density Poly (*N*-isopropylacrylamide) (PNIPA) constructed on silicon surface by Atom Transfer Radical Polymerization (ATRP)

**Abstract.**

High-density polymer brushes were grown from the silicon surface by atom transfer radical polymerization of Poly(*N*-isopropylacrylamide) (PNIPA) at different polymerization conditions. PNIPA brushes were prepared using CuCl/tris(2-(dimetylamino)ethyl)amine ($Me_6$TREN) as a catalytic system in DMSO at 20 $^{o}$C. Free polymer formed during the brush formation was characterized by gel permeation chromatography. The grafting densities up to 0.52 chains/nm$^2$ were obtained. The layer thickness of polymer brush increases with the increase of conversion of the monomer conversion as well as polymerization time. Atomic force microscopy and air bubble contact angle under pH solution were employed to study the surface morphology, reversible conformational changes of and stimulus-response behavior. PNIPA brushes exhibited a different nanomorphology after treatment with different pH solution. It also revealed a unique reversible wetting behavior with pH. The reversible properties of the PNIPA brushes can be used to regulate the adsorption of the sulfonated PS nanoparticles.

## 5.1. Introduction.

Microscopic structures of polymers are emulated on macroscopic characteristics, which is also dependent on the conformational change of the polymer. It is generally known that, many nonionic water-soluble polymers have phase transition properties. Thermoresponsive surfaces with temperature responsive properties are most important among smart surfaces since temperature can be easily controlled as a stimulant. By applying external stimuli (e.g. adhesion, wettability, friction, roughness, reactivity, biocompatibility, selectivity etc.) on "smart" materials, it switch and/or tune the properties of the coatings.[1] That's the reason for developing many thermoresponsive surfaces.[2] Poly (*N*-isopropylacrylamide) PNIPA, which has the nonfouling function and has excellent resistance to nonspecific protein absorption, is the most important materials to fulfill specific binding capacity for the biomolecules and a nonfouling background. [3] If grafting density of polymer chains on solid surface is adequately high, polymer chains are constrain to stretch away from the surface. This arrangement of solution polymer is called as "Polymer brushes".[4] Theoretical studies of polymer brushes using self-consistent-field calculation depend on Huggins interaction parameter (*ø*), overall molecular weight (*N*), volume fraction of one block (*f*), Kuh length (flexibility of backbone), grafting density, environmental conditions (solvent, temperature), and surface free energy of each block in the air.

Because of the performance to control the thickness and the composition of polymer brush, living radical polymerization is the most important among all the polymerization for synthesis of polymer brush. A variety of monomer such as styrene, methyl (meth)acrylate, methyl acrylate, 2-hydroxyethyl (meth)acrylate, 4-vinylpyridine, acrylamide etc can be used, and the polymerization can be performed at ambient temperature for homocopolymerization or block-copolymerization.[5] Atom transfer radical polymerization (ATRP) is one of the well-developed controlled living polymerization.[6-9] Another advantage of this method is that the end of the polymer chain is capped with an active halide atom that can be reinitiated to form block copolymer brushes with addition of fresh catalyst and monomer.[10] There are two different way for graft polymerization, which is, "grafting to" and "grafting from." [4] Polymer chains contain reactive moieties at chain ends and/or side chains are covalently attached to reactive surface in case of grafting to technique. Grafting density is also lower in this process; this is because

previously grafted chain prevents later chain to approach on the surface. Whereas high density polymer brushes with well controlled structure can be synthesized by the grafting from method, but characterization is a little bit difficult. However the difficulties can be overcome by using surface-initiated living polymerization techniques. [11]

Naturally hydrophobic interactions are thermodynamic in nature. If water structure forms around hydrophobic groups, gained entropy is reduced by accomplishing hydrophobic species.[12] To study alteration of polymer brushes few research groups used AFM method and presumed that if temperature raised over LCST, brush thickness will decrease. [13] To establish PEG-based thermoresponsive surfaces for biological and medical application this work exposed an innovative approach. The phase behavior of block copolymer has been widely studied. [14] In case of diblock copolymers with immiscible components, microphase separation occurs. Under a robust isolation limit, linear diblock copolymers in the bulk exhibit ordered morphologies that depend on the volume composition. [15] When the diblock copolymer is near a surface or confined between two solid surfaces, , diblock copolymer self-assembles into an ordered structure with a specific microdomain orientation, either parallel or normal to the surfaces depending on the interaction between the blocks in the copolymers and interfaces [16-20]

In the last two decades, Many researchers have focused on the stimuli responsive behavior of polyelectrolyte hydrophobic polymer brushes, e.g., PMMA, polystyrene (PSt),[21] PAAM,[22] quarternized poly (4-vinylpyridine) [23] and polyelecrolyte block copolymer brushes of P2VP-b-PAA. [24] The coil-globule transition has been extensively studied as it is related with phase separation of polymer solution, morphological formation of a biopolymer and collapse of a polymer gel.[25] PNIPA which has both hydrophilic amide and hydrophobic isopropyl group might be interesting for this types of studies, because it is related to stimuli responsive or smart surface coatings [26] and biosensors. [27]

In this study PNIPA brushes were grown on a silicon surface by ATRP under different reaction conditions and examined the kinetics of the surface initiated ATRP of that system. We also observed the pH responsive surface properties of the polymer brush at room temperature and analyzed the AFM image by autocorrelation functions to observe pH responsive change of the

brush membrane. The result was also explored by the measurement of air bubble contact angle of the polymer brush under the aqueous solution of different pH values.

### 5.2. Experimental Section.

Materials. *N*-isopropylacrylamide (Nippon Sokubai, 97%) was recrystallized two times from the mixture of tolune and hexane (1/7, v/v). Copper(II) chloride (99.99%), methanol (99.99%) and Ethylenediaminetetraaceticacid (EDTA) were purchased from Aldrich and were used without further purification. 2-Chloropropionyl chloride was purchased form Kishida chemical and used as received. $Me_6$TREN was prepared according to literature procedure. [28] Silicon wafers with one side polished were purchased form Kishida chemical Tolune was distilled under nitrogen atmosphere from sodium/benzophenone. Tetrahydro furan (THF), n-hexan were bought from Kanto chemical company and was used is at is.

### 5.3. Self-Assembly of Initiator Monolayer on Silicon Wafers.

The surface-attachable ATRP initiator(11-(2Chloro)propionyloxy) undecyl dimethylchlorosilane (CPU-dMCS), was synthesized by the hydrosilylation of 10-undecen-1-yl 2-chloropropionate (Mw : 260.80e) with chlorodimethylsilane (Mw : 94.62, density : 0.852) in presence of Karsted catalyst at room temperature for 6 hours, 10-undecen-1-yl 2-chloropropionate was synthesized by an addition reaction of 10-undecen-1-ol (MW : 170.29, density : 0.85) with 2-chloropropionyl chloride (MW : 126.97, density : 1.281). Silicon wafers were pretreated as described previously. [29] 100 μl CPU-dMCS was added into 100ml dry tolune inside glovebox which was used as a silane coupling solution. Treated silicon wafers were then immersed into silane coupling solution and were kept into a woven for at 60 $^{o}$C temperature for 84 hours to form a self-assembled initiator monolayer with a thickness of 1.9 ( 0.2 nm. The silicon wafers were then removed from solution, ultrasonically cleaned in dry toluene, rinsed sequentially with toluene and methanol, and then dried in an argon stream. The successful of the ATRP initiator layer was verified by X-ray photoelectron spectroscopy (XPS).

### 5.3.1. Synthesis procedure of the ATRP initiator.

As an ATRP initiator, propargyl 2-Chloropropionate (PCP) was used. PCP was synthesized by an esterification reaction of propargyl alcohol with 2-Chloropropionyl chloride in presence of dry trimethyl amine and THF. A typical procedure was as follow. A 250 ml round –bottom flask was charged with trimethyl amine (1.98ml, 101.19 gm/mol, density 0.726 gm/cc), Propargyl alcohol (1.98 ml) and dry THF (40 ml). Air was removed from the flask by freeze pump thaw cycle. The reaction mixture was cooled to 0 $^{o}$C in an ice-water bath. 2-chloropropanioyl chloride (3.37 ml, 126.97 gm/mol, density 1.281 gm/cc) was added dropwise under magnetic stirring over a period of 1hour. The mixture was stirred at 0 $^{o}$C for 1 hour and at room temperature whole night. Then n-hexane (the volume is same with THF) was added with the solution to dilute it. The mixture was filtrated by suction filtration to remove *N,N'*-dicyclohexylurea,. The filtrate was washed with 10% HCl solution, $NaHCO_3$, Brine and miliQ water. Dried $MgSO_4$ was added and was kept over night to remove water form the mixture. To remove $MgSO_4$, the mixture was filtrate and was concentrated by evaporator. For further purification, a silica gel column chromatography was used using n-hexane: ethyl acetate=9:1 as the eluent. The solvent was then removed by rotary evaporator and residue was distilled under reduced pressure. A colorless liquid was obtained with 74% yield. $^{1}$H NMR ($CDCl_3$, δ, ppm): 4.86 (2H, -C*H*2O-), 4.42 (H, -C*H*Cl-), 2.53 (H, -CtC*H*), and 1.695 (3H, -C*H*3).

### 5.3.2. Preparation of the Free Polymers and polymer Brushes simultaneously.

A polymerization tube was charged with the monomer NIPA (1.65 gm) and 3ml di-methylsulfoxide (DMSO) (DMSO wad added inside glovebox). The solution was degassed by three consecutive freeze– pump–thaw cycles and backfilled with nitrogen gas (procedure repeated three times). In the glovebox, the polymerization tube was again charged with copper chloride (3.6 mg,), $Me_6$TREN (10.03 µl,) and PCP (3.6 µl). A self-assembled monolayer silicon substrate was inserted into the solution of the tube very carefully under a nitrogen atmosphere. The tube was then sealed with stopper by using laboratory film paper. The grafting process was carried out at 20 $^{o}$C with continuous shaking by a shaker (Model: EYELA, NTS-4000) at different pre-planned time. The tube was exposed to air to terminate the polymerization reaction after desired time period. To determine the conversion of the monomer a sample was prepared for NMR with Hydoquinone and DMSO as a solvent. Then the solution was dissolved in THF,

and passed through a short silica column to remove the catalyst. After concentrating the solution by vacuum rotary evaporator, the solution was dissolved with methanol and purified by dialysis against methanol solution for 5 days. The eluents were concentrated, dissolved in THF and precipitated into an excess of n-hexan. The product was then separated by a centrifuge ( Model: KOKUSAN, H-18F) at 2500 rpm for 20 minutes. This purification cycle was repeated three times. The obtained product was dried overnight in a vacuum dryer. The molecular weight distribution of the polymer was measured by gel permeation chromatography (GPC). On the other hand the polymer-grafted silicon wafer was then ultrasonically cleaned in methanol, rinsed thoroughly into EDTA solution and dried in an argon stream.

### 5.3.3. Treatment of the PNIPA Brushes by Different pH Aqueous Solution.

The PNIPA brush was treated by aqueous solution with different pH values. To adjust the pH value of the solution a desired amount of aqueous solution was added and removed with the corresponding amount of 0.1 M HCl or 0.001 M NaOH solution to obtain a defined pH value. The modified substrate was immersed in a water bath with defined pH value for 10 min and then withdrawn from the water bath and was dried by nitrogen gas immediately.

## 5.4. Characterization.

Average molecular weights and molecular weight distributions were determined by GPC on a Waters GPC system consisting of a Waters 515 HPLC pump, a Waters 717plus Autosampler, three Waters Styragel columns (HR2, HR3, and HR4; 30 cm × 7.8 mm; 5μm particles; exclusion limits: 500-20000, 500-30000, and 5000- 600000 g/mol, respectively) maintained at 40 °C, and a Waters 2414 refractive index detector maintained at 35 °C. THF containing 0.25% (w/v) tetrabutylammonium bromide was used as the mobile phase (1.0 mL/min), and monodisperse poly(methylmethacrylate) (PMMA) standards (Polysciences, Inc.) were used to calibrate the molecular weights. The molecular weights of the PMMA standards were 350,000, 127,000, 30,000, and 6000 g/mol.

### 5.4.1. Fourier Transform Infrared Spectroscopy (FT-IR).

Fourier transform infrared (FT-IR) spectra were recorded on a Varian 640 –IR spectrometer. The spectra were collected at 128 scans with a spectral resolution of 4 cm-1. Thickness of the brush surfaces were measure by using a AFM Nanoscope IIIa controller (Digital Instruments, Santa Barbara, CA), equipped with an atomic head of 100_100 μm2 scan range (Nanopics 2100, NPX2100).

### 5.4.2. Atomic force microscopy (AFM).

Atomic force microscopy measurements were performed on a multimode commercial scanning probe microscope (SPA- 400). AFM measurements were performed at air in contact (???) and phase mode using a commercially manufactured V-shaped silicon nitride (Si3N4) cantilever with gold on the back for laser beam reflection. Air bubble Contact angle measurements were made with a Data Physics telescopic goniometer with a Hamilton syringe with a flat-tipped needle at ambient temperature. The static water contact angle was measured by using deionized water with drop size 4 μl. The contact angle was determined by using sessile drop method. The static and dynamic contact angle was averaged over three measurements.

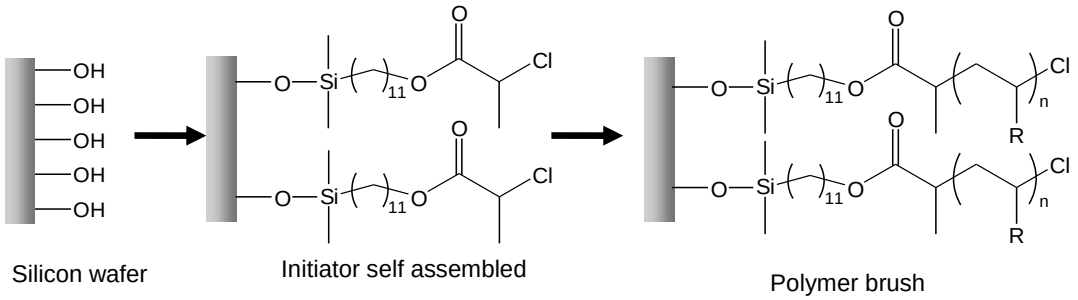


Scheme 2. Synthetic Routes for the Preparation of Poly(*N* isopropylacrylamide), brushes on silicon substrate via ATRP.

## 5.5. Result and discussion.

Scheme 1 shows the preparation of PNIPA brushes on silicon surface. ATRP of PNIPA on the silicon surface was accomplished in presence of a free initiator at CuCl/$Me_6$Tren system and DMF as a solvent. For the ATRP of PNIPA the addition of catalyst $CuCl_2$ is not necessary. [31-32] During polymerization reaction a minimum amount of deactivator is require for controlled surface initiator ATRP. Monomer conversions were observed by $^1$H NMR based on integration areas. At resonance peak 4.0 ppm was considered as PNIPA monomer and PNIPA polymer, the integration factor was assented to 1 and the resonance peak 6.0-6.4 ppm (vinyl portion of PNIPA) as monomer. By GPC analysis number average molecular weight, $M_n$ and molecular weight distribution, $M_w/M_n$ was obtained. Typical PDI's vary based on the mechanism of polymerization and can be affected by a variety of reaction conditions. Due to the reactant ration this value can vary for synthetic polymers. But low PDI value indicates a good distribution of individual molecular masses in this batch of polymers as shown in the figure 5-1. As the polymer chains approach uniform chain length, the PDI approaches to a low value (1.15 ~ 1.27). Low PDI values were also observed even at lower polymerization time. According to the fig. 5-1, there is a slightly fluctuation of PDI values, which might be the narrow molecular weight distribution of the free polymer.

Figure 5-2 showed the graft density of the surface attached chains of the different polymer sample. Graft density of the surface attached polymer chains could be obtained from the molecular weight of the polymer chain and the film thickness. For the same material, unknown material density of polymer in the monolayer was considered to be similar to the mass density. In all cases, the graft density was around 0.45 to 0.50 chain/nm$^2$. These values seemed to be constant except a small deviation at lower polymerization time. During separation of the polymer low molecular weight samples get precipitate and the molecular weight of these samples might be overestimated which is the causes of molecular weight loss. The rate of exchange between active and sluggish chain was swift, that's why all chains arose slowly and almost at the same rate with the number of chain remaining constant. This criterion also implies that polymer chains are highly extended states regardless of the polymerization time.

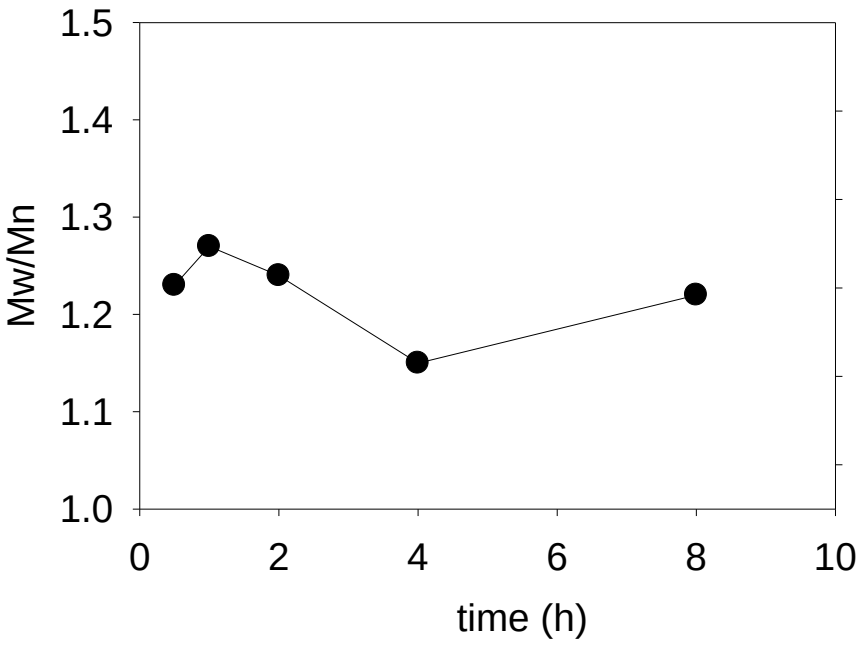


Figure 5-1. Polydispersity ($M_w/M_n$) of free polymer for the ATRP of PNIPA in DMSO as a function of the

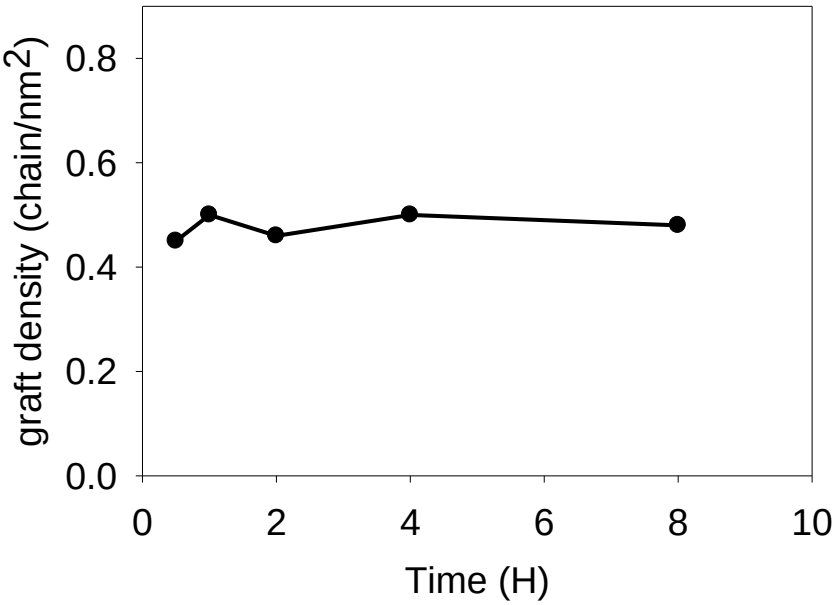


Figure5- 2. Graft density of the surface attached PNIPA brushes as a function of polymerization time.

Film thickness of monolayer is plotted against the molecular weight of free polymer (Figure 5-3). A linear relation is between film thickness and $M_n$ was obtained. Film thickness is increased linearly with $M_n$ of the free polymer. So the number average molecular weight of grafted polymer is either similar or proportional to the free polymer. This linear relationship also indicates that, the chain that attached on the surface and the chain that grown in the solution were almost similar molecular weights.

Figure 5-4 and 5-5 shows the compared surface morphologies of the PNIPA brush on silicon surface with 15 nm thickness as observed by AFM after treatment with different pH values. The surface roughnesses observed in AFM studies were consistent with contact angle observations. Part (a, b, c) of the Fig.5-4 are the height images of the brush surface at pH value 1.2, 5.3 and 11.5 respectively and the part ($a_1$, $b_1$, $c_1$) of the fig. 5-5 are the phase image of the same surface. At lower pH value (pH 1.2), the surface fluctuating amplitude and the phase contrast of the brush surface were around 12 nm and 9 $^o$ respectively. But the surface fluctuating amplitude and the phase contrast were remarkably decreased to 5 nm and 2.5 $^o$ at pH 5.3. This value did not change significantly (surface fluctuating amplitude is 5.9 nm and phase contrast is 3.8 $^o$) also at higher pH ( pH 11.5) values. The morphology of the PNIPA brush varies with the strength of pH values. The brush surface exhibits hydrophobic phenomena strong acidic conditions, whereas the surface tends to become hydrophilic state at moderate acidic and strong basic conditions. Weak acid and strong base modified surface exhibited distinct and deeper features than strong acid treated PNIPA grafted membrane. There are two possible explanations for such a difference in the surface roughness values. First, polymer was synthesized on the silicon substrate at "grafting form" method, which leads to a high grafting density of chains on the surface. Strong base solution may cause topology-induced reduction of chain graft density and the brush surface resembles mushrooms shape. During formation of polymer brush on the silicon surface, although all the chains are initiated at the same time, as branching proceeds, chain crowding prevents uniform growth, which leads to an unequal chain lengths. Secondly, by the mixture of acid and base a salt is being produced in the solution, which occupied some of the chains of the polymer brush because of the common ion effect. Using an image processing techniques, such as autocorrelation function, we established an independent measure to observe the change of the morphology of the brush membrane.

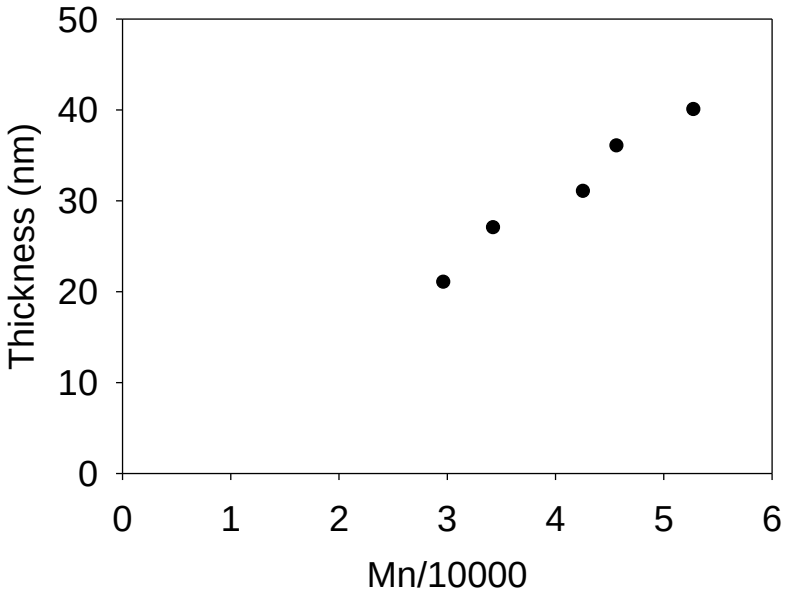


Figure 5-3. Correlation of the monolayer film thickness with the molecular weight (Mn) of free PNIPA produced by ATRP in DMSO

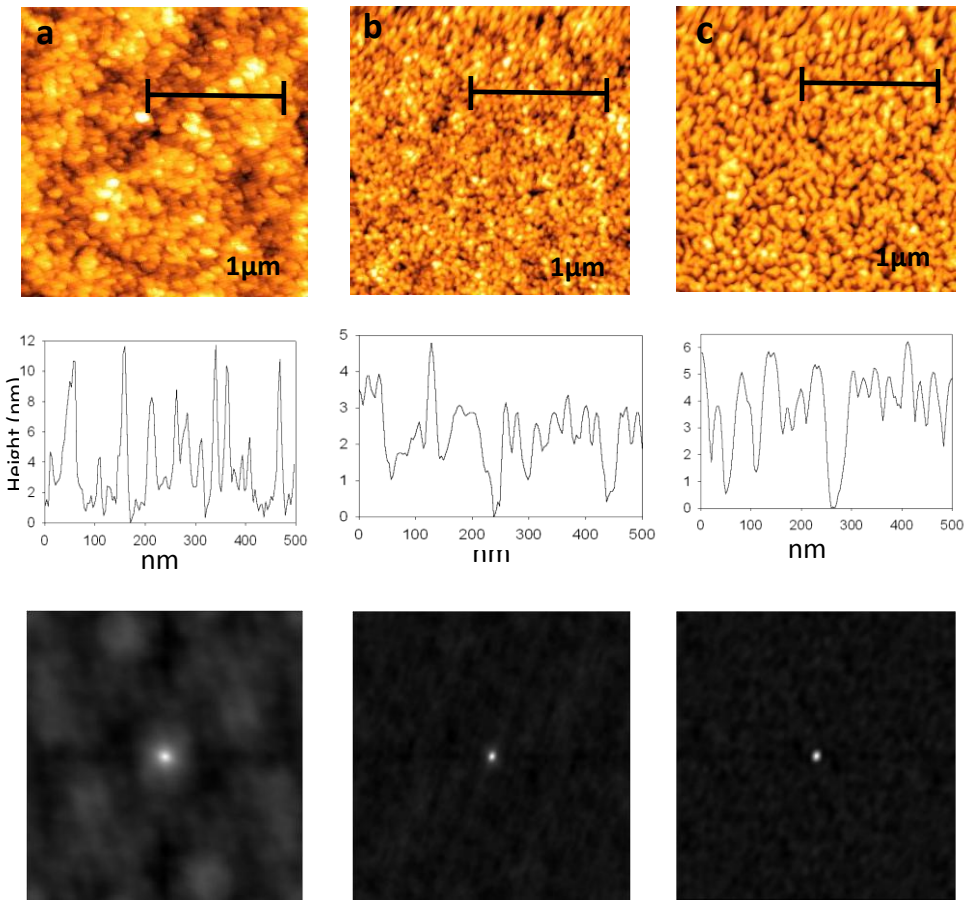


Figure 5-4. The height image (a,b,c) and the autocorrelation function of the AFM image ($a_1$,$b_1$,$c_1$) of the PNIPA brushes after treatment by aqueous solution with different pH values (a), pH 1.2, (b), pH 5.3 and (c), pH 11.5.

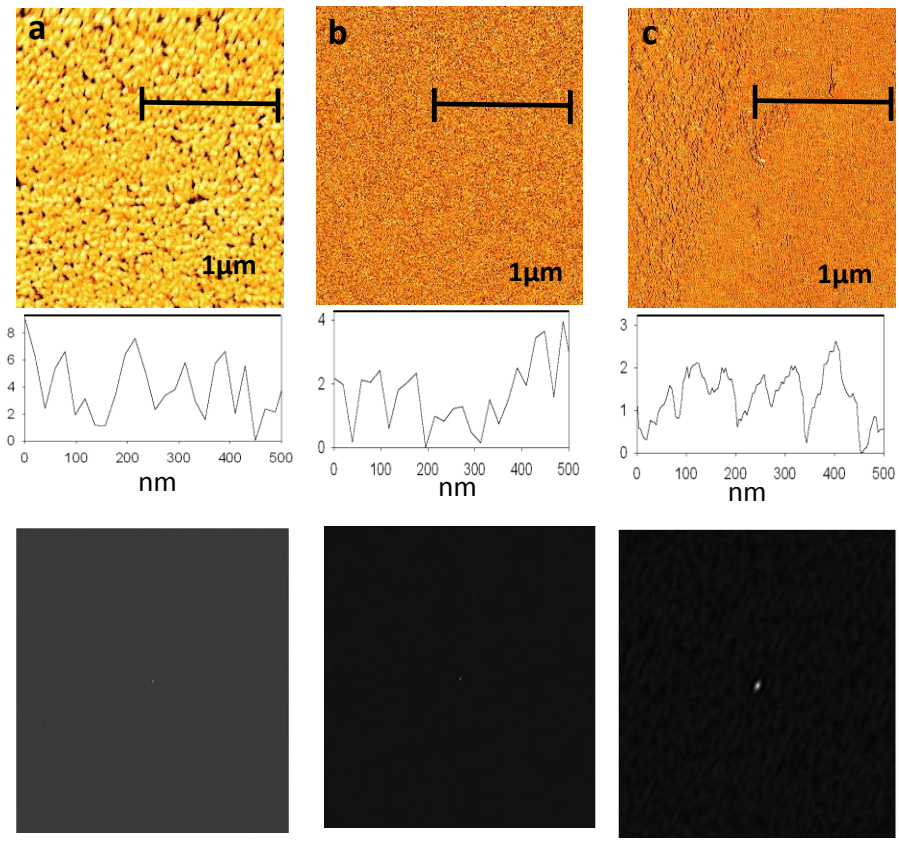


Figure 5-5. The phase image (a,b,c) of the PNIPA brushes after treatment by aqueous solution with different pH values. (a), pH 1.2, (b), pH 5.3 and (c), pH 11.5.

The autocorrelation function is an approach to enhance the interpretation of such data based on the combination of linear correlations of the same feature in one AFM image. The AFM image was resized to a power of 2 (such as 256 x 256 pixels), and the autocorrelation function (Fig. 5-4($a_1$,$b_1$,$c_1$)) was obtained from the AFM image. In the case of the pH strength above 5.5, the resulting frequency plot of treated sample contains pixel (Fig. 5-4($b_1$,$c_1$),) concentrated along a specific axis. The frequency plots or power spectra, of the strong acid treated grafted membrane (Fig 5-4. ($a_1$)) contains cluster as circular patterned around the origin. Almost same types of image was found in the case of weak acid and strong base treated sample, which is also a strong affidavit of the explanation of the AFM images.

Grafted polymer brushes have been used for making smart surfaces in the literatures. [32-38] Different surface properties on the surface exposes by the treatment of different solvents that modulate surface properties. As a result, the surface can switch between hydrophilic and hydrophobic, protein-adsorbing and protein-repelling, acidic and basic, conductive and nonconductive, etc., according to the chemical composition of grafted surface.

## 5.6. Conclusion.

ATRP of PNIPA in DMSO to a narrow-disperse of NIPAM with high conversion and good molecular weight was shown. The PNIPA brush can be grown under mild conditions at low temperature. Analysis of the grafting density and molecular size of the chains indicates that polymerization was carried out in a control manner as affirmed by the narrow molecular weight distributions of the grafted PNIPA chain. AFM analysis of PNIPA brushes illustrated that, surface rearrangement occurred during the treatment of the PNIPA brushes by aqueous solution with different pH values. We also used an independent image processing technique to observe the change of brush morphology. The responsive change of the brush surface was also explored by the air bubble contact angle measurements under pH solution.

**References and notes**.


(1) John.D,:Logor L,;Manred S, *Polymer materials: sci & eng*. **2002**, 87, 187

(2) Xiang G.;Norbert K.; Heather S. *Langmuir* **2009**, DOI: 10.1021/la901086e

(3) *Langmuir* **2008,** *24*, 8303-8308

(4) Zhao, B.; Brittain, W. J. *Prog. Polym. Sci.* **2000**, *25*, 677.

(5) (Heskins, M.; Guillet, J. E. J. Macromol. Sci., Chem. **A2,**1441 (1968).

(6) For review papar, see: Patten, T. E.; Matyjaszewski, K. *Adv. Mater*. **1998**, *10*, 901.

(7) Xia, J.; Zhang, X.; Matyjaszewski, K. *Macromolecules* **1999**, *32*, 3531.

(8) Uegaki, H.; Kotani, Y.; Kamigaito, M.; Sawamoto, M. *Macromolecules* **1997**, *30*, 2249.

(9) Nishikawa, T.; Kamigaito, M.; Sawamoto, M. *Ibid*. **1999**, *32*, 2204.

(10) Sedjo RA, Mirous BK, Brittain WJ. Macromolecules 2000;33: 492.

(11) Kato, K.; Uchida, E.; Kang, E. T.; Uyama, Y.; Ikada, Y. Prog Polym Sci 2003, 28, 209

(12) (a) Arieh, B. N. *Hydrophobic Interaction*; Plenum Press: New York, **1980.** (b) Chandler, D. Nature (London) **2005**, 437, 640–47. (c) Meyer, E. E.; Rosenberg, K. J.; Israelachvili, J. N. Proc. Natl. Acad. Sci. U.S.A. 2006, 103, 15739–746.

(13) Glinel, K.; Jonas, A. M.; Jouenne, T.; Leprince, J.; Galas, L.; Huck, W. T. S. Bioconju gate Chem. 2009,

*20(1*),71–77.

(14) Bates, F. S. *Science* **1991**, *251*, 898-905. (17) Bates, F. S.; Fredrickson, G. H. *Annu. Re*V. *Phy. Chem.* **1990**, *41*, 525-557.

(15). Bin Zhao, William J. Brittain ,*J. Am. Chem. Soc.* **2000,** *122*, 2407-2408

(16).Russell, T. P. *Curr. Opin. Colloid Interface Sci.* **1996**, *1*, 107-115.

(17) Huang, E.; Rockford, L.; Russell, T. P.; Hawker, C. J. *Nature* **1998**, *395*, 757-758.

(18) Mansky, P.; Russell, T. P.; Hawker, C. J.; Pitsikalis, M.; Mays, J. *Macromolecules* **1997**, *30*, 6810-6813.

(19) Lambooy, P.; Russell, T. P.; Kellogg, G. J.; Mayes, A. M.; Gallagher, P. D.; Satija, S. K. *Phys. Re*V. *Lett*. **1994**, *72*, 2899-2902.

(20) Koneripalli, N.; Singh, N.; Levicky, R.; Bates, F. S.; Gallagher, P. D.; Satija, S. K. *Macromolecules* **1995**, *28*, 2897-2904.

(21) (a) Grimaud, T.; Matyjaszewski, K. *Macromolecules* **1997**, *30*, 2216. (b) Matyjaszewski, K.; Patten, T. E.; Wang, J. *J. Am.Chem. Soc*. **1997**, *119*, 674.

(22). (a) Huang, X.; Doeski, L. J.; Wirth, M. J. *Anal. Chem*. **1998**, *70*, 4023. (b) Huang, X.; Wirth, M. J. *Macromolecules* **1999**, *32*, 1694.)

(23) Biesalski, M.; Ru¨ he, J. *Macromolecules* **1999**, *32*, 2309.

(24) Kai Y. Langmuir 2007, 23, 1443-1452

(25) Heskins M, Guillet JE, James E. J Macromol Sci Chem A2, **1968**;1441–55.

(26) Moya, S.; Azzaroni, O.; Farhan, T.; Osborne, V. L.; Huck, W. T. S. *Angew. Chem., Int. Ed.* **2005**, *44*, 4578.

(27) Tugulu, S.; Arnold, A.; Sielaff, I.; Johnsson, K.; Klok, H.-A. *Biomacromolecules* **2005**, *6*, 1602

(28) Ciampolini, M.;Nardi, N.*inorg.Chem.* **1966**, 5, 41-44.

(29) Gao, X.; Feng, W.; Zhu, S. P.; Sheardown, H.; Brash, J. L. Langmuir 2008, 24(15), 8303–8308.

(30)Xia, Y.; Yin, X. C.; Burke, N. A. D.; Stover, H. D. H. *Macromolecules* **2005**, *38*, 5937.

(31) Masci, G.; Giacomelli, L.; Crescenzi, V. *Macromol. Rapid Commun.* **2004**, *25*, 559

(32) Zhao, B.; Brittain, W. J. *J. Am. Chem. Soc.* **1999**, *121*, 3557.

(33) Minko, S.; Muller, M.; Motornov, M.; Nitschke, M.;Grundke,K.; Stamm, M. *J. Am. Chem. Soc.* **2003**, *125*, 3896.

(34) Xu, C.; Wu, T.; Drain, C. M.; Batteas, J. D.; Fasolka, M. J.; Beers, K. L. *Macromolecules* **2006**, *39*, 3359.

(35) Minko, S. *Polym. Re*V. **2006**, *46*, 397.

(36) Zhou, F.; Huck, W. T. S. *Phys. Chem. Chem. Phys.* **2006**, *8*, 3815.

(37) Luzinov, I.; Minko, S.; Tsukruk, V. V. *Prog. Polym. Sci.* **2004**, *29*, 635.

**Publications.**

1. Suzuki H., **Huda M. Nurul**, Seki T., Kawamoto T., Haga H., Kawabata k., Takeoka Y.. "*Precise Synthesis and Physicochemical Properties of High-Density Polymer Brushes designed with Poly(N-isopropylacrylamide)* " Macromolecules (DOI: 10.1021/ma101439f).

2. **Huda M. Nurul**., Seki T., Suzuki H., A.N.M Hamidul K., Harun-ur- R., and Takeoka Y.. "*Characteristics of High-Density Poly(N-isopropylacrylamide) (PNIPA) Brushes on Silicon Surface by Atom Transfer Radical Polymerization"* Transactions of the Materials Research Society, Japan (in press).

3. Md.Mominul Huque, A.N.M.Hamidul Kabir, **M. Nurul Huda**, Shaila K. *"Physio – Chemical study of Paraetamol and Aspirin in water – Ethanol system".* Bangladesh Pharmaceutical journal, 2010, Vol 13, No 2, 13-19.

4. Huda M.Nurul. Seki T. Takeoka Y. *"Dominant influence of the terminal molecule of PNIPA grafted membrane obtained by Atomic Transfer Radical Polymerization*" In prerparation.

5. Huda M.Nurul. Seki T. Takeoka Y. *"Stimuli responsive behavior of high density Poly (N-isopropylacrylamide) (PNIPA) constructed on silicon surface by Atom Transfer Radical Polymerization (ATRP).* In preparation

**Conferences.**

1. **Muhammad Nurul Huda**, Hiromasa Suzuki, Takahiro Seki, Yukikazu Takeoka, "*Characteristics of disperse poly(N-isopropylacrylamide) (PNIPA) brushes on silicon surfaces by Atom transfer radical polymerization.*", 19th Academic Symposium of MRS-J, Yokohama, Japan, Dec.07-09, 2009.

2. **Muhammad Nurul Huda**, Hiromasa Suzuki, Takahiro Seki, Yukikazu Takeoka, "*Characteristics of stimuli responsive poly(N-isopropylacrylamide) (PNIPA) brushes on silicon surfaces by Atom transfer radical polymerization* ", 59th Polymer conference, Yokohama, Japan, May 26-29 , 2009.